

AN INVESTIGATION
OF WIND TUNNEL WALL EFFECTS
AT HIGH MACH NUMBERS

Thesis by

Lieutenant Commander John K. Leydon, USN
and
Lieutenant Commander Walter B. Miller, USN

In Partial Fulfillment of the
Requirements for the
Degree of Aeronautical Engineer

California Institute of Technology
Pasadena, California

CONFIDENTIAL

ACKNOWLEDGEMENT

The authors are indebted to the staff of the Guggenheim Aeronautical Laboratory, California Institute of Technology.

In particular they wish to express their appreciation to Dr. Hans Wolfgang Liepmann, Mr. A. E. Puckett and Dr. A. Fejer for valuable help and criticism, and to Mr. Richard Schamberg for material assistance during the course of the investigation.

CONFIDENTIAL

TABLE OF CONTENTS

<u>PART</u>		<u>PAGE NOS.</u>
I	Summary	1.1
	Introduction	1.2
	Equipment	1.4
	Procedure	1.7
	Results and Discussion	1.11
	Conclusions	1.18
	Recommendations	1.19
	References and Bibliography	1.20
II	Figures	2.1

* 1.1 *

SUMMARY

This paper presents the results of an investigation of wind tunnel wall interference in a two-dimensional wind tunnel at high Mach numbers. The results are presented in the form of curves of lift coefficient versus the ratio of model chord to tunnel height, as functions of Mach number and angle of attack. The investigation was carried out by the authors at the Guggenheim Aeronautical Laboratory of the California Institute of Technology during the school year 1944-45.

Tests were carried out on the NACA low drag airfoil section 65,1-012 at Mach numbers from .60 to .80, and angles of attack of from 1 to 3 degrees. Models were of 1", 2", 4" and 6" chord, giving values of the chord to tunnel height ratio of .1 to .6. Schlieren photographs were made of shock waves where they occurred.

INTRODUCTION

Many attempts have been made to determine wind tunnel interference effects at high Mach numbers using a purely theoretical approach. It was felt that an experimental investigation might also be of value, if not quantitatively, at least qualitatively, to indicate the general nature of these effects.

A complete systematic investigation involves a considerable number of parameters, measurements, and calculations, all of which require more time than was available for this investigation. Therefore, tests were restricted to one airfoil section, the NACA symmetrical low drag section 65,1-012, varying only chord length, Mach number, and angle of attack.

The general approach to this problem was to show the variation in C_L versus the non-dimensional parameter c/h , for several Mach numbers and angles of attack. By extrapolation to $c/h = 0$, corresponding to $h = \infty$, the free stream values of C_L were obtained for comparison.

Since one of the limitations of the equipment was the accuracy of the angle of attack setting, recourse was made to incompressible theory in order to establish a uniform criterion for the angle of attack.

Schlieren photographs were taken in all cases where shock waves existed, principally to indicate the extent of the shock

wave and the possibility of tunnel blocking.

These investigations were conducted at the Guggenheim Aeronautical Laboratory of the California Institute of Technology during the school year 1944-45.

EQUIPMENT

The tunnel is described in detail in Ref. 1, and is shown in Fig. 1A. It is a closed throat, open return, induction tunnel, capable of reaching a Mach number of .91 with no model installed. The jets are located in a rectangular section downstream of the test section and are followed by a constant area mixing section which discharges into the diffuser. Filters are installed at the entrance and exit sections of the tunnel.

Air is supplied to the jets by two rotary, positive displacement type compressors in series, capable of delivering a pressure of 100 lbs/in². A remotely controlled by-pass valve enables accurate control of the pressure delivered to the tunnel. This in turn allows precise speed adjustment.

The test section is rectangular, one inch wide by ten inches high, and twenty inches long. The side walls are of 3/4 inch plate glass, gasketed to the structure. The top and bottom walls are laminated phenolic resin blocks with 23 flush static pressure orifices in each. The orifices cover 17 inches of the blocks and are spaced $\frac{1}{2}$ inch apart in the region of the model, and one inch apart elsewhere. The test section is tapered in the one inch dimension from 0.900 inches at the entrance to 1.000 inches at the exit, to allow for boundary layer growth.

The model is supported at its 25% chord point in the center of the test section by a through bolt which is held by

trunnions inserted in oblong slots cut in the glass. The model is gasketed to the glass and to the trunnions. The trunnions and the model are held together by the through bolt which is set up with nuts at each end, thus fixing the model position with respect to the trunnions. Since the trunnions cannot rotate in their oblong slots, restraint is exercised on the model. It is also restrained from rotation by pressure exerted upon it by the glass side walls when they are tightened in place.

The models used in this investigation are of the NACA 65,1-012 low drag section. They are of 1", 2", 4", and 6" chord, machined from brass to tolerances of .001".

The wall block static pressure orifices were connected to a closed system multiple manometer containing butyl alcohol when possible, and acetylene tetrabromide (Sp. Grav. 2.96) when a higher specific gravity fluid was required. An orifice having a relatively positive pressure was connected to the reservoir and used as a reference. A mercury manometer vented to the atmosphere was connected to the orifices used for determining free stream pressure and hence Mach number.

The optical system consists of standard schlieren equipment, and was used for visual and photographic observations. An incandescent light source employing a projection type bulb was used for visual observation. A high intensity spark giving an exposure time of the order of 10^{-4} seconds was used for photographic purposes.

CONFIDENTIAL

* 1.6 *

Relative humidity was measured for each series of runs using a wet and dry bulb hygrometer.

CONFIDENTIAL

PROCEDURE

The project included the setting up of the wind tunnel in a special room which was so narrow that a modification of the former optical system was required. This involved redesign of the light system to maintain a proper length of light path. To maintain proper distances it was necessary to bend the light by introducing plane mirrors into the system. Incidental to this redesign a more powerful focusing lens was installed for the photographic apparatus. The entire system as modified is shown schematically in Fig. 1B, and can be seen in the photographs of Fig. 1A. Work required to accomplish the above included the design of mirror and prism mounting brackets and holders.

Prior to the actual calibration of the tunnel, it was found that the pressure distribution along the tunnel wall blocks was quite uniform except at the leading orifice. By the second orifice from the entrance, both top and bottom, the flow had stabilized. These orifices, therefore, were connected to the mercury manometer to determine p of the free stream. Using the relationship

$$\frac{P}{P_0} = \left(1 + \frac{\gamma-1}{2} M^2\right)^{\frac{\gamma}{1-\gamma}} \quad \checkmark$$

a scale was made to read Mach number directly for each pressure. The area contraction ratio from the entrance filter to the test section being 60, the pressure drop across the filter was negligible. This was proved by the fact that the indicated Mach number did not change with removal of the filter during operation. Since it was desired to use the average of top and bottom pressures for

a more representative free stream reading, the scale was mounted on the manometer board between the tubes indicating each of these pressures. They did not differ materially, so that it was possible to average them visually and read the Mach number corresponding to this average.

After the wind tunnel and the optical system had been successfully assembled, actual research was begun. Several calibration runs were made, at Mach numbers of .50, .60, .70, and .80, with no model in the tunnel. From the data obtained during these runs, correction curves were drawn for each pressure orifice.

Zero degrees angle of attack was determined by trial and error by measuring lift on the six inch airfoil and shifting the angle of attack setting until zero lift was obtained. Using a ten inch steel rule as a protractor, the zero reference setting was inscribed on the tunnel and additional angle of attack references were computed and located.

The procedure for setting angle of attack required that the protractor first be set and then the model adjusted by visually aligning both the chord line scribed on the model and the trailing edge of the model with the protractor.

The zero angle of attack setting was checked by measuring the lift on the one inch airfoil at that setting. The agreement was excellent, as should have been expected.

For all runs the tunnel wall pressures were recorded for each orifice. These were actually pressure differences with respect to a chosen orifice having a relatively positive pressure. The recorded pressures were reduced to $\Delta p/q$ and the orifice corrections applied. Values of q were computed from the relation $q = \frac{\gamma}{2} M^2 p$, where the value of p was the same as that which determined M . The curves for upper and lower orifice blocks were superimposed in order to measure the lift on the airfoil by the area enclosed between the curves. The areas were evaluated by means of a planimeter and lift coefficients were calculated in the usual manner.

Runs were made on the 1", 2", and 4" chord models at angles of attack of 1°, 2°, and 3°, and Mach numbers of .60, .65, .70, .75, and .80. With the six inch model installed, the tunnel choked at Mach numbers between .75 and .80, depending on the angle of attack. It was impossible, therefore, to reach a Mach number of .80 with this model, but the other corresponding runs were made. Schlieren photographs were taken for each run in which shock waves existed. The Mach number at which the shock waves first appeared was noted.

Oil from the compressor system quickly filled the room during each run so that it was necessary to dismantle the test section and clean the glass walls frequently. This was held to a minimum, nevertheless, by running at the highest Mach number first

* 1.10 *

and taking photographs, if any, while the glass was relatively clean. By the time the glass became clouded, a lower Mach number had been reached, where no shock waves existed and no photographs were required.

The one inch airfoil was so thin that its gasket would not cover the holes in the glass walls. It was necessary, therefore, to mask these holes from the outside by means of scotch tape. This masking obscured all but the trailing edge of the model and made it impossible to determine the first occurrence of the shock wave, or its extent, until it had progressed beyond the masked area.

At the higher values of Mach number and angle of attack, for the four inch and six inch models, individual pressures were so large that the alcohol head in the manometer was insufficient to balance them. For these runs, acetylene tetrabromide was substituted for the alcohol as manometer fluid.

The run numbers were assigned successively as each run was made. Because of the shift from alcohol to acetylene tetrabromide and the necessity of doing the higher Mach numbers first, as previously mentioned, these run numbers do not follow a systematic progression and are of use only in relating the final values with the original data.

RESULTS AND DISCUSSION

Values of corrected $\Delta p/q$ versus distance along the test section are shown plotted for all runs in Figs. 1 to 57 inclusive. It will be noted that the curves are smooth, which is a justification for the use of an orifice by orifice correction method. In some cases the curves do not close at the ends of the orifice region. This results in a measured lift lower than actual. The percentage error made in C_L is not determinable but the results should be comparable with any tests made, using the wall pressure method of measuring lift. An apparent scatter exists in the curves for the one inch airfoil since the area of influence of this small chord is so light that the scale of the graph must be enlarged to a point where the accuracy of the readings themselves causes scatter.

Schlieren photographs of shock waves where they existed at test points are shown in Figs. 58 - 62. The photographs were so taken as to show the upper and lower surface of the model and the top tunnel wall, which appears as the horizontal boundary at the top of each picture. This allows observation of the full extent of the shock wave on the upper surface and the position of the shock wave on the lower surface. Fig. 62 shows an example of the shock wave extending to the tunnel wall, at which point the tunnel is choked.

The values of C_L obtained were plotted versus Mach number

and angle of attack in Figs. 63 - 66 and 68 - 71 respectively. The latter showed that the values of C_L did not lie on a straight line themselves, nor did any straight line passing through the origin appear to approximately satisfy the points. Since the angles of attack used were small, and the airfoil section is a symmetrical one, some linear variation of C_L with α was to be expected, even at the high Mach numbers, provided no shock waves were encountered.

For this reason, an attempt was made to check the angle of attack by some other means. The procedure adopted utilized known two-dimensional incompressible wind tunnel wall correction data and preserved as much as is possible the identity of the experimental results. Prandtl-Glauert curves were fitted to the curves of C_L versus M , and C_L for $M = 0$ determined from the Prandtl-Glauert formula. (See Figs. 63 - 66). While the Karman-Tsien method, Ref. 2, would also have been useful, data on C_p variation was not available, thereby obviating the use of this method.

The free stream slope of the lift curve for this airfoil was obtained from Ref. 3. Using the method outlined in Ref. 4, offsets from this curve were obtained to determine the line of C_L versus α for various values of c/h at $M = 0$. Whereas Ref. 4 concerns itself with the same problem which is here trying to be determined, the equations therein when used with $M = 0$ are merely incompressible theory. These curves are shown in Fig. 67.

Entering the curve for the appropriate c/h value with the C_L for $M = 0$ found from the Prandtl-Glauert extrapolation of test points, gave values of angle of attack differing markedly from those set on the models. These results are listed below:

α set	C_L for $M = 0$	α derived	$\Delta\alpha$
1" chord			
1	.092	.80	-.20
2	.184	1.60	-.40
3	.238	2.06	-.94
2" chord			
1	.064	.55	-.45
2	.150	1.27	-.73
3	.271	2.28	-.72
4" chord			
1	.123	.98	-.02
2	.202	1.60	-.40
3	.289	2.28	-.72
6" chord			
1	.080	.57	-.43
2	.198	1.40	-.60
3	.288	2.05	-.97

The accuracy of the setting of angle of attack in the tunnel is considered to be within .2 degrees. The above results tend to indicate otherwise. It is believed that the discrepancy is not entirely attributable to angle of attack setting but that the Prandtl-Glauert approximation also is involved. However, in order to coordinate the data, the derived angles of attack were used as obtained. Replotting C_L versus α_d , on Figs. 68 - 71,

gives excellent agreement of the data, being straight lines passing through the origin.

To correlate data between the different chord models, common values of α_d were chosen. These were $3/4^\circ$, $1\frac{1}{2}^\circ$, and $2\frac{1}{4}^\circ$, since these values were not only evenly spaced but also were quite close to the mean of the derived angles obtained.

In shifting the C_L values either ahead or back to the chosen α_d , it was impossible to determine whether this shift was of sufficient magnitude either to obtain or lose shock waves, as the case may be. For this reason, the points in which shocks were present were kept in the same position relative to the other points. It should therefore be understood that this is not to be used as a guide in determining the exact angle of attack at which shock waves occur, but should be used only to obtain qualitative differences between points with shock waves and those without in their behaviour so far as wind tunnel wall effect is concerned. It can be seen that lift continued to increase with increasing Mach number even after the shock wave had formed.

Having reduced C_L values to a common denominator in angle of attack, curves of C_L versus c/h for these angles were plotted in Figs. 72 - 74. No attempt was made to draw curves above a Mach number of .70, since this whole approach to the subject is not valid when there is a large supersonic zone of flow or there exists a shock wave. By extrapolating these curves to a c/h of zero, a

qualitative measure of wind tunnel interference was obtained. The curves are all of the same character and consistently indicate the change to be expected with increasing M and c/h .

In the derivation of these curves, as is explained previously, every attempt was made to retain the individuality of the experimental points. However, in striving for a common basis in angle of attack, the quantitative value of the results may have been destroyed. The qualitative value of the results has been preserved. In applying these results, therefore, to any similar wind tunnel investigation, they should be used only to indicate trends rather than exact corrections. In a completely similar tunnel they could possibly be considered to indicate order of magnitude.

A composite of these curves is given in Fig. 75, by plotting $dC_L/d\alpha$ versus c/h for values of M .

Throughout the whole investigation, no Reynolds number effect has been included in any discussion of the results. This effect is not yet well enough understood to apply to an interpretation of experimental work.

The Mach number at which a shock wave first appeared for each series of runs is tabulated below. The choking Mach number, where encountered, is also tabulated below. The Mach number at appearance of shock wave decreased with increasing angle of attack and with increasing values of c/h with complete regularity. In

comparing these results with those of Ref. 1, it must be noted that Mach number determination in that investigation was not based on free stream values exactly, since the pressure used was in the positive pressure region of the tunnel when a model was installed.

Table II

Chord	α set	M at appearance of shock	M at choking
1"	1	*.--	--
	2	*.770	--
	3	*.760	--
2"	1	.785	--
	2	.765	--
	3	.725	--
4"	1	.765	--
	2	.755	--
	3	.725	--
6"	1	.735	.770
	2	.725	.765
	3	.705	.765

*When shock wave appeared from behind masing on side walls.

The choking Mach number for the 6" airfoil as determined from one-dimensional theory is .72.

There are several salient features to be noted in the schlieren pictures. In spite of the results of other investigators, in particular those of Ref. 1, the shock waves were here found to be straight and devoid of triangulation at their base. The straightness of the shock wave is believed to be indicative of smooth flow. The humidity throughout the course of the investigation was between 48% and 52%. In general, however, particularly on the upper surface, there was only one shock wave apparent.

Visual observation of the shock waves during the course of the investigation showed very little, if any oscillation of the wave, either at its base or at its extremity. Several time photographs were taken, using the incandescent bulb as light source. These, however, showed no differences whatever over the spark pictures, no zone of shock wave travel could be discerned.

The quality of the shock wave pictures indicates that no loss in effectiveness results from injecting extra bends in the light path of the schlieren system.

CONCLUSIONS

The investigation showed the variation of wind tunnel wall effect with chord to tunnel height ratio and with Mach number. It demonstrated that lift coefficient continues to increase with increasing Mach number after the shock wave is formed and that the shock waves are in general straight and non-oscillatory.

It was also shown that the wall pressure method of measuring lift in a small two-dimensional tunnel should be confined to models giving intermediate chord to tunnel height ratios.

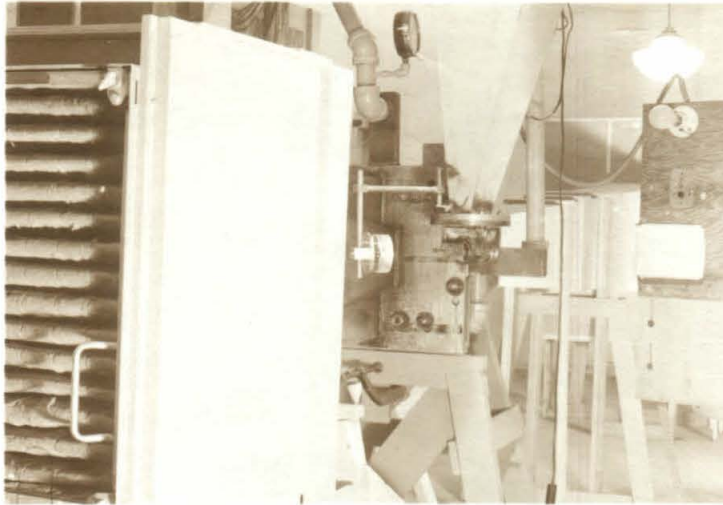
RECOMMENDATIONS

1. Some means of accurately setting the angle of attack of a model should be developed for this tunnel, employing a precision instrument and optical setting methods.
2. An extension of these results should be made, employing airfoils of the NACA 65,1 series with sections of different thickness ratios.
3. The results of this investigation should be applied to existing theoretical wind tunnel wall effect correction methods to determine whether agreement exists.
4. Future work in this wind tunnel should employ models of 2", 3", 4", and 5" chords, since they are best adapted to the wall pressure method of measuring lift.

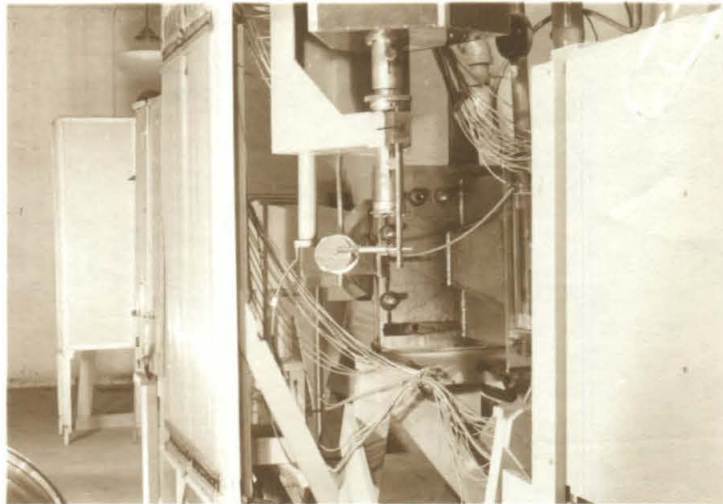
References and Bibliography

1. Chambers, L. S.; Doll, R. E.; and Harrell, D. A.
"An Investigation of the Effects of Angle of Attack and Airfoil Model Size on the Occurrence of Shock Waves in a Two Dimensional Wind Tunnel." C.I.T. Thesis 1944.
2. von Karman, Th; "Compressibility Effects in Aerodynamics." Journal Inst. Aer. Sc., July 1941.
3. Jacobs, E. N.; Abbott, I. H.; and Davidson, M.
"Preliminary Low-Drag-Airfoil and Flap Data at Large Reynolds Numbers and Low Turbulence." NACA Advanced Confidential Report, 1942.
4. Allen, H. J. and Vincenti, W. G., "Wall Interference in a Two-Dimensional-Flow Tunnel with Consideration of the Effect of Compressibility." NACA ARR 4K03.

CONFIDENTIAL



View of tunnel from left side of
entrance section, looking aft.

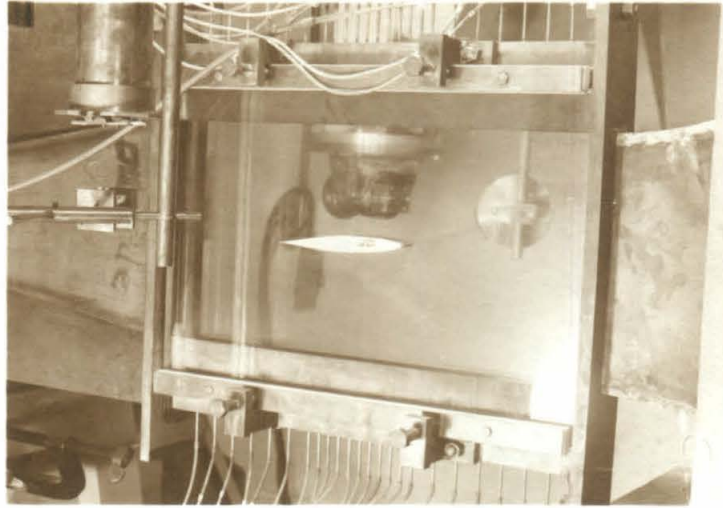


View of tunnel from right side
of entrance section, looking aft.

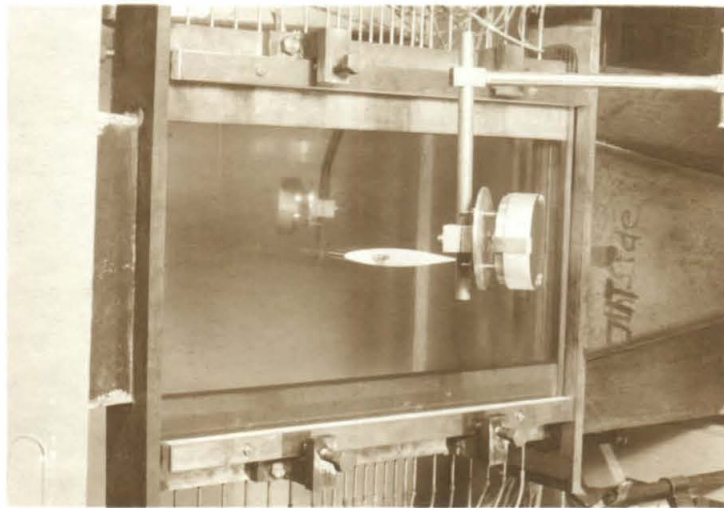
Fig. 1A

CONFIDENTIAL

CONFIDENTIAL



Left side of test section.



Right side of test section.

Fig. 1A'

CONFIDENTIAL

CONFIDENTIAL

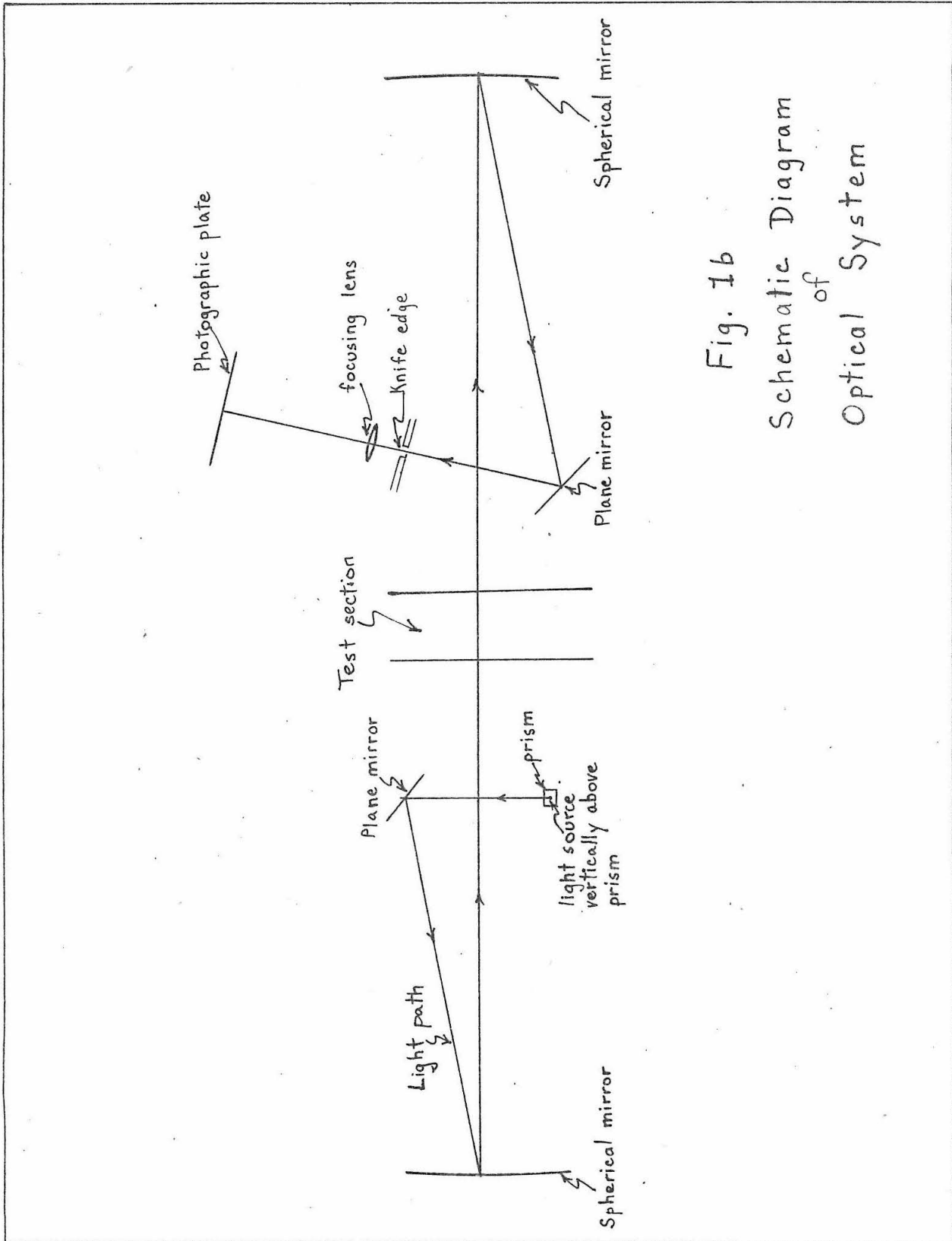


Fig. 1b
 Schematic Diagram
 of
 Optical System

CONFIDENTIAL

Figure 1c

Run 15
1" chord $\alpha = 1^\circ$
M = 60 $C_L = 1.20$

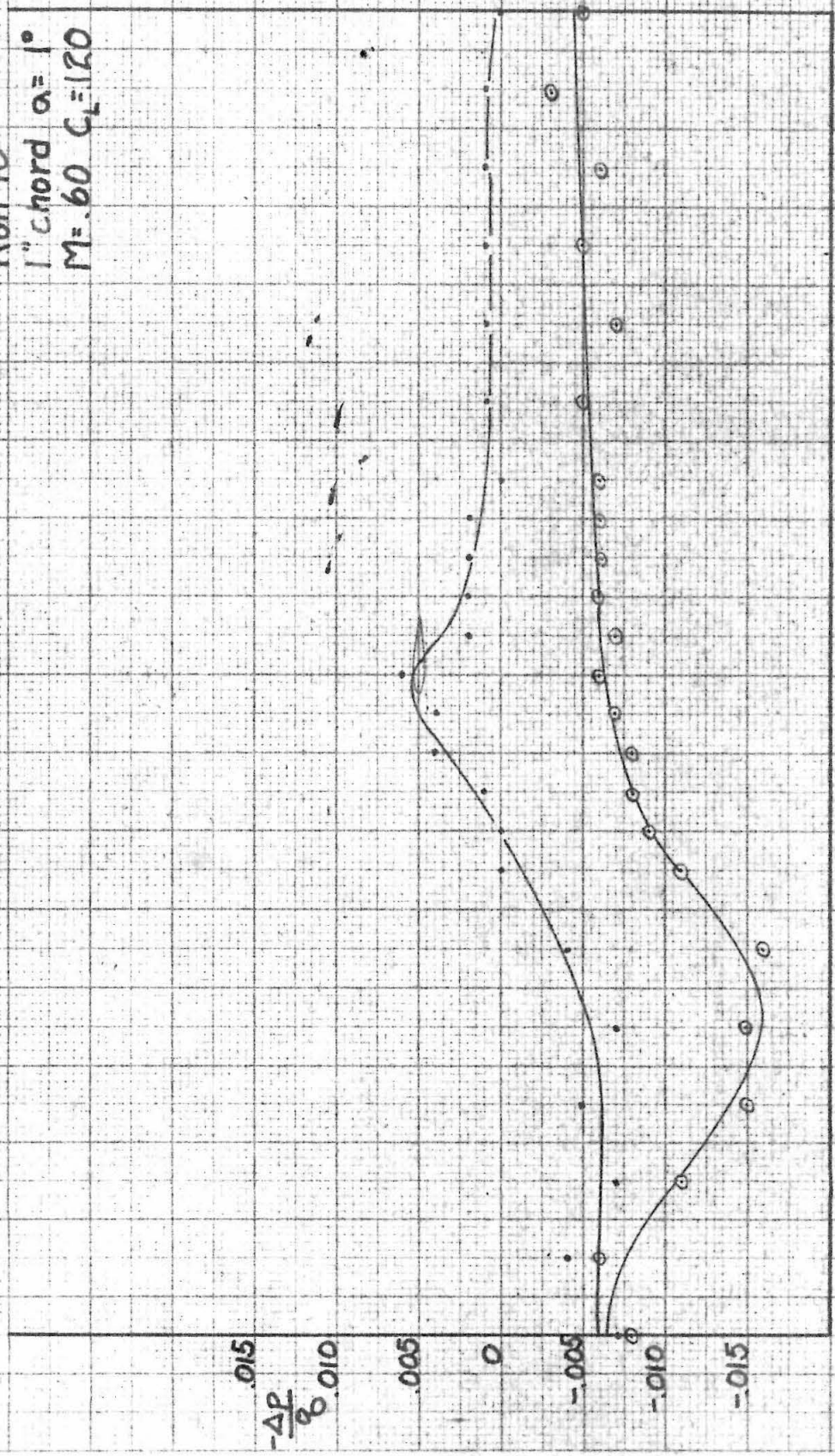
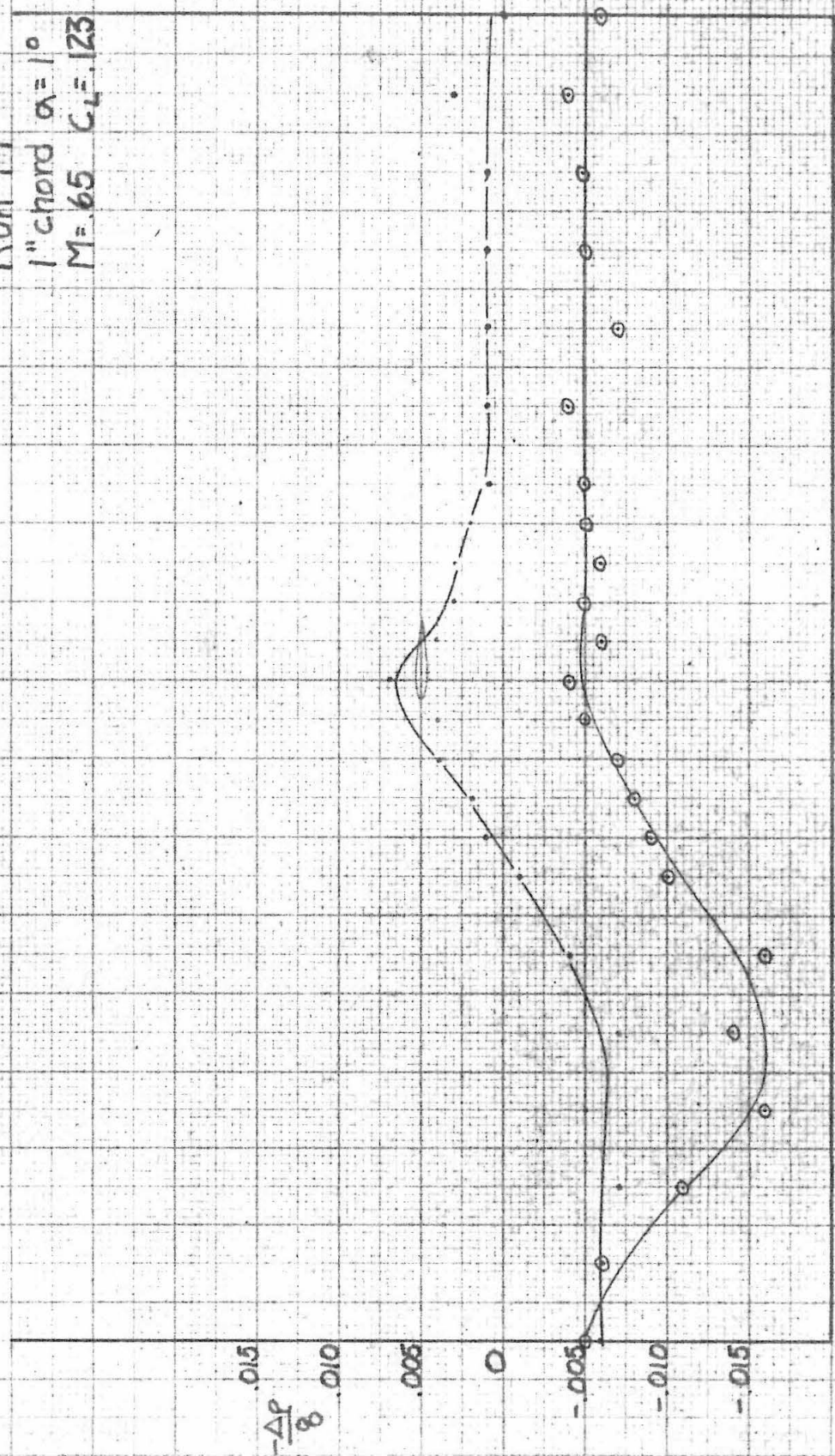


Fig. 2

Run 1A
1" chord $\alpha = 1^\circ$
M = 65 $C_L = .123$



5

0

5

Chords from a.c.

Fig. 3

Run 13

1" chord $\alpha = 1^\circ$

$M = .70$ $C_L = .122$

.01

$-\frac{\Delta p}{\rho}$

0

-.01

8

6

4

2

0

2

4

6

8

Chords from a.c.

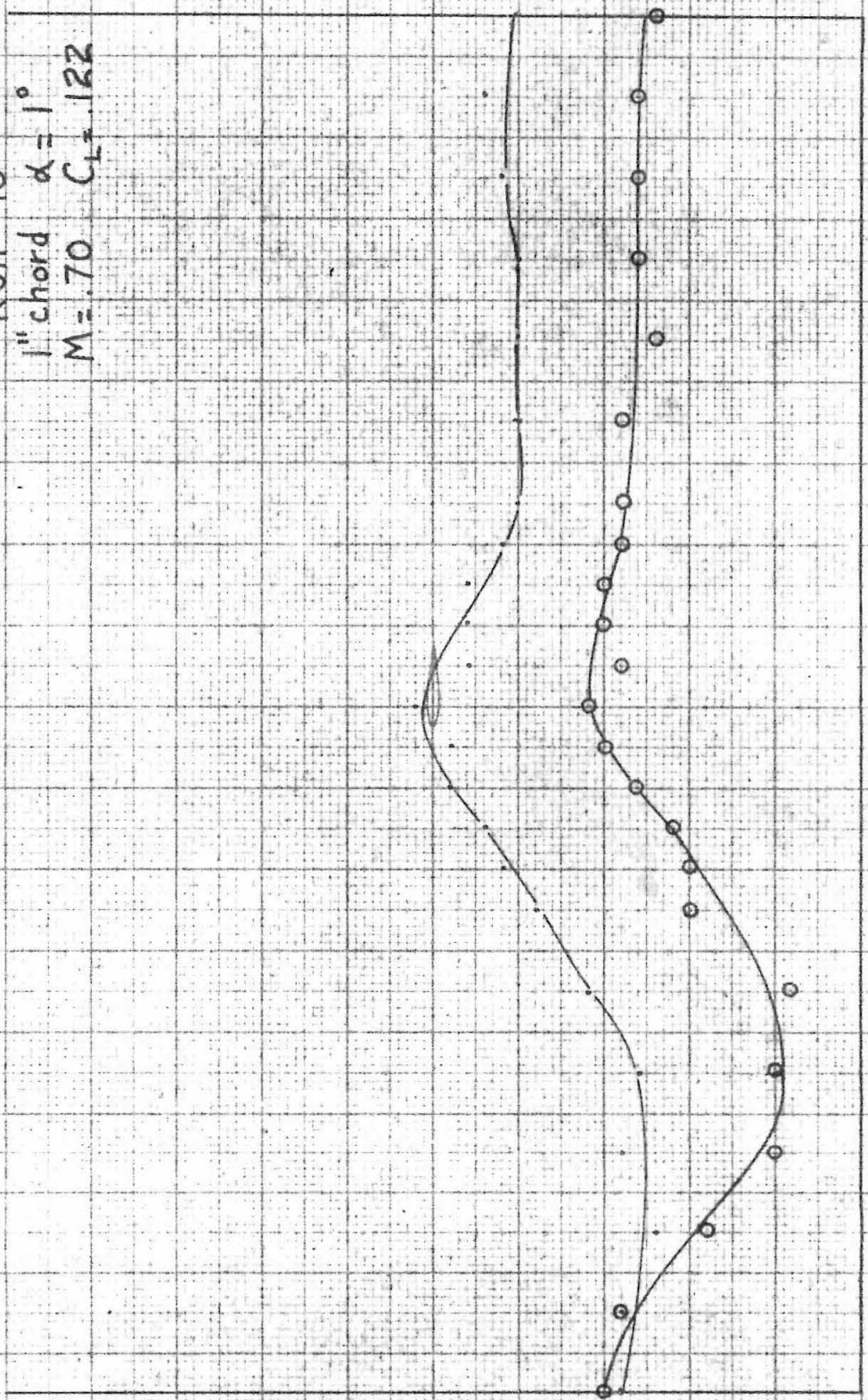


Fig. 4

Run 12
1" chord $\alpha = 1^\circ$
 $M = .75$ $C_L = .136$

$\frac{\Delta p}{\rho}$

Chords from a.c.

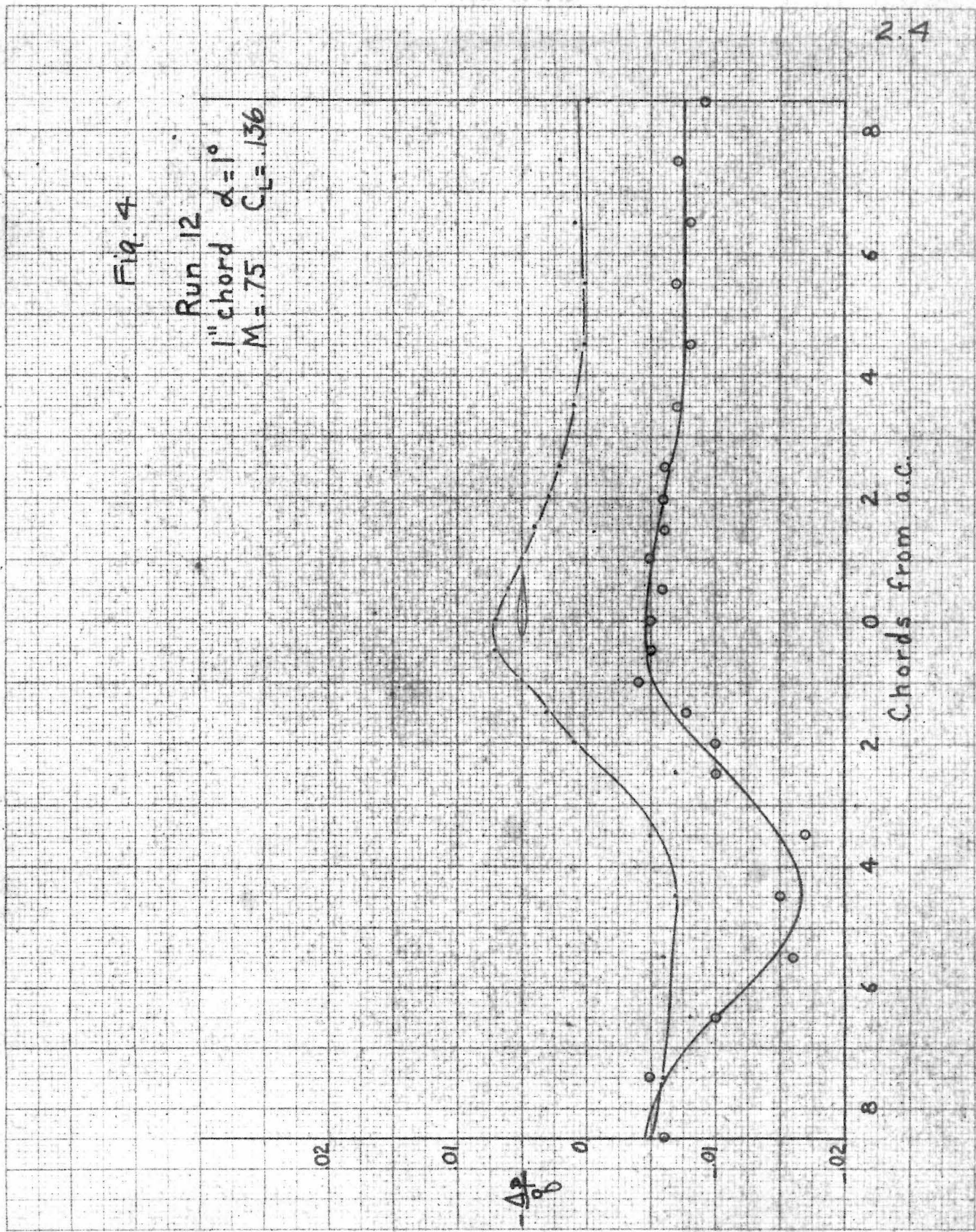


Fig. 5

Run II
1" chord $\alpha = 1^\circ$
M = .80 $C_L = 1.08$

$-\frac{\Delta P}{\rho}$

Chords from a.c.

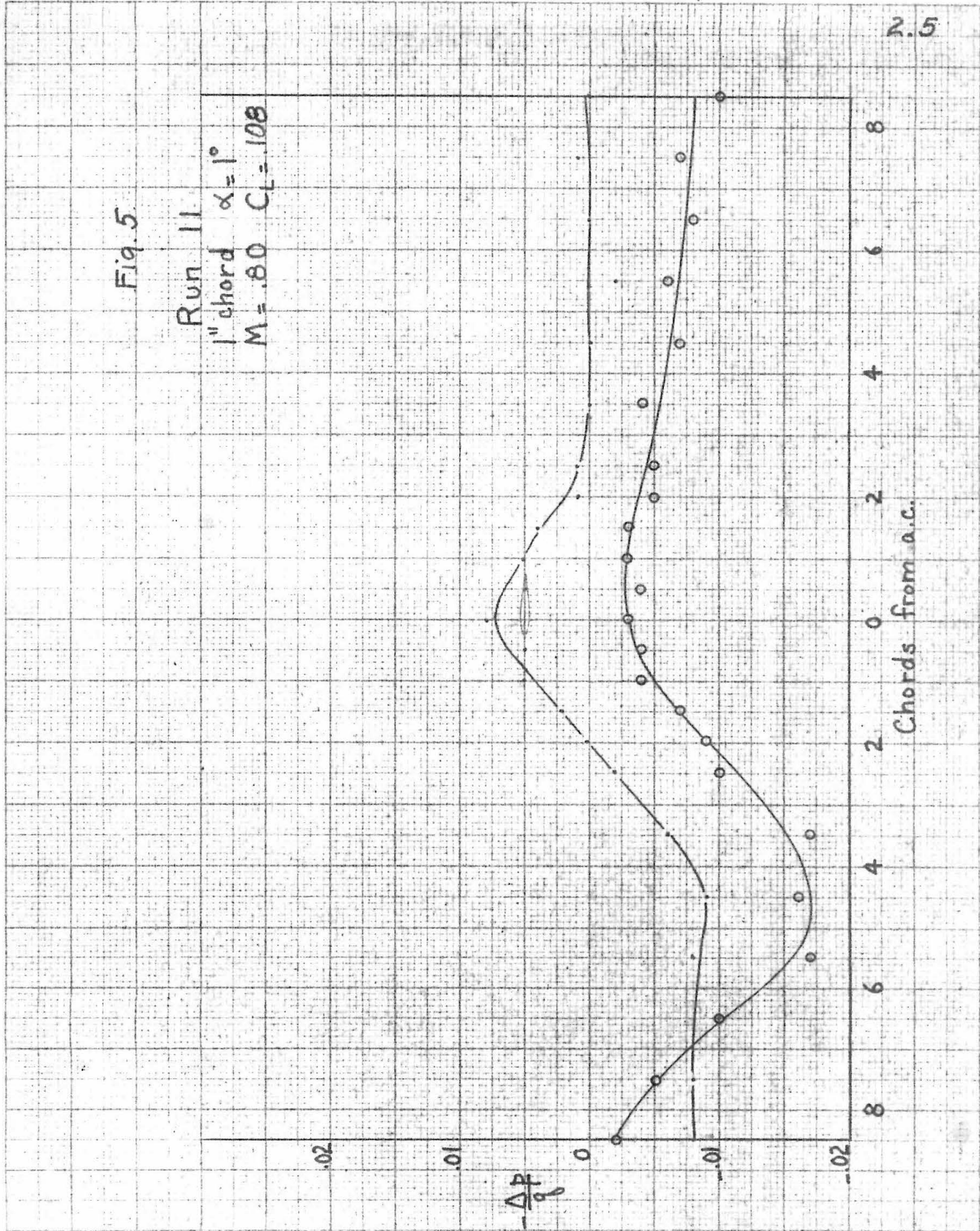
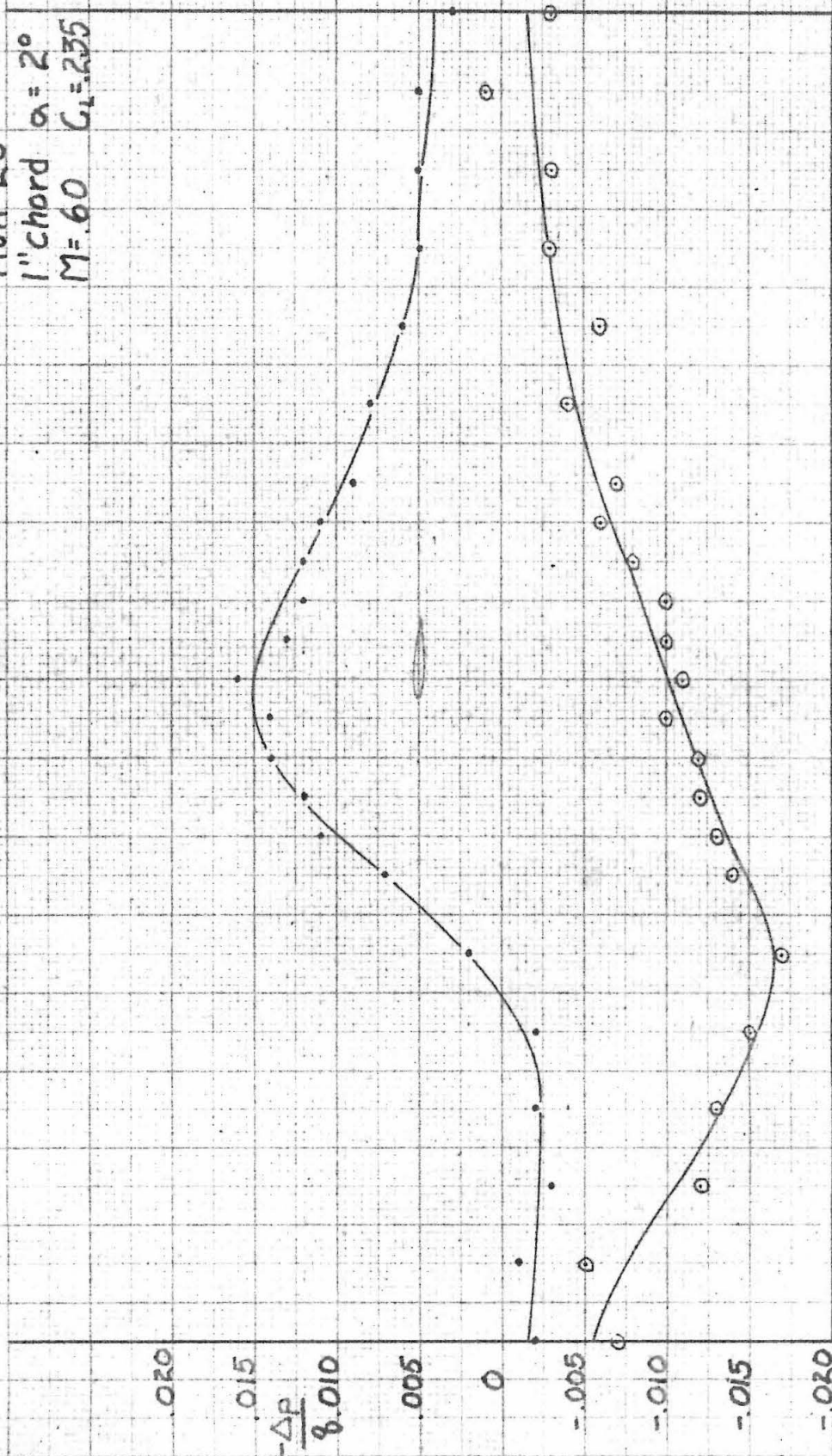


Fig. 6

Run 20
1" chord $\alpha = 2^\circ$
M = 60 $C_L = 2.35$



5

Chords from a.c.

5

Fig. 7

Run 19
1" chord $\alpha = 2^\circ$
M=65 $C_L = 257$

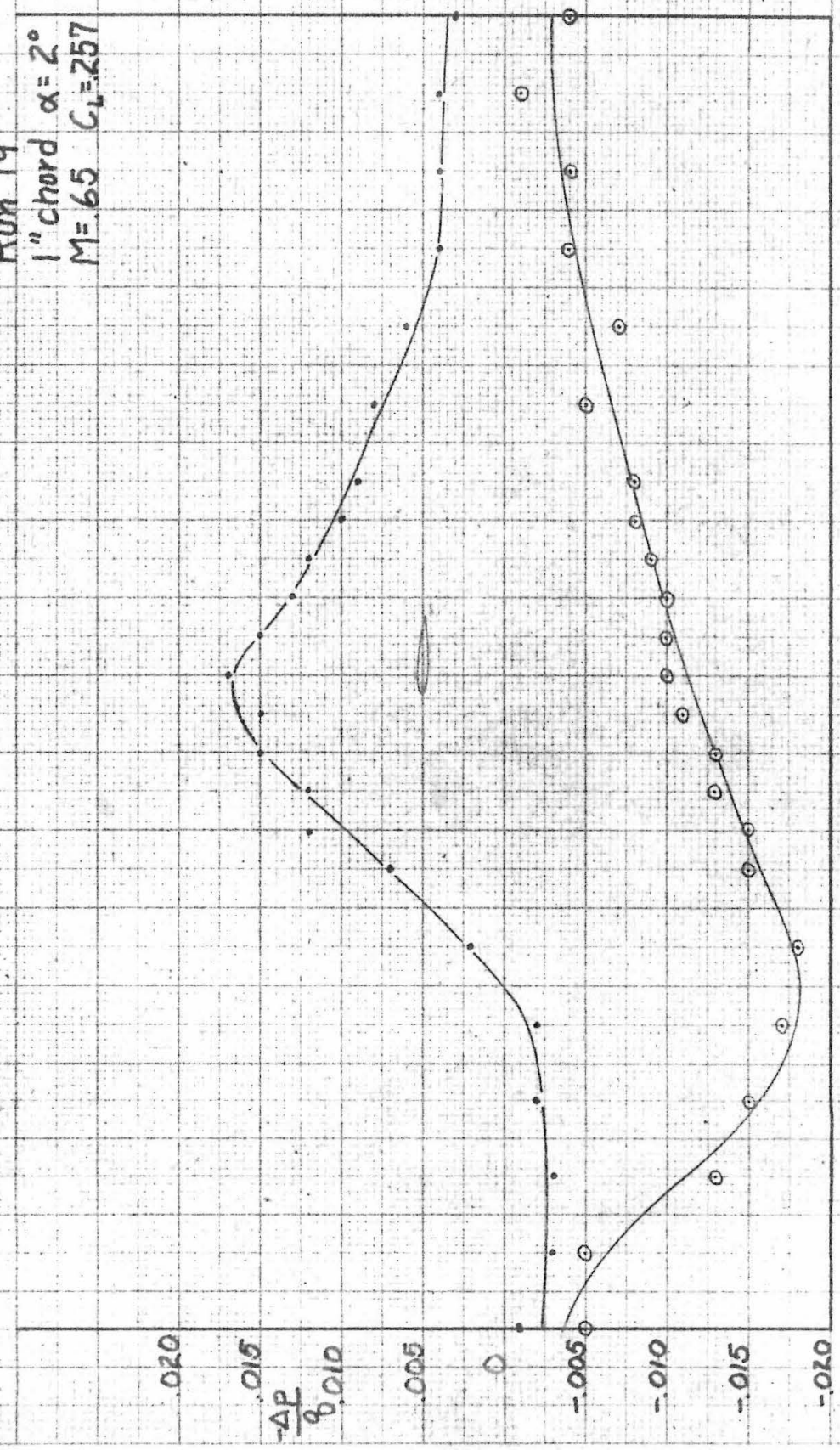


Fig. 8

Run 18
1" chord, $\alpha = 2^\circ$
 $M = .70$ $C_L = .252$

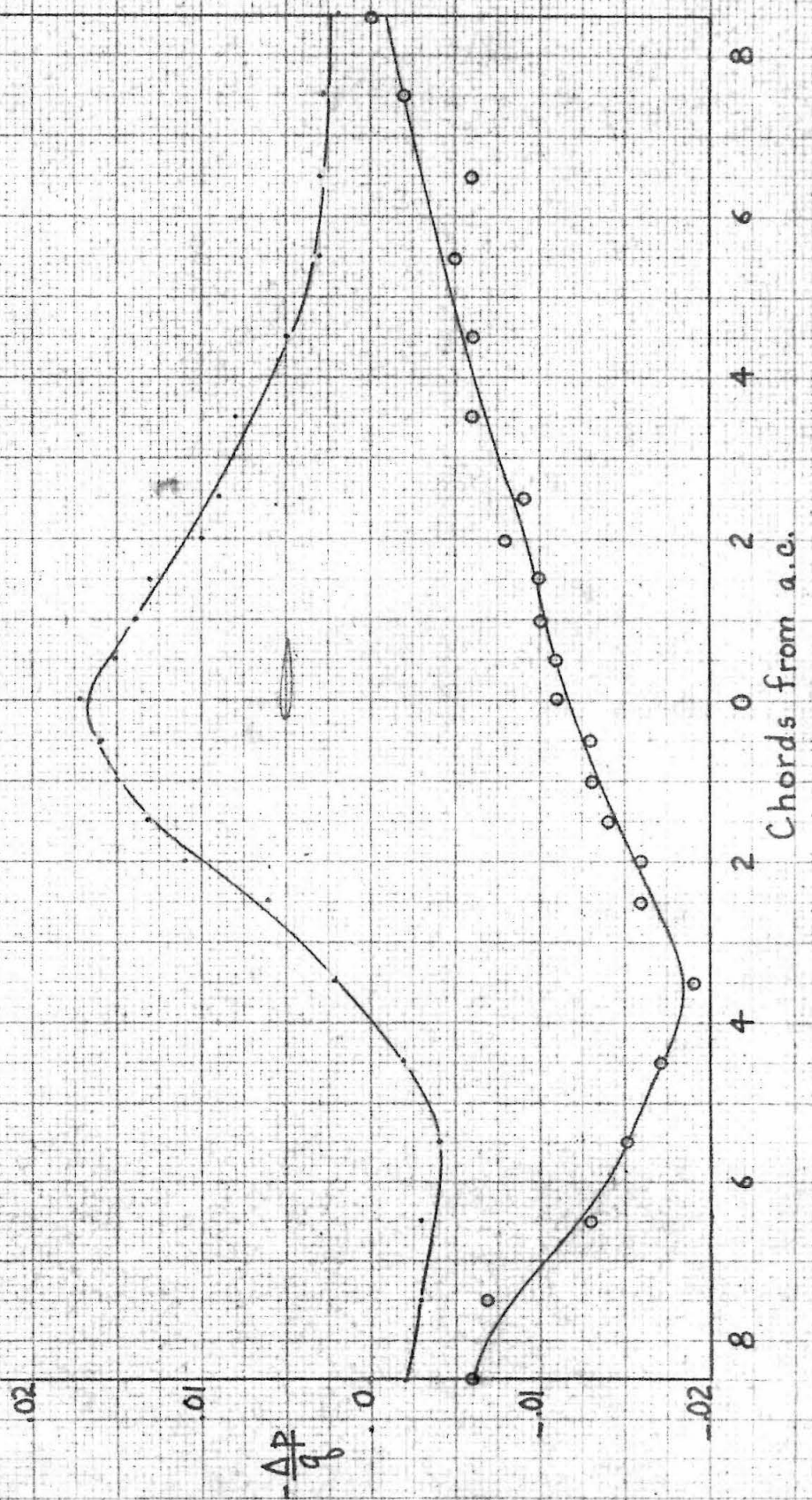


Fig. 9

Run 17

1" chord $\alpha = 2^\circ$

M=7.5 $C_f = 254$

$\frac{-\Delta P}{\rho U^2}$
.020
.015
.010
.005
0
-.005
-.010
-.015
-.020

5

0

5

Chords from a.c.

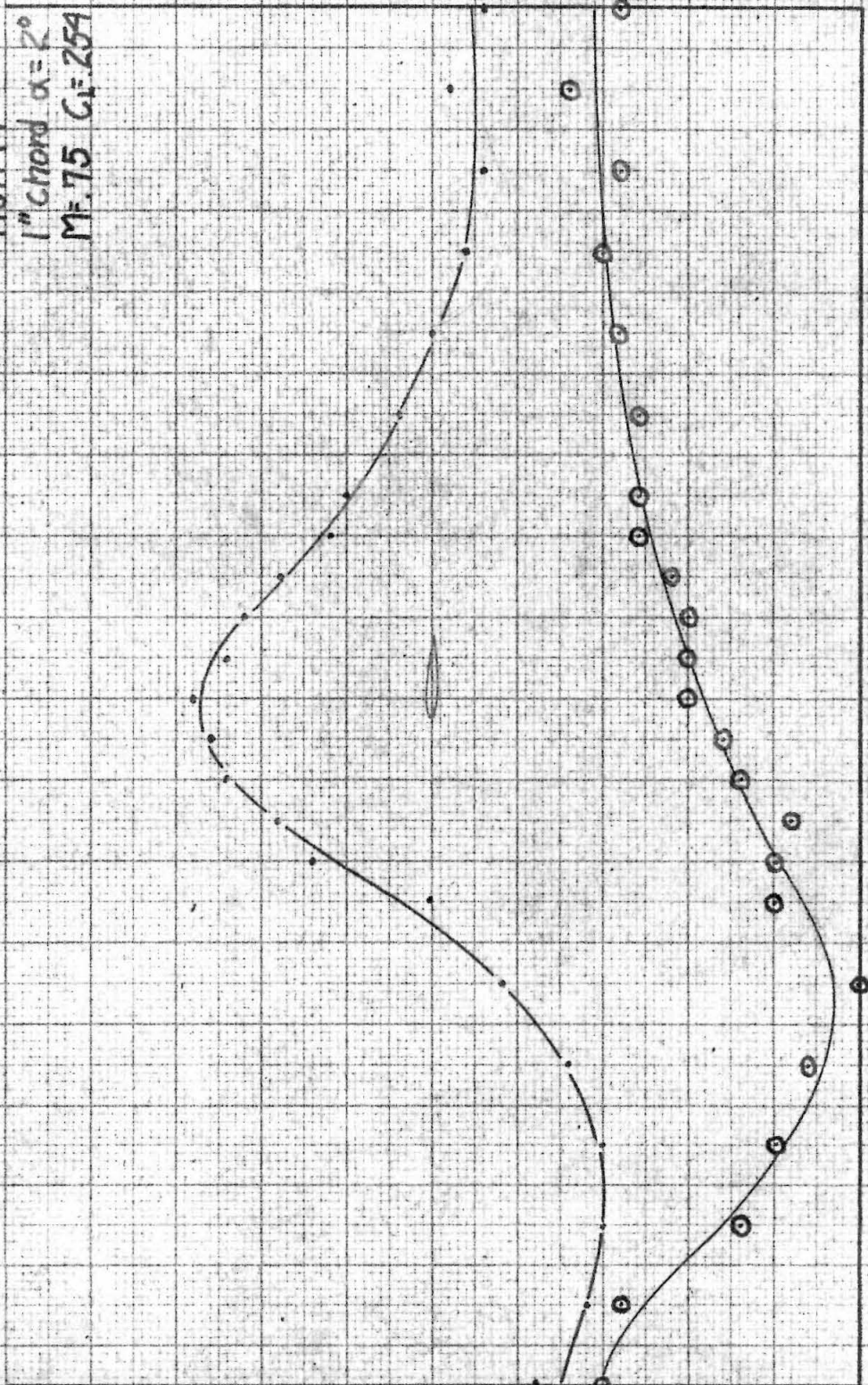


Fig. 10

Run 16
1" chord $\alpha = 2^\circ$
M = 80 $C_L = 228$

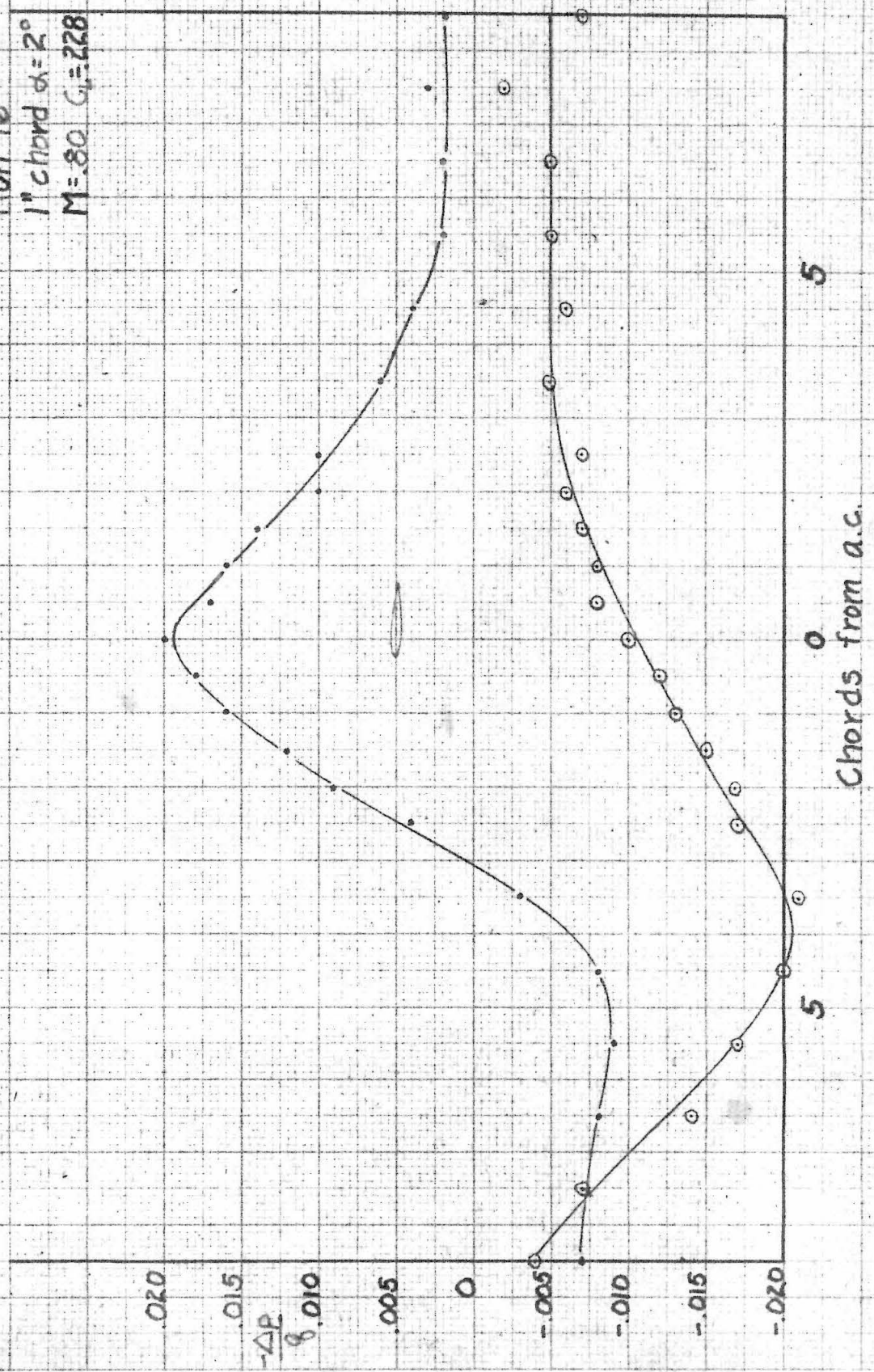
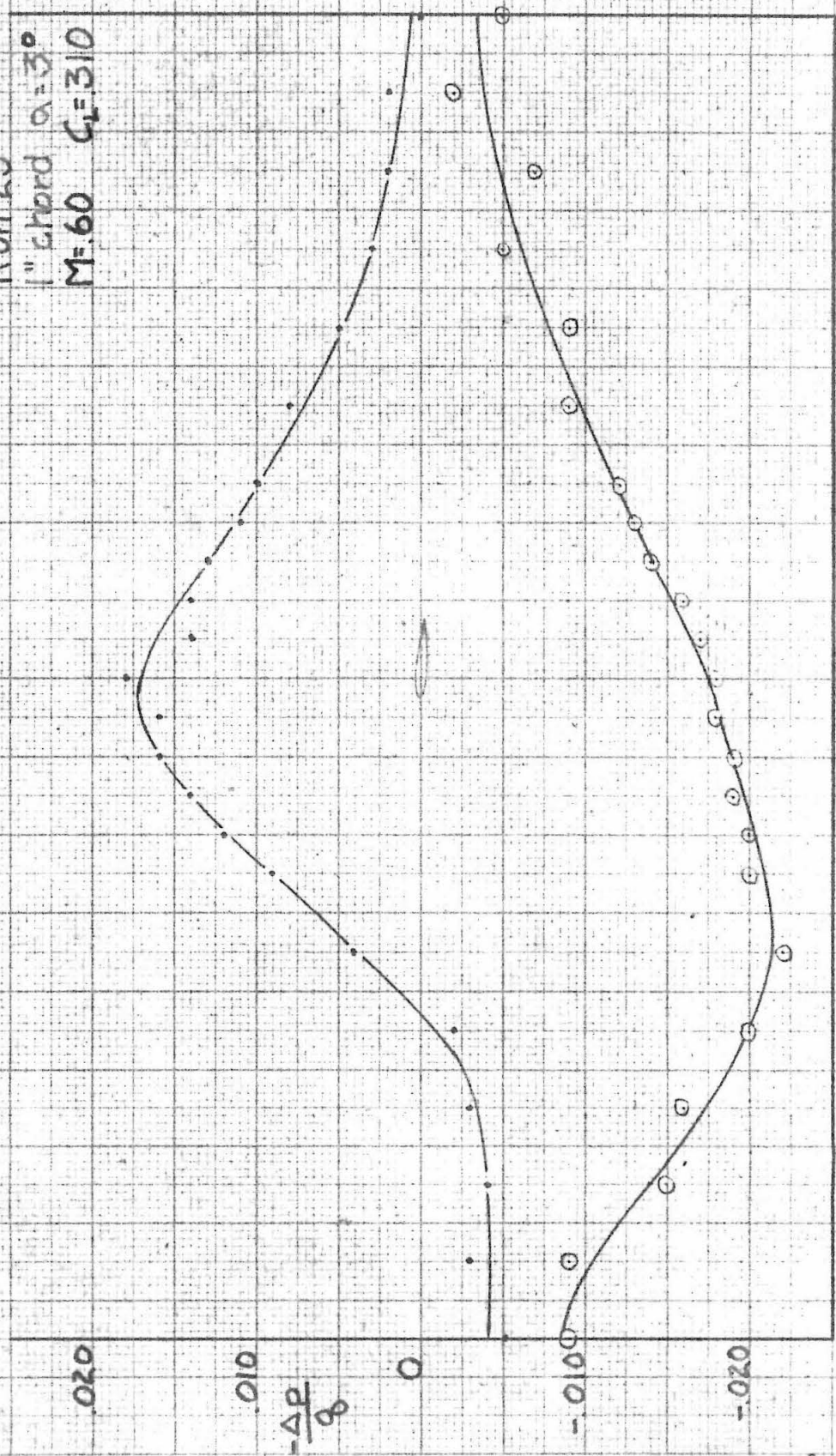


Fig. 11

Run 25
1" chord $\alpha = 3^\circ$
M=60 $C_L = 3.10$



5

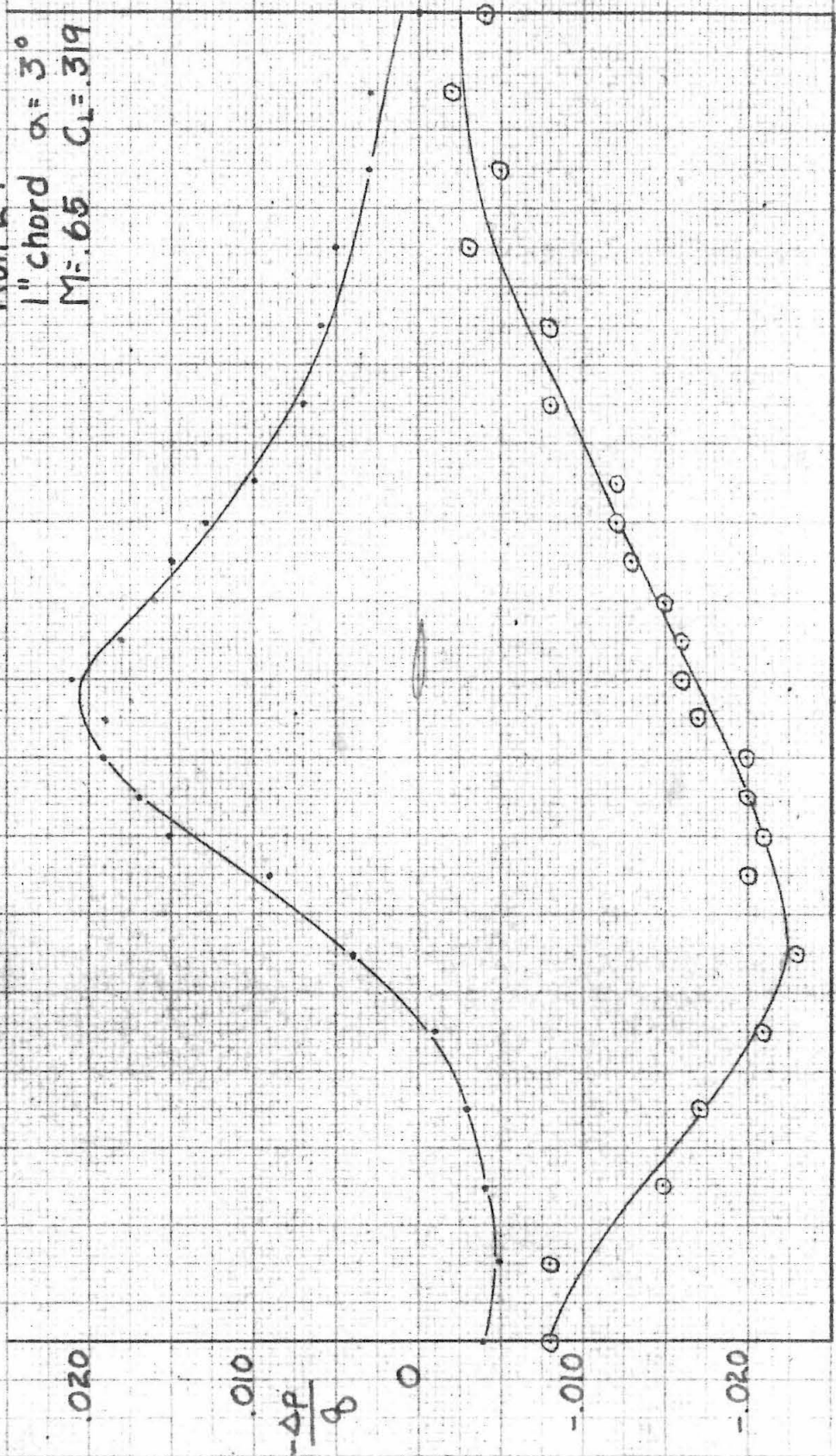
0

5

Chords from a.c.

Fig. 12

Run 24
1" chord $\alpha = 3^\circ$
M = 65 $C_L = 319$



5

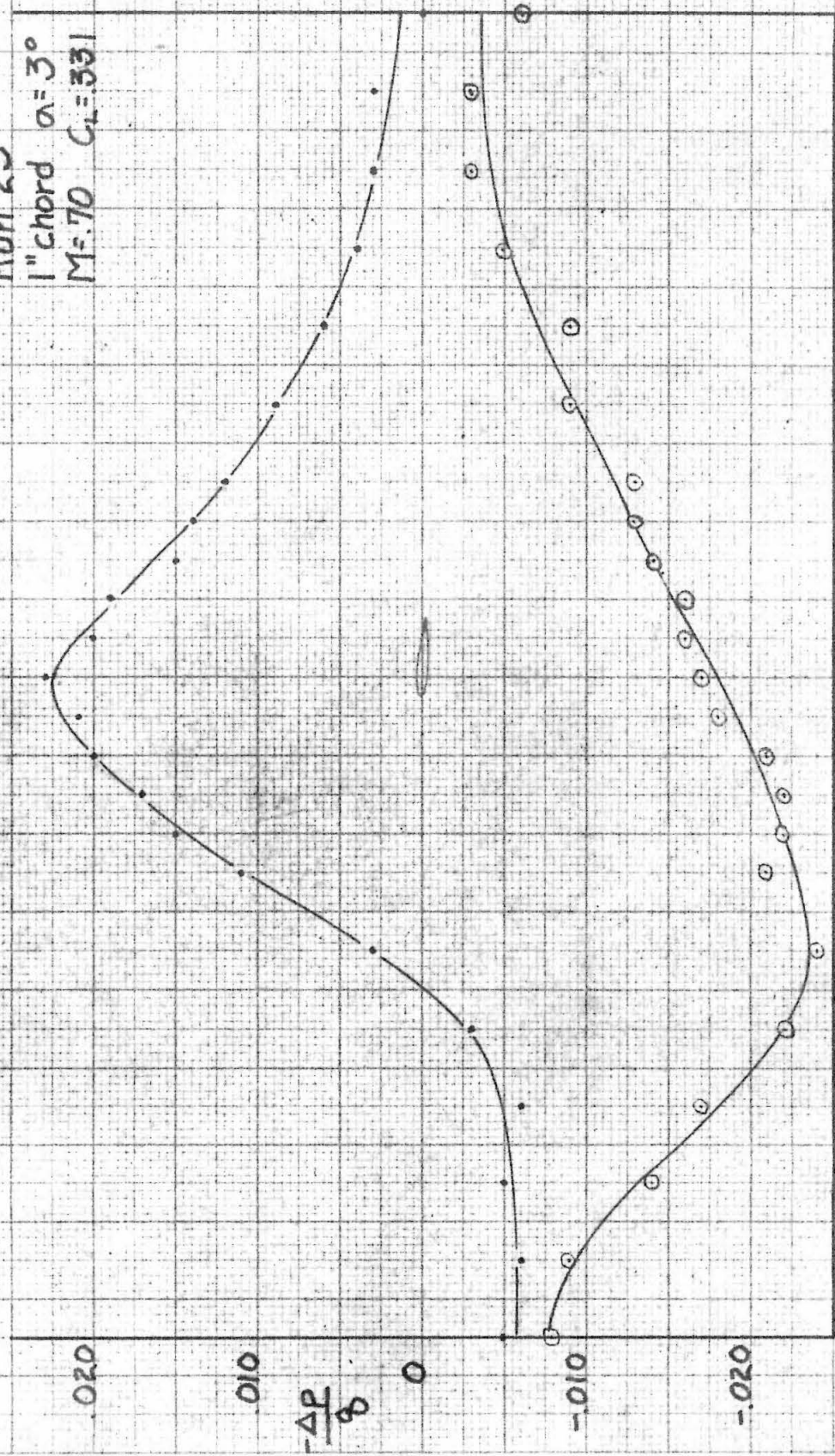
0

5

Chords from a.c.

Fig. 13

Run 23
1" chord $\alpha = 3^\circ$
M=70 $C_L = 331$



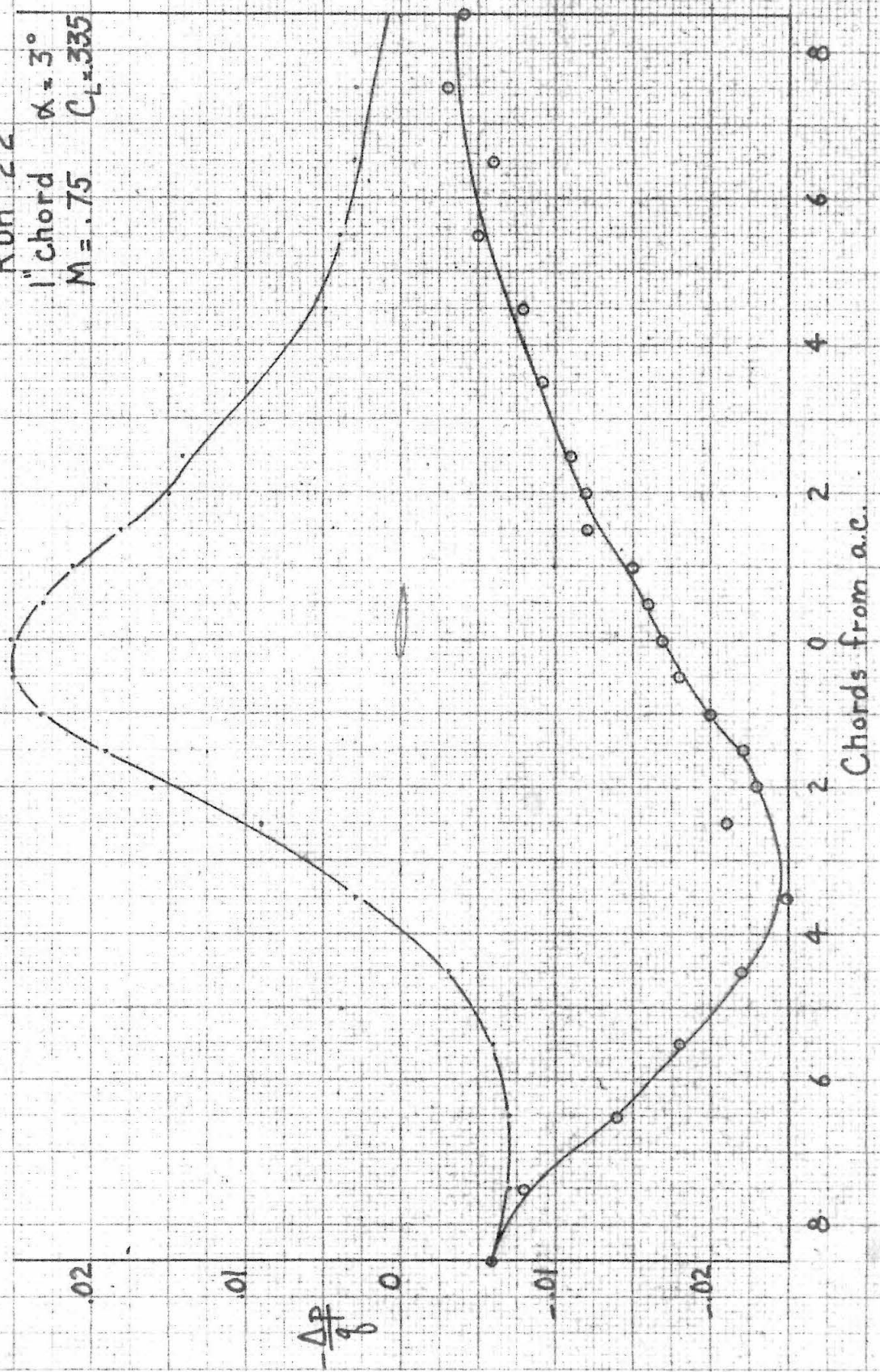
5

5

Chords from a.c.

Fig. 14

Run 22
1" chord
M = .75
 $\alpha = 3^\circ$
 $C_L = .335$



Run 21
 1" chord $\alpha = 3^\circ$
 $M = .80$ $C_L = .313$

Fig. 15

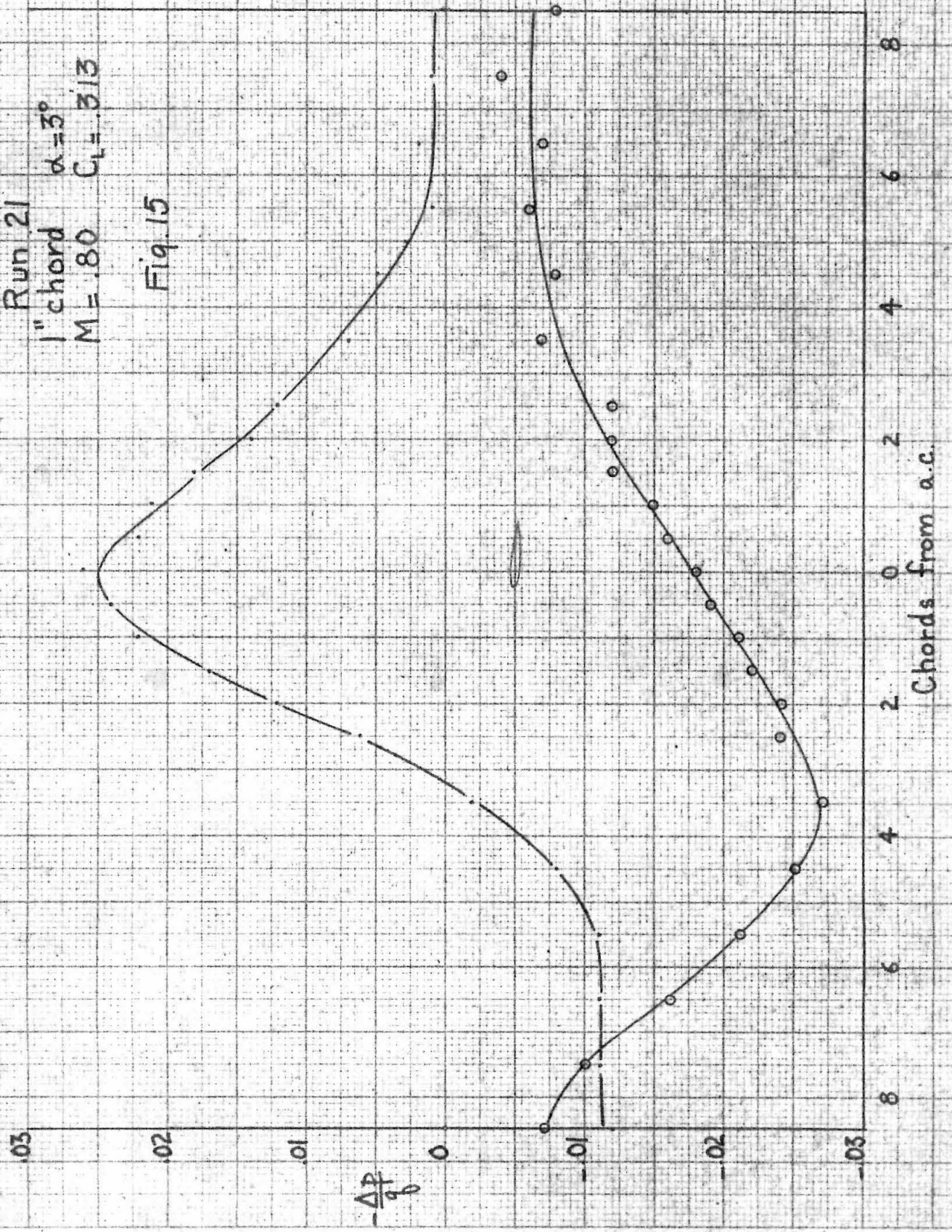


Fig. 16

Run 35
2" chord $\alpha = 1^\circ$
M = .60 $C_L = .079$

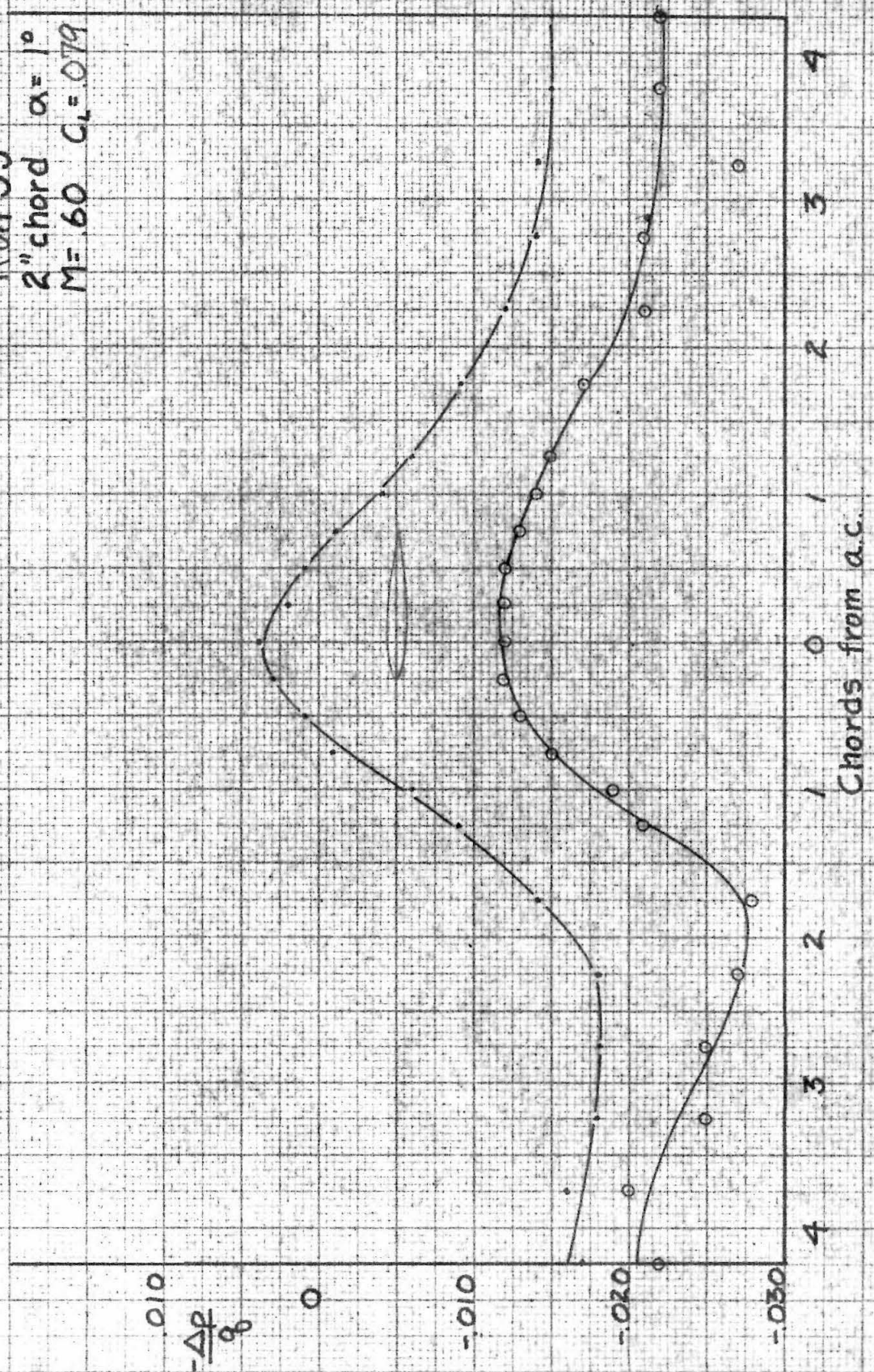


Fig. 17

Run 34
2" chord $\alpha = 1^\circ$
M = .65 $C_L = .085$

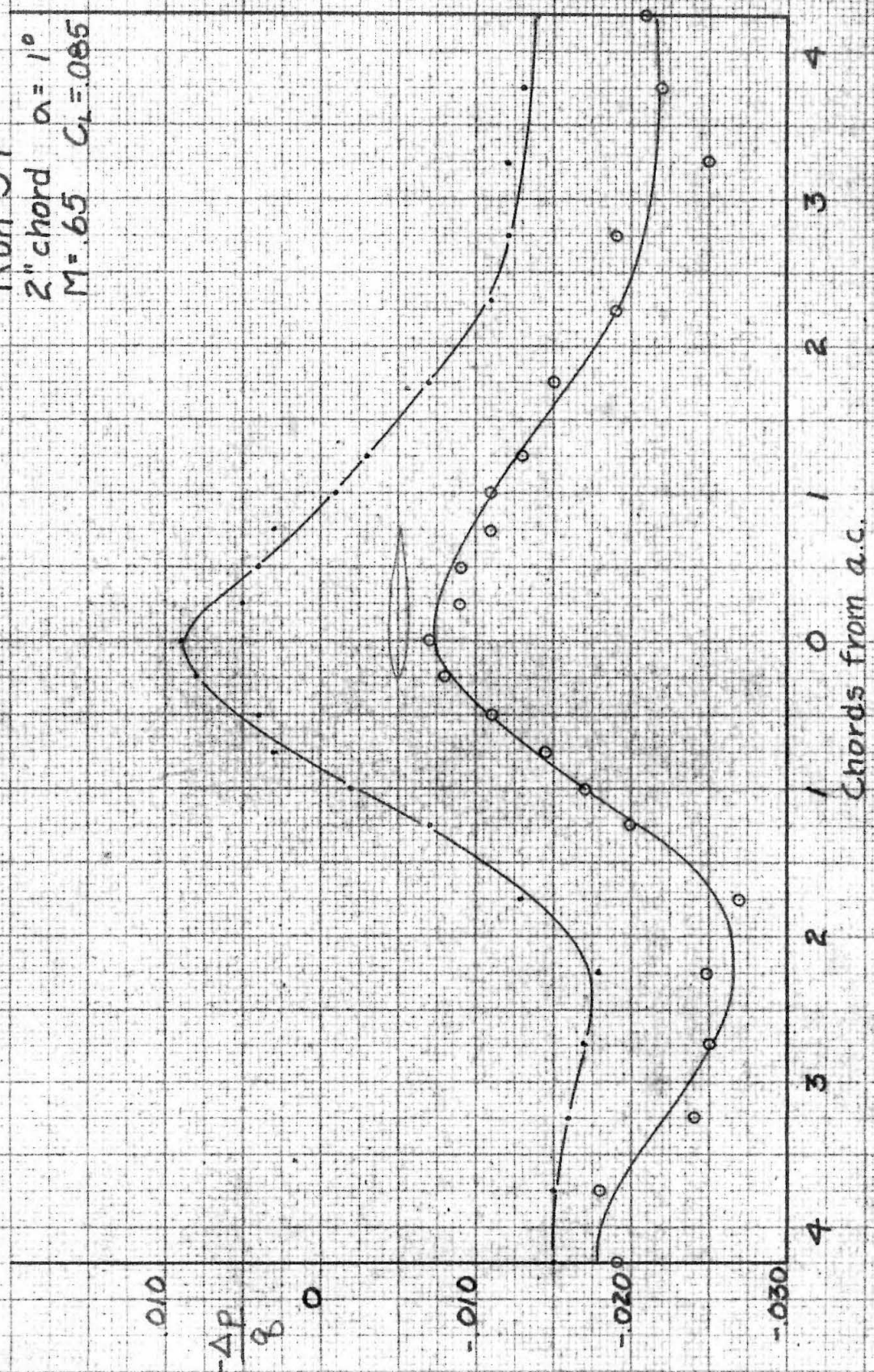


Fig. 18

Run 33
2" chord $\alpha = 1^\circ$
M = .70 $C_L = 0.92$

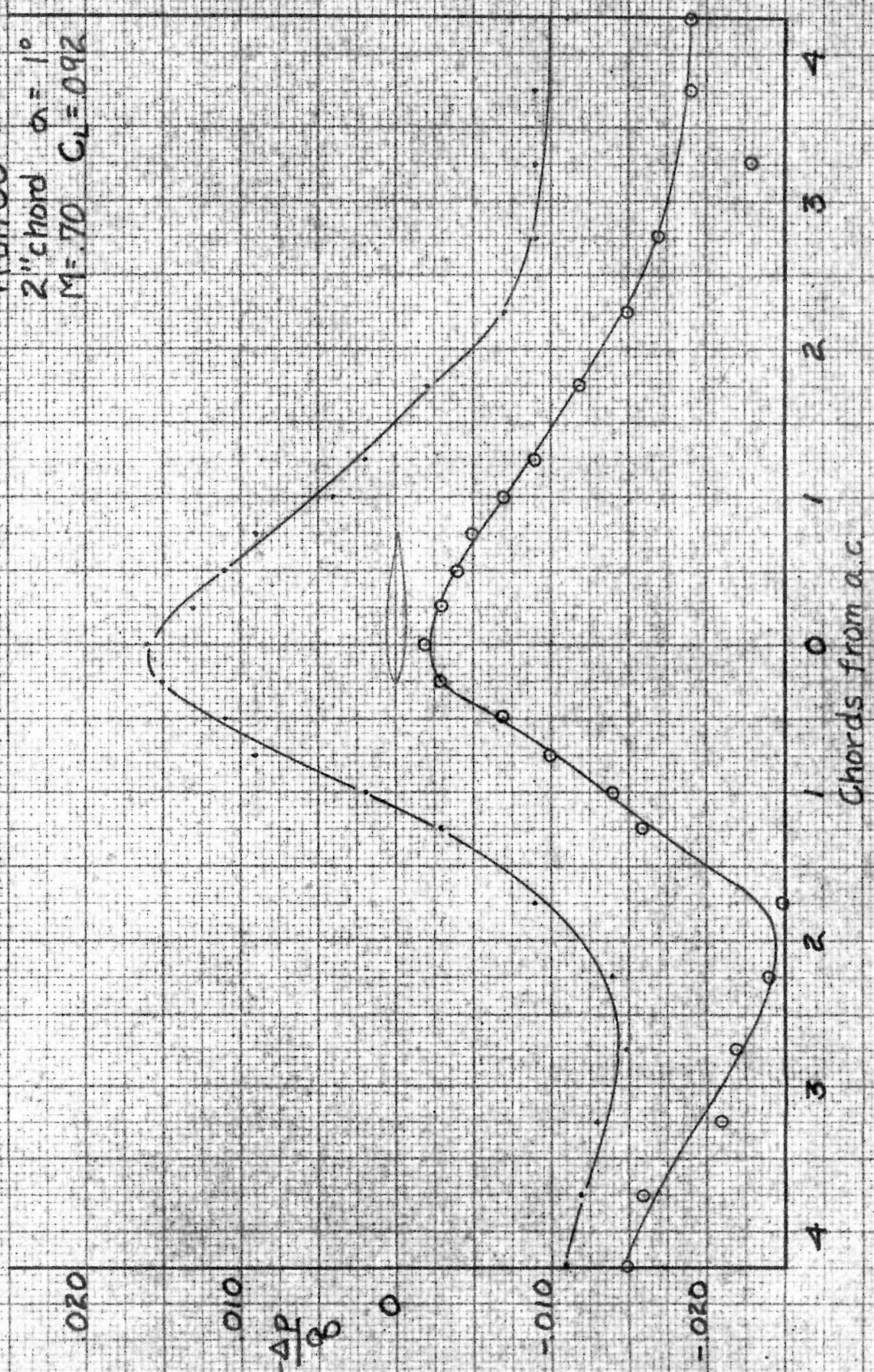


Fig. 19

Run 32
2" chord $\alpha = 1^\circ$
M = 1.75 $C_L = 0.95$

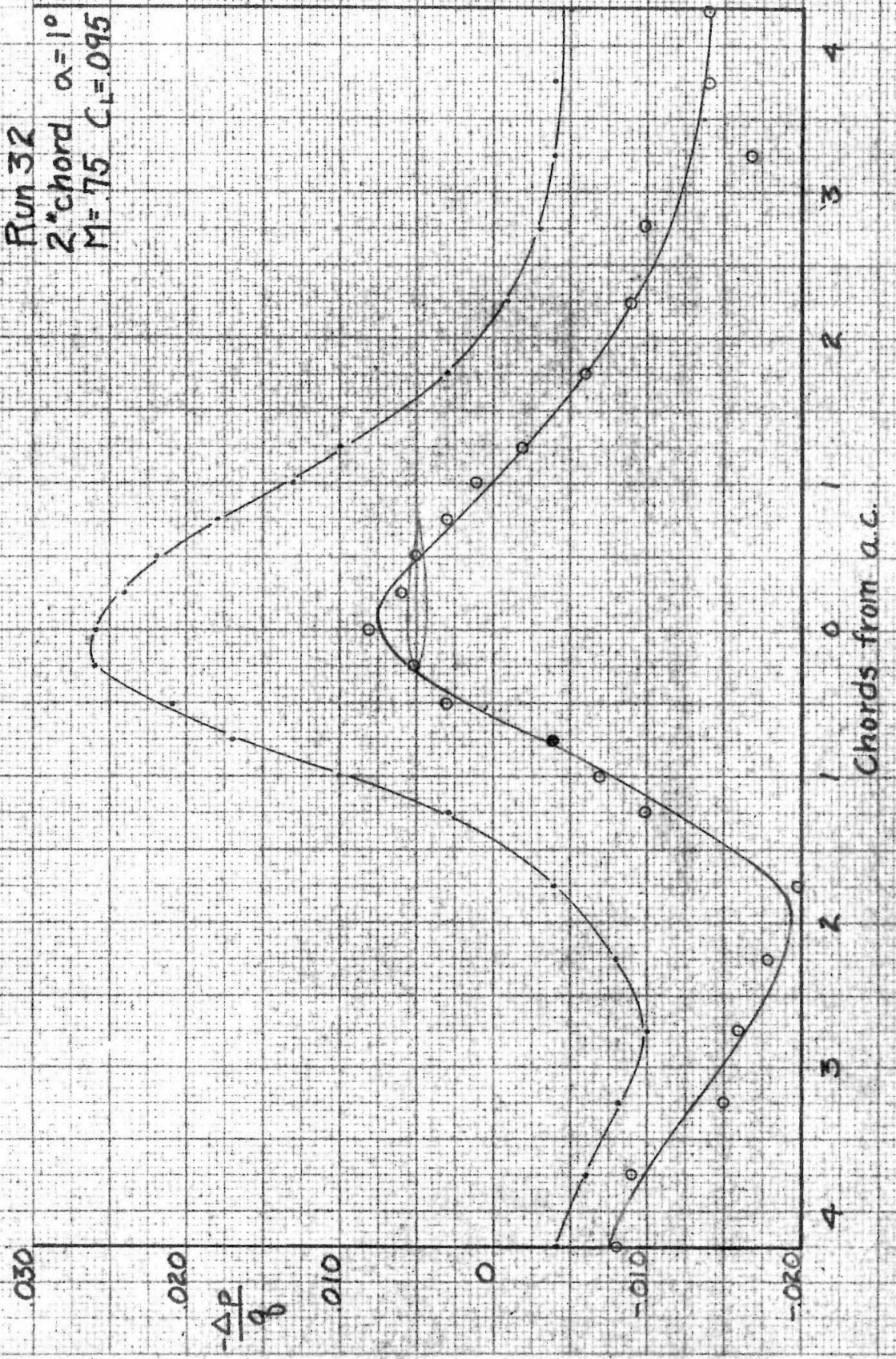


Fig 20

Run 31
2" chord $\alpha = 1^\circ$
M = 80 $C_L = .092$

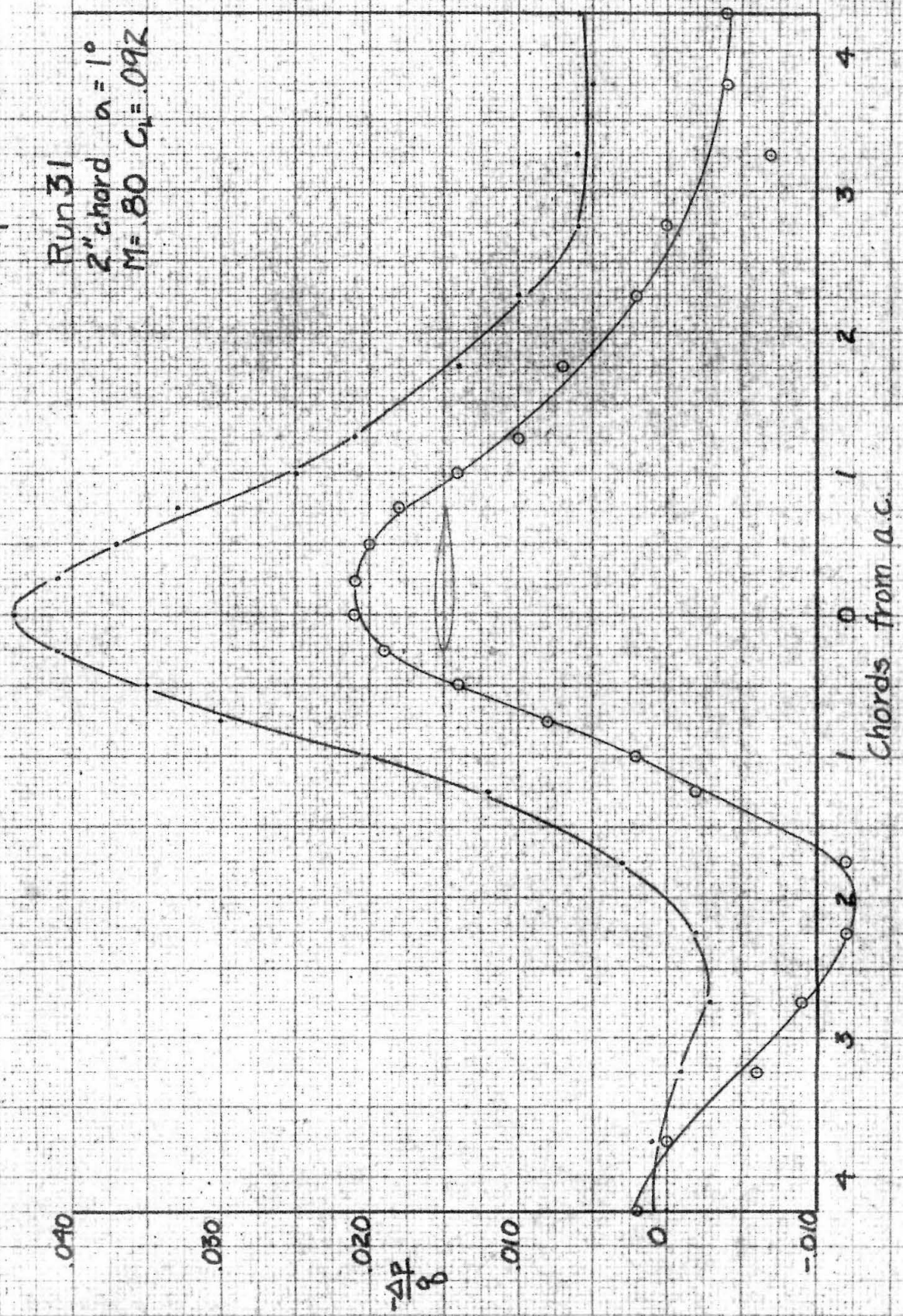


Fig. 21
 Run 40
 2" chord $\alpha = 2^\circ$
 $M = .60$ $C_L = .184$

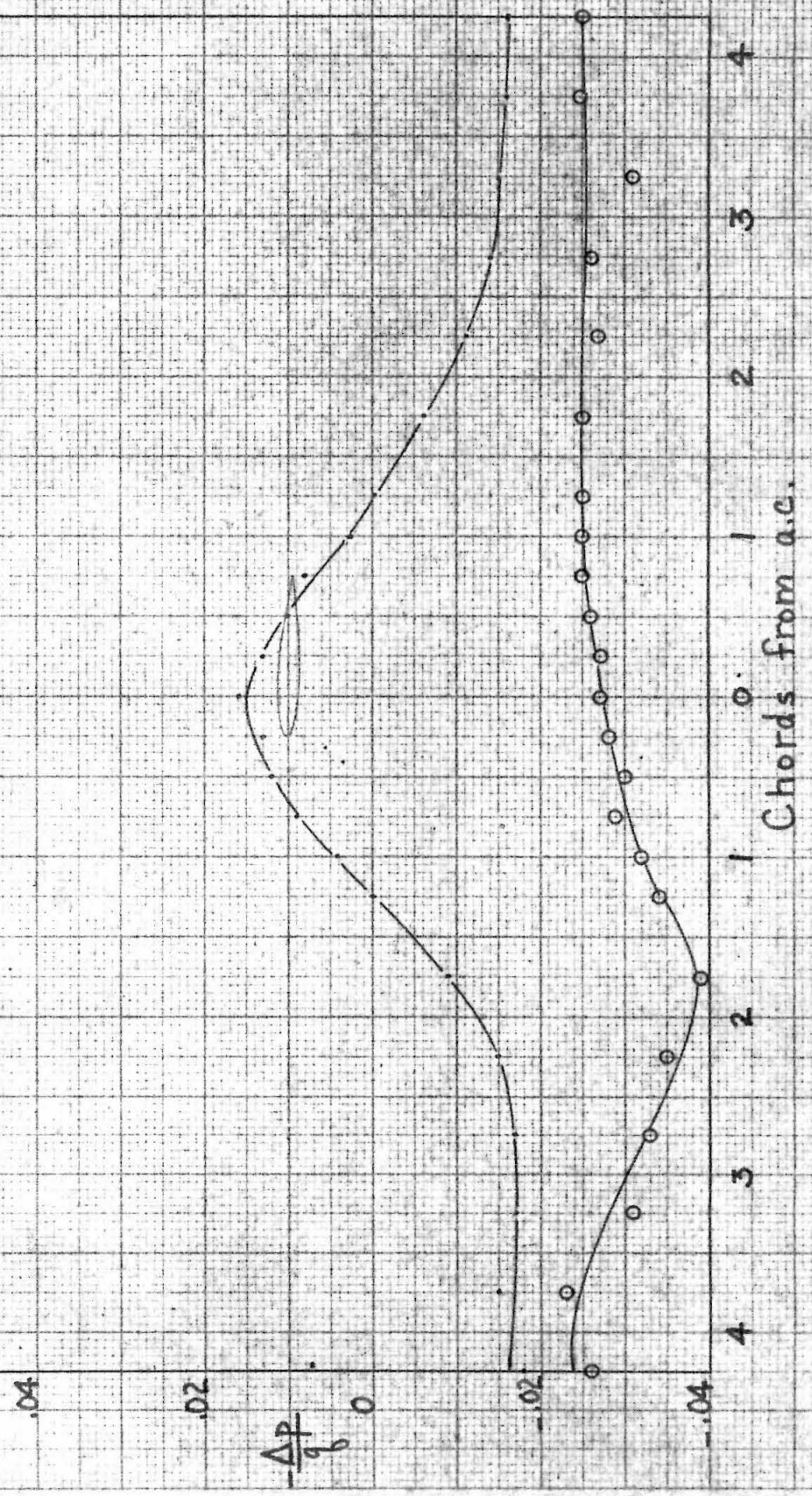


Fig. 22

Run 39
2" chord $\alpha = 2^\circ$
 $M = 65$ $C_L = 1.99$

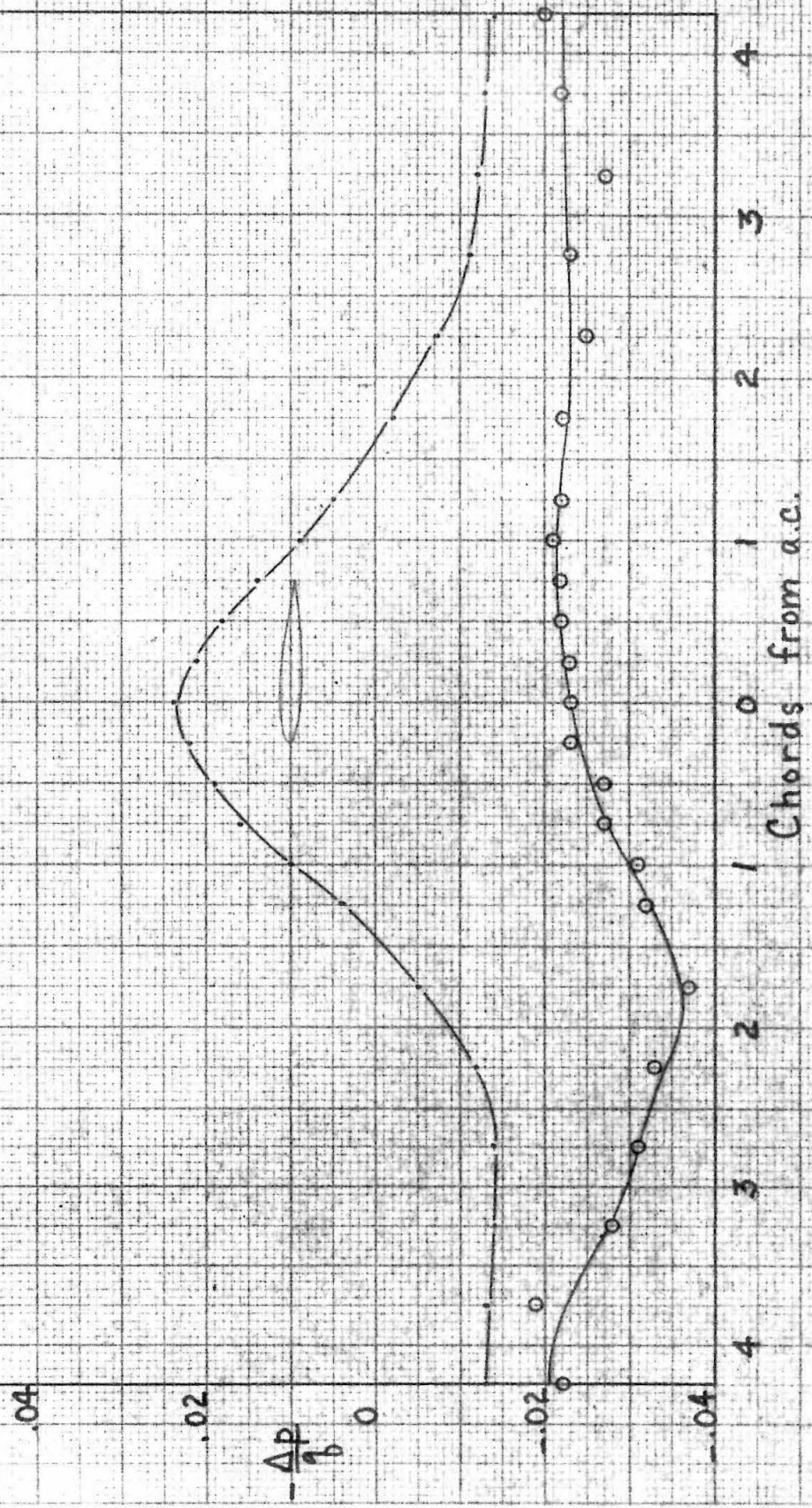


Fig. 23

Run 38

2" chord $\alpha = 2^\circ$

$M = .70$ $C_L = .214$

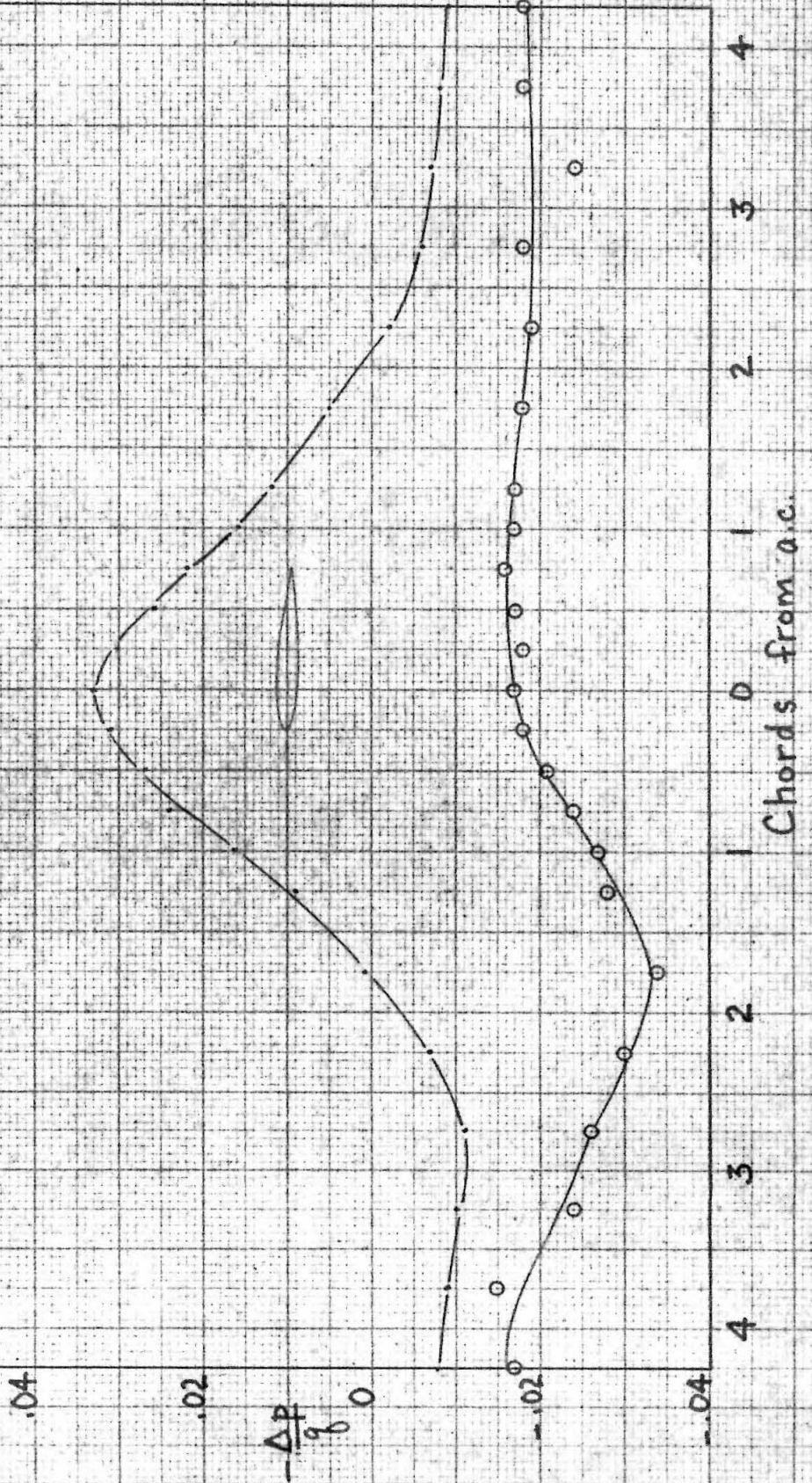


Fig. 24

Run 37
2" chord $\alpha = 2^\circ$
 $M = .75$ $C_L = .222$

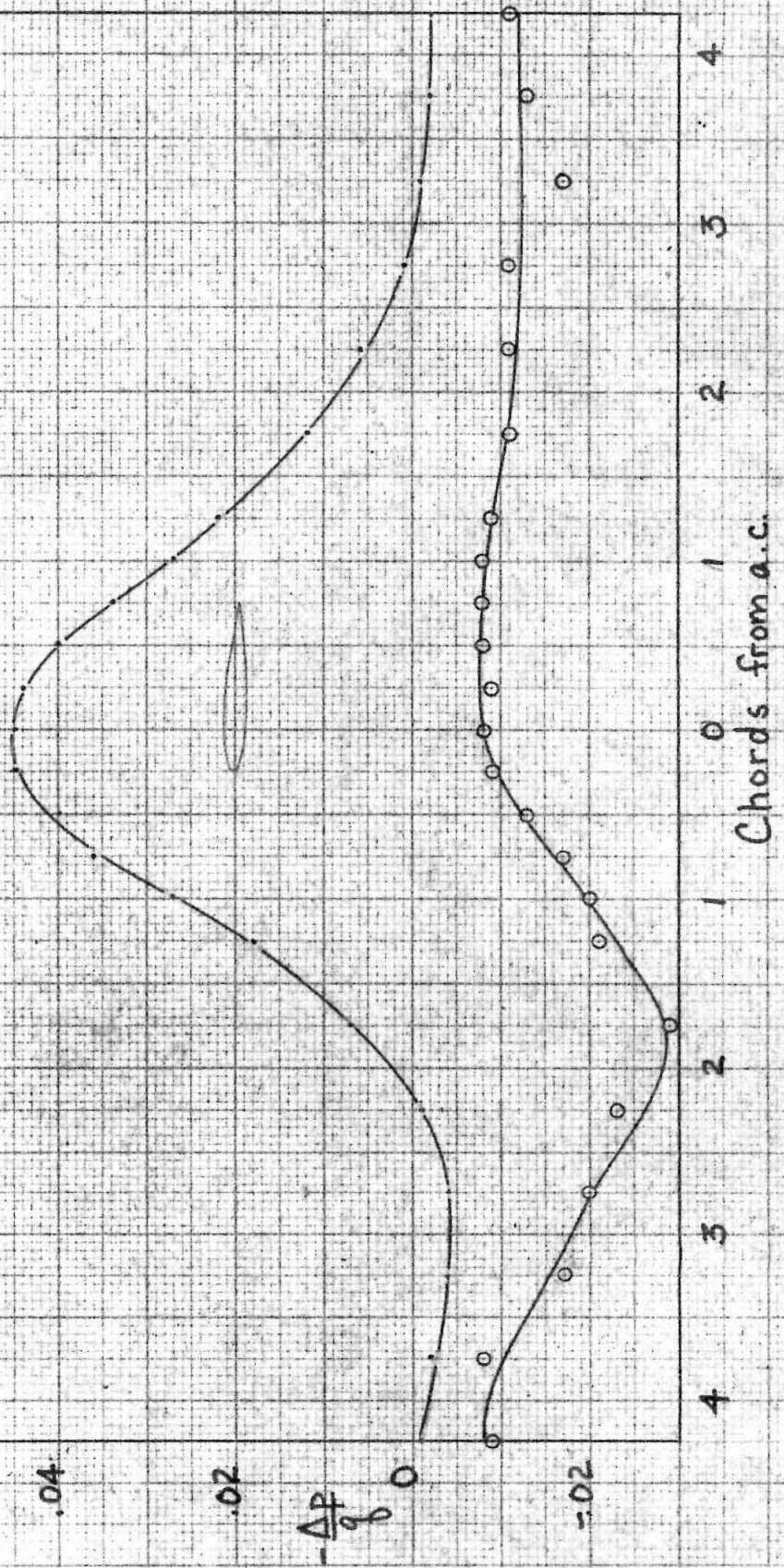


Fig. 25

Run 36
2" chord $\alpha = 2^\circ$
M = .80 $C_L = .230$

.08

.06

.04

$\frac{\Delta p}{\rho}$

.02

0

-.02

4

3

2

1

0

1

2

3

4

Chords from a.c.

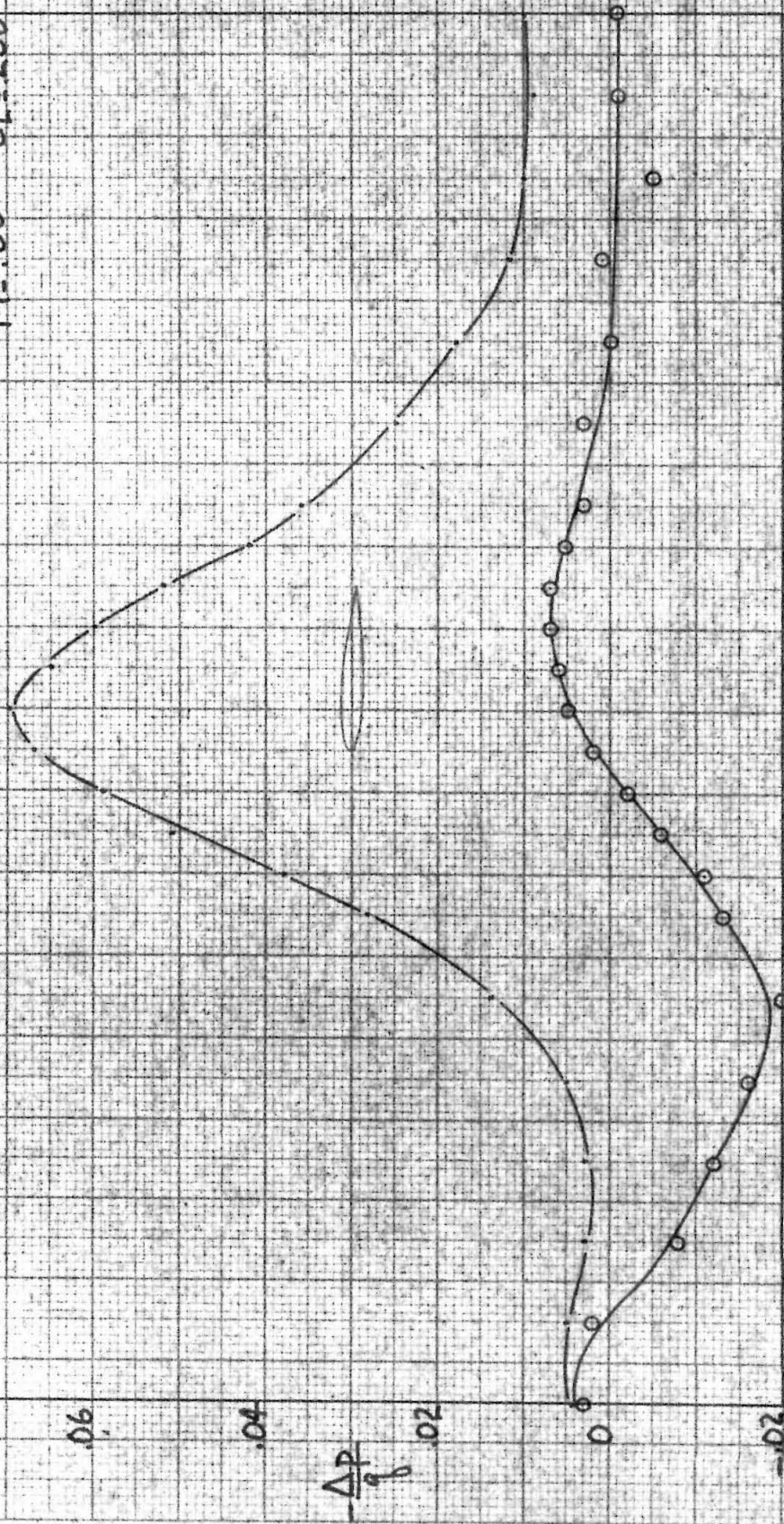


Fig. 26

Run 45
2" chord $\alpha = 3^\circ$
M = 6.0 $C_L = .338$

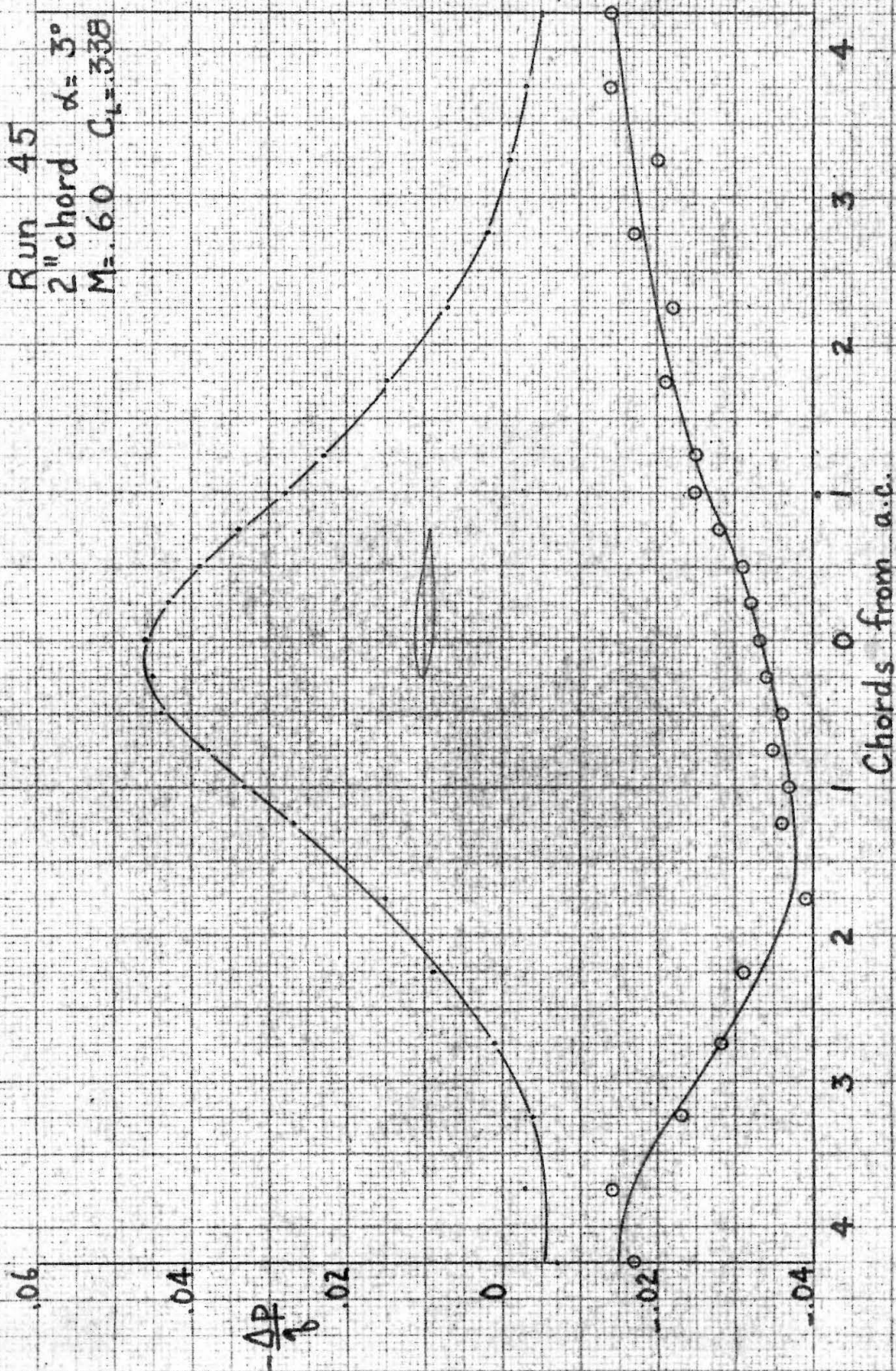


Fig. 27

Run 44

2" chord $\alpha = 3^\circ$

$M = .65$ $C_L = .357$

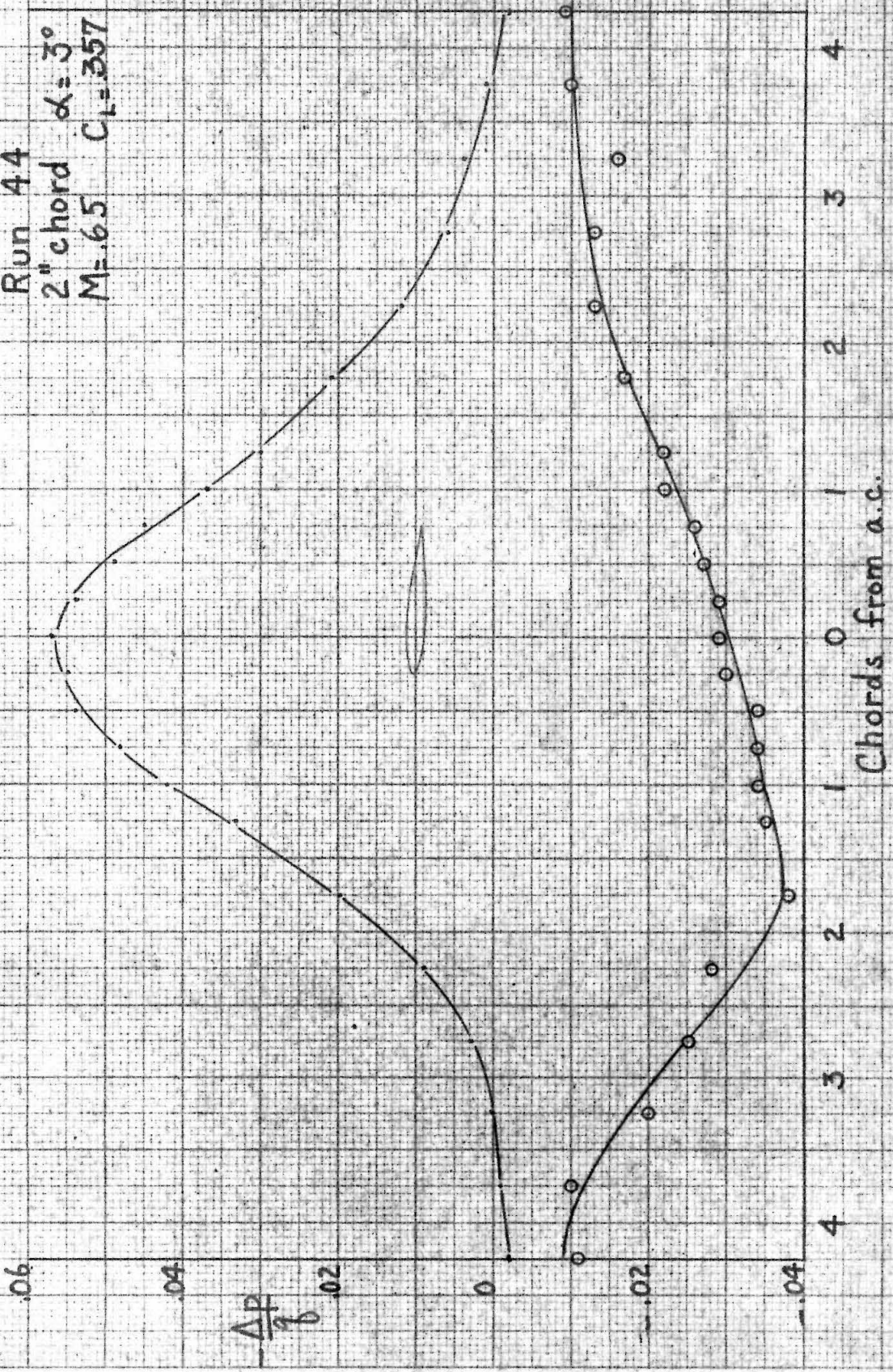


Fig. 28

Run 43
2" chord $\alpha = 3^\circ$
M=70 $C_L = .384$

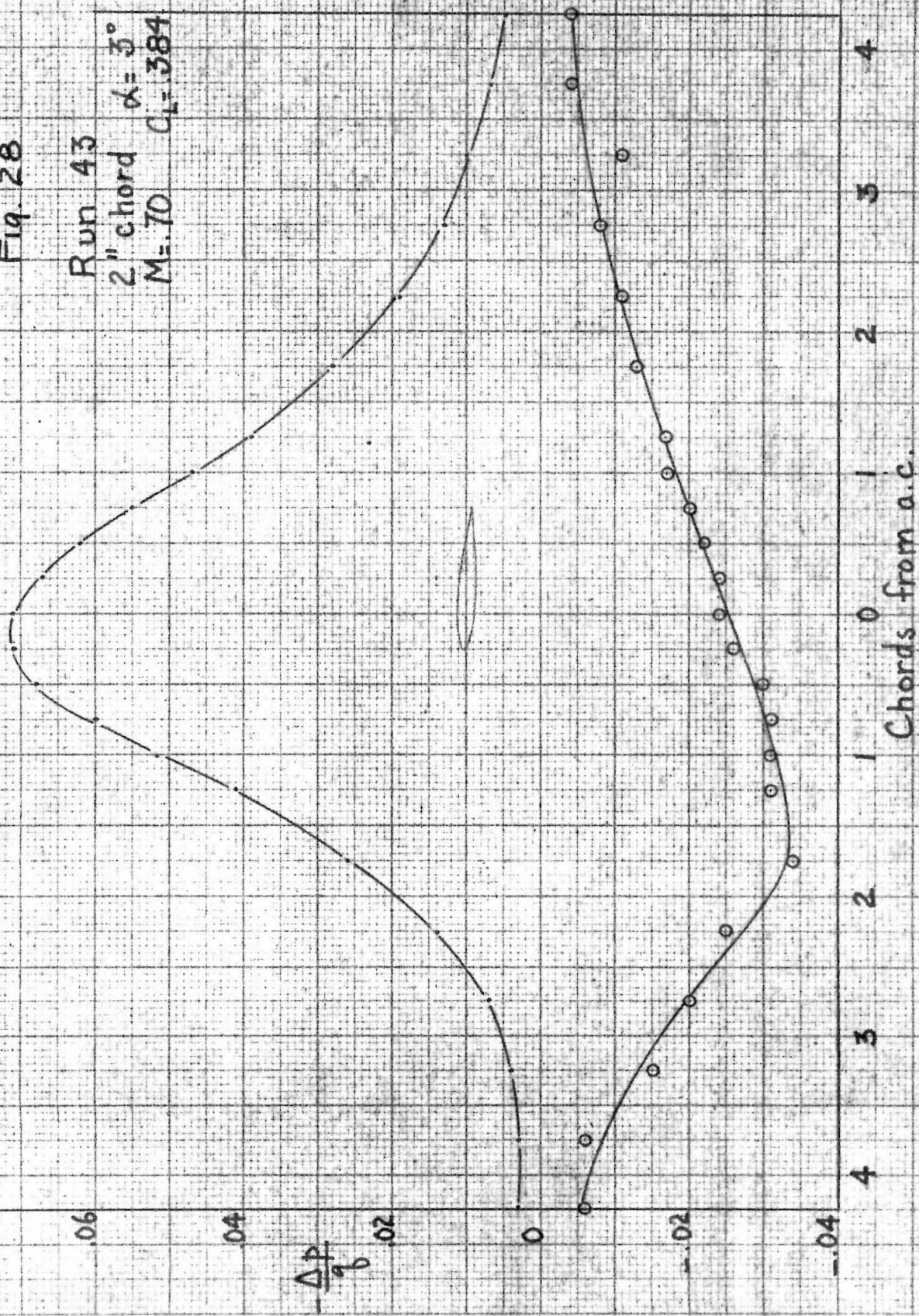


Fig. 29

Run 42
2" chord $\alpha = 3^\circ$
 $M = .75$ $C_L = .404$

.12

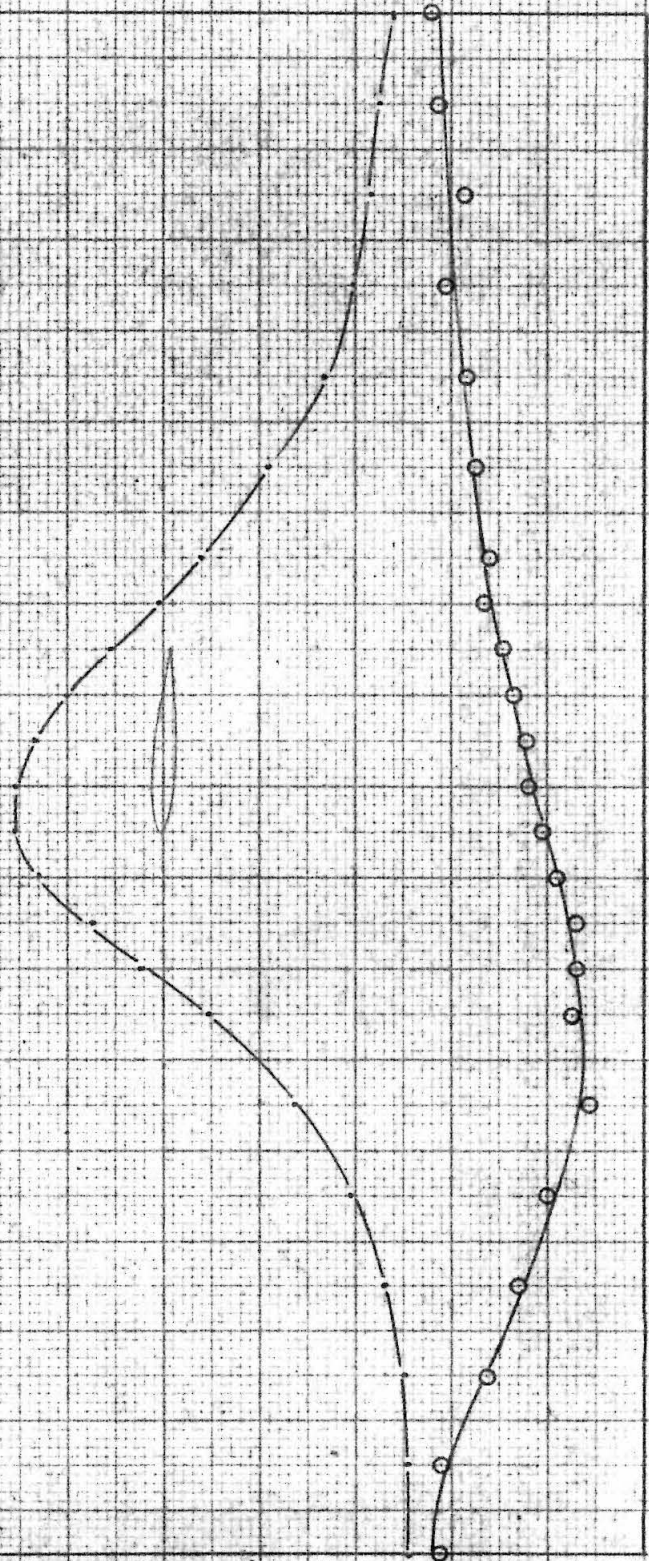
.08

.04

0

-.04

$\frac{\Delta p}{\rho}$



4 3 2 1 0 1 2 3 4

Chords from a.e.

Fig. 30

Run 41
2" chord $\alpha = 3^\circ$
M = .80 $C_L = .386$

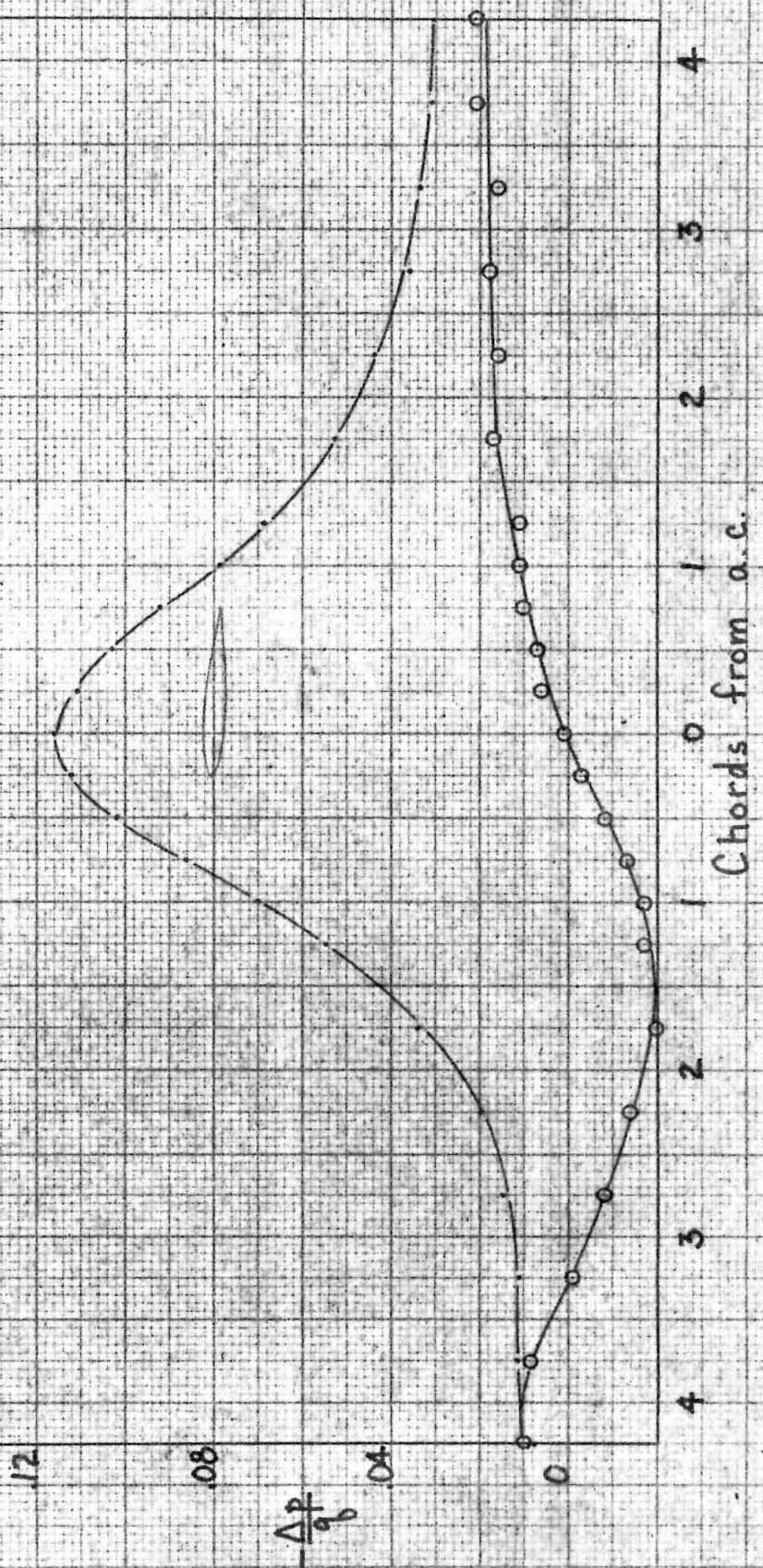
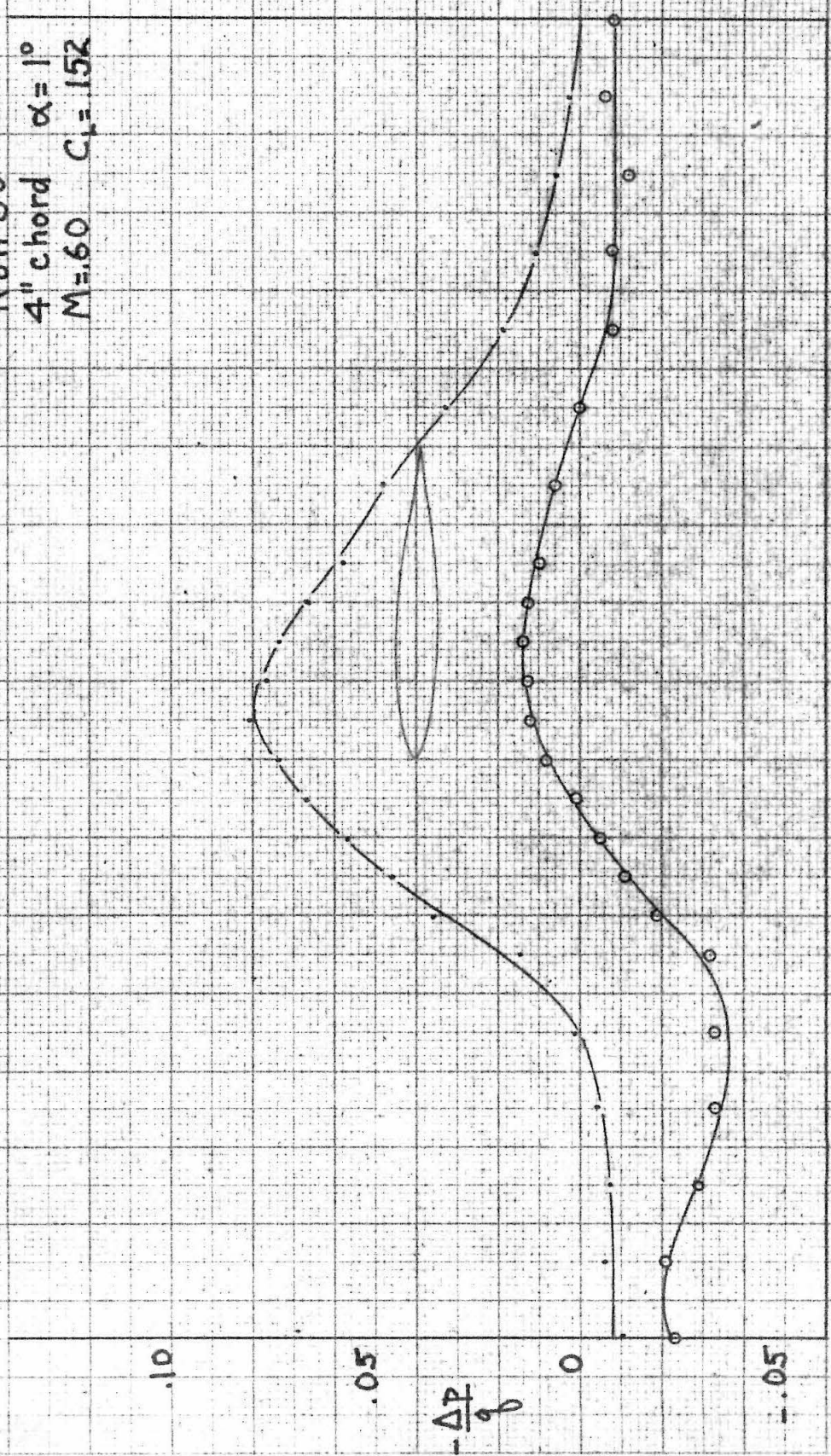


Fig. 31

Run 30
4" chord $\alpha = 1^\circ$
M=60 $C_L = 152$



Chords from a.e.

Fig. 32

Run 29
4" chord $\alpha = 1^\circ$
M = 65 $C_L = .161$

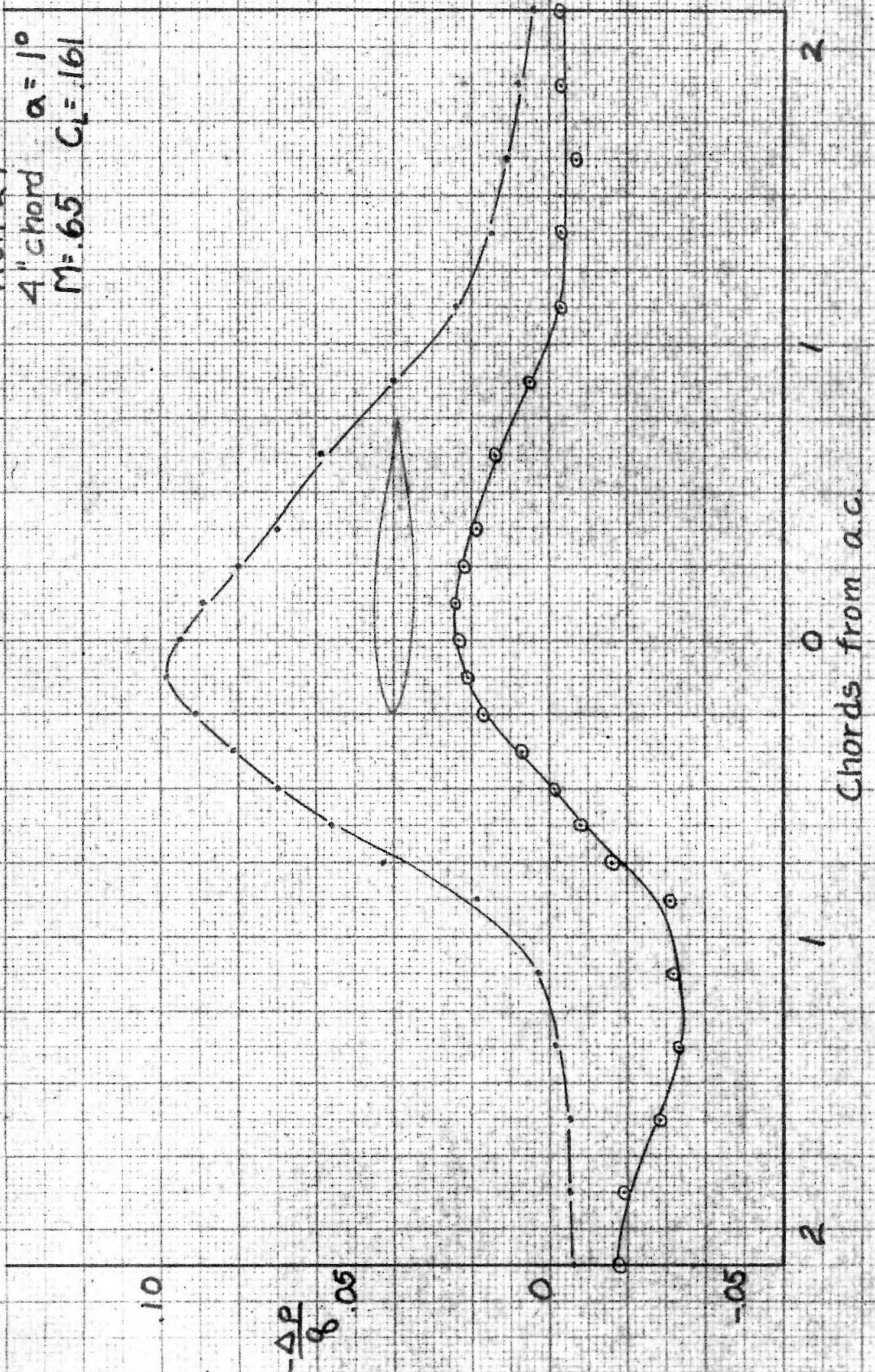
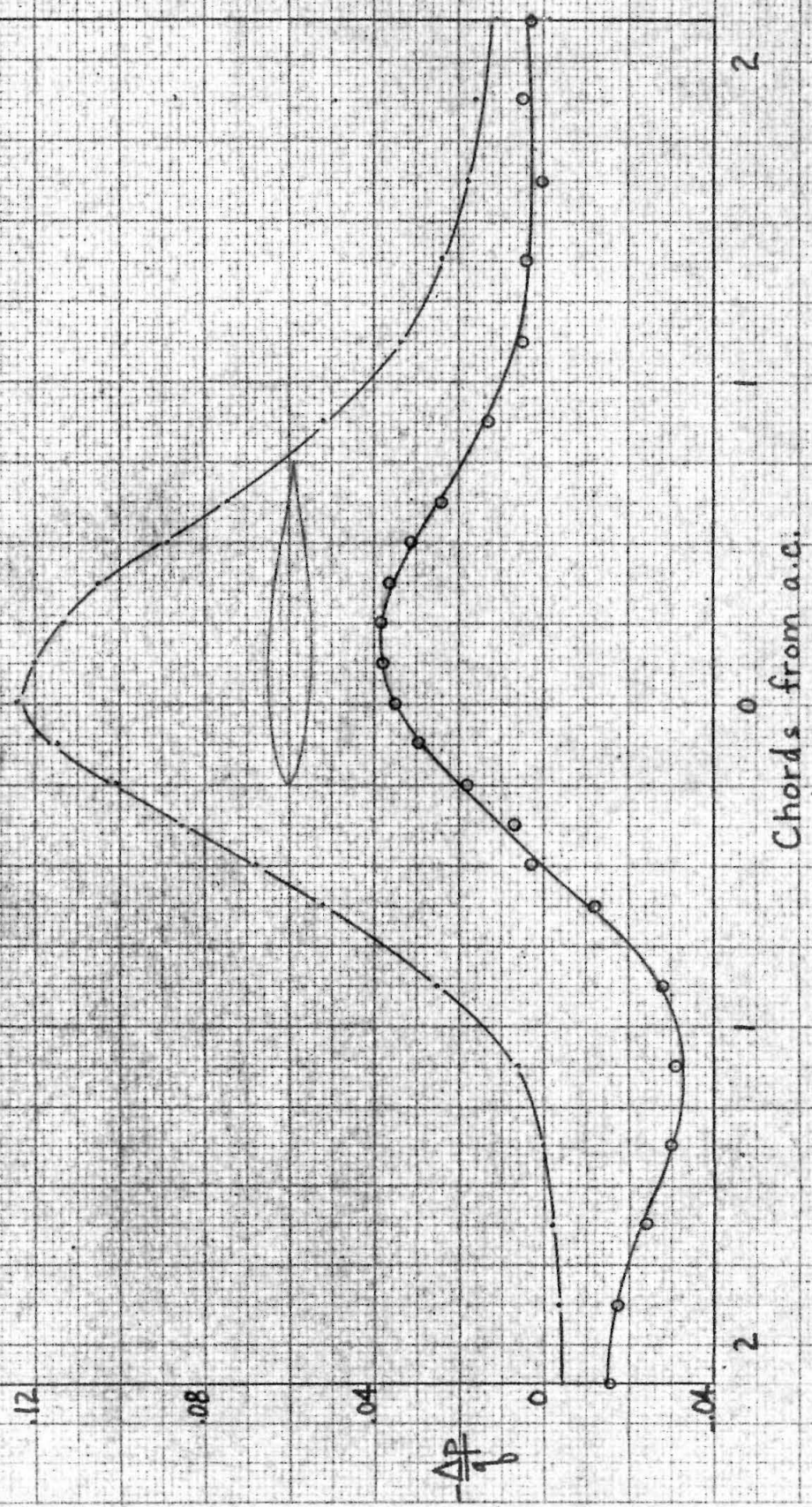


Fig. 33

Run 28
4" chord, $\alpha = 1^\circ$
 $M = .70$, $C_L = .176$

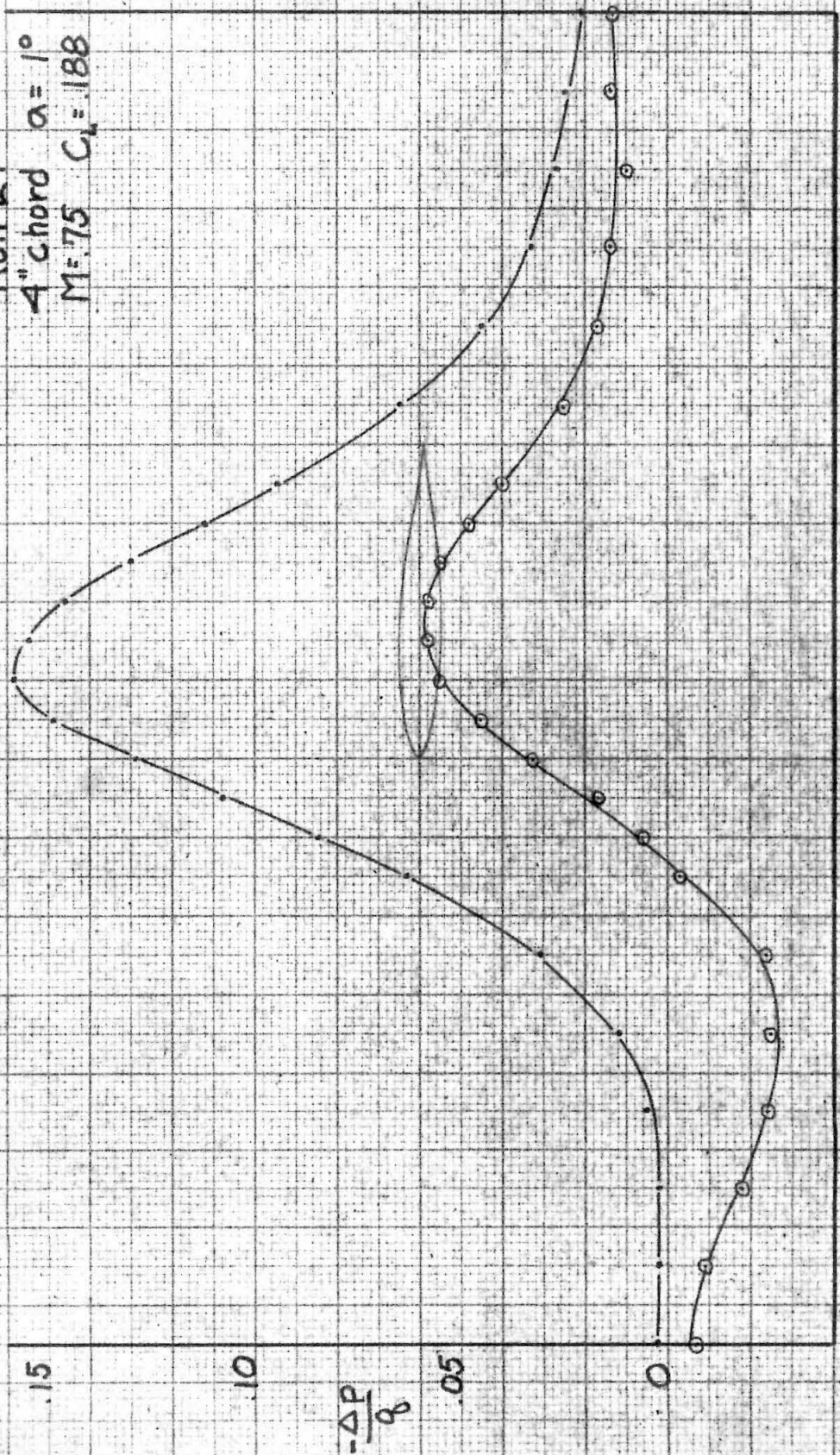


2

2

Fig 34.

Run 27
4" chord $\alpha = 1^\circ$
M:75 $C_L = .188$



2

1

0

1

2

Chords from a.c.

Fig. 35

Run 26
4" chord $\alpha = 1^\circ$
M=80 $C_c = .209$

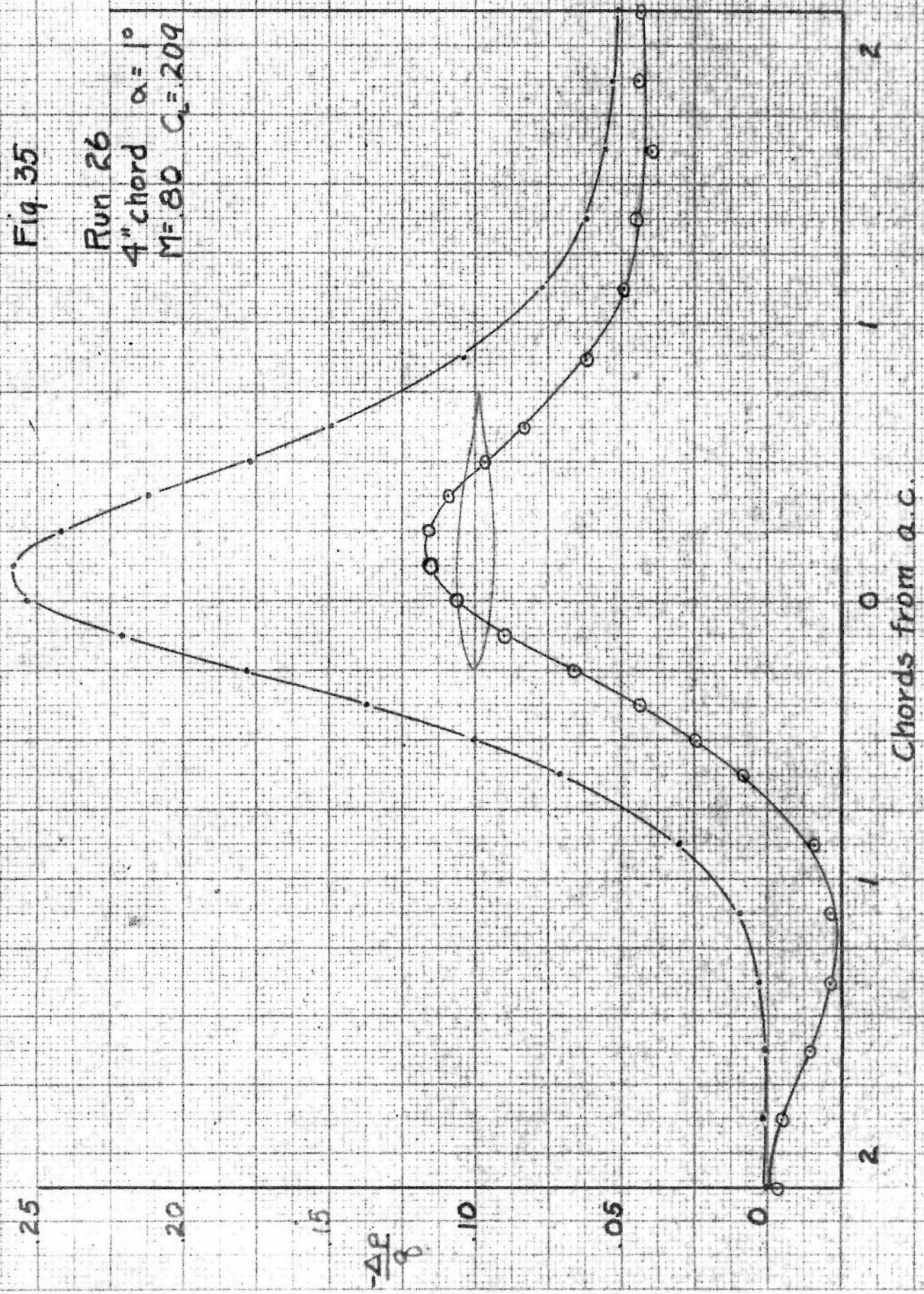


Fig. 36

Run 50
4" chord $\alpha = 2^\circ$
M = 60 $C_L = 242$

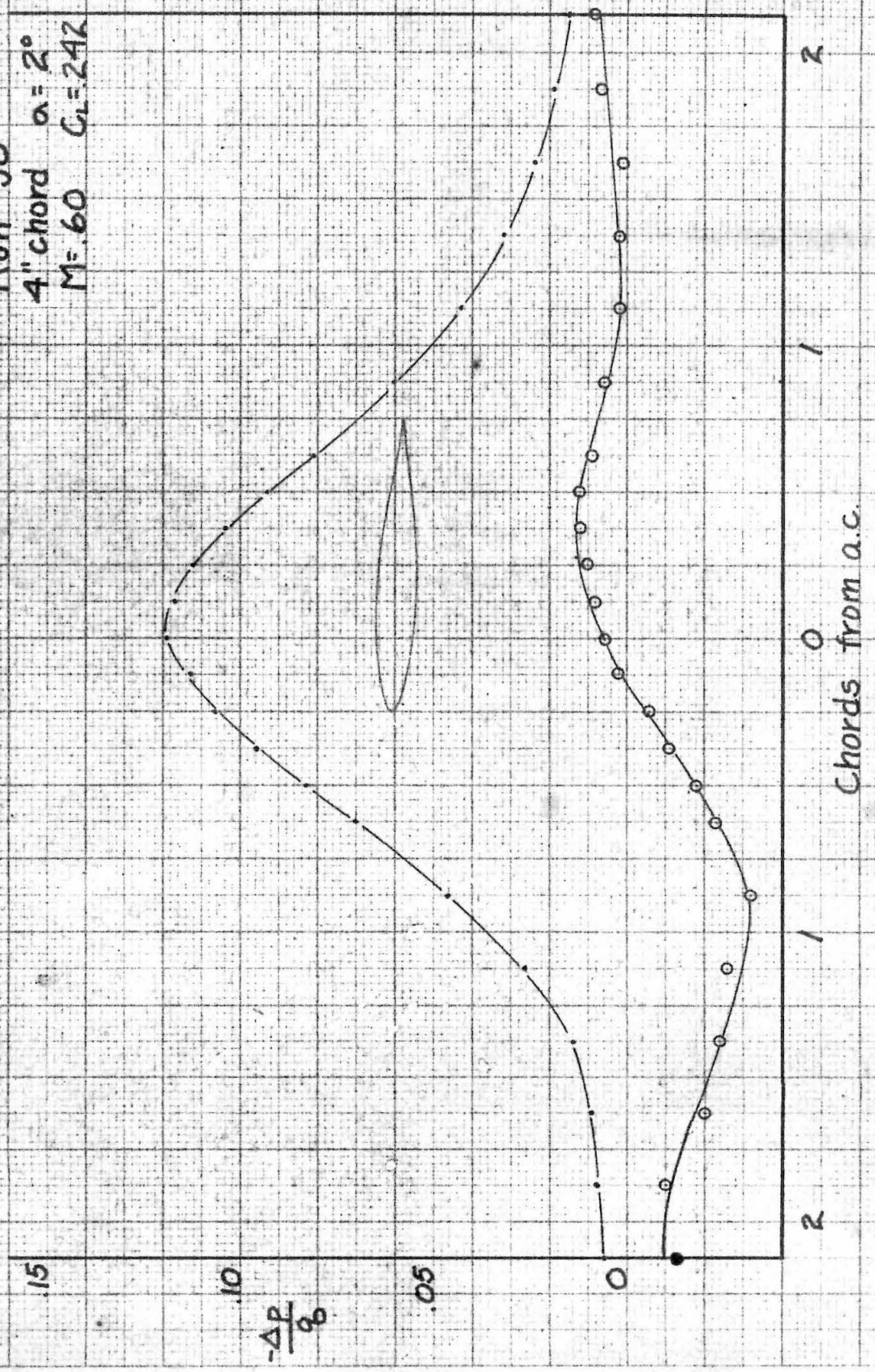
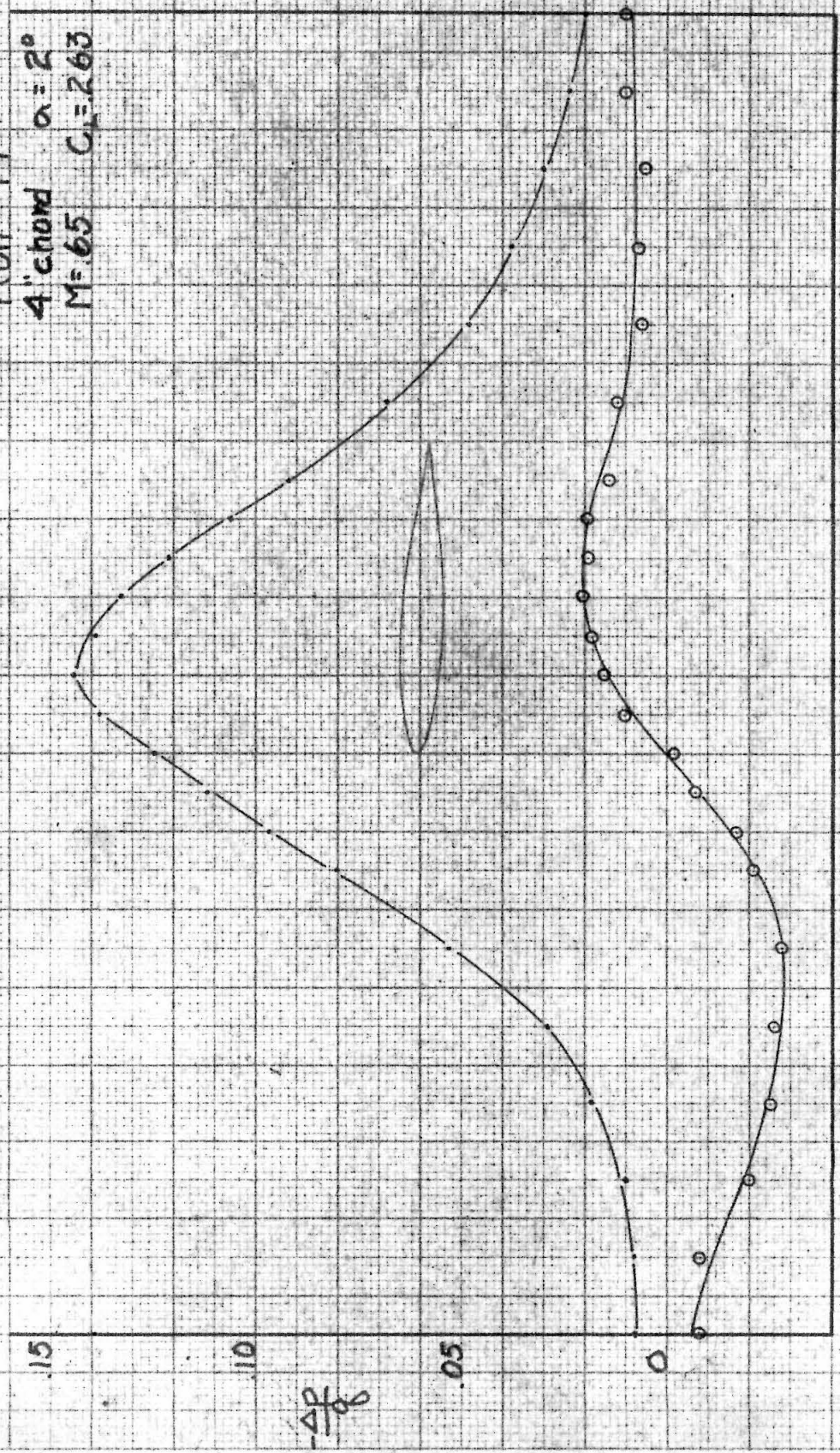


Fig 37

Run 49
4' chord $\alpha = 2^\circ$
M = 65 $C_L = 2.63$



Chords from a.c.

Fig. 38

Run 48
4" chord $\alpha = 2^\circ$
M = 70 $C_L = 2.83$

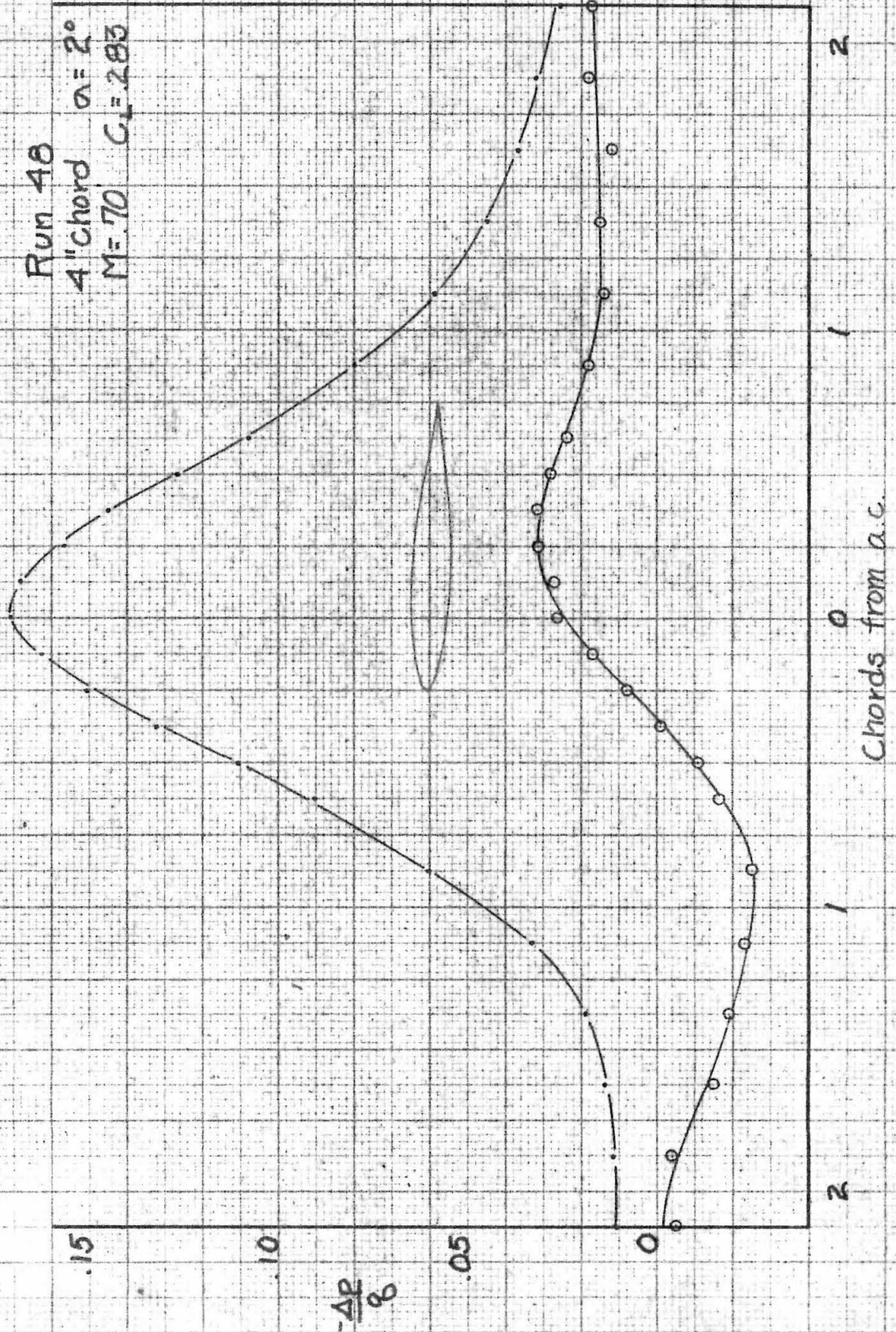
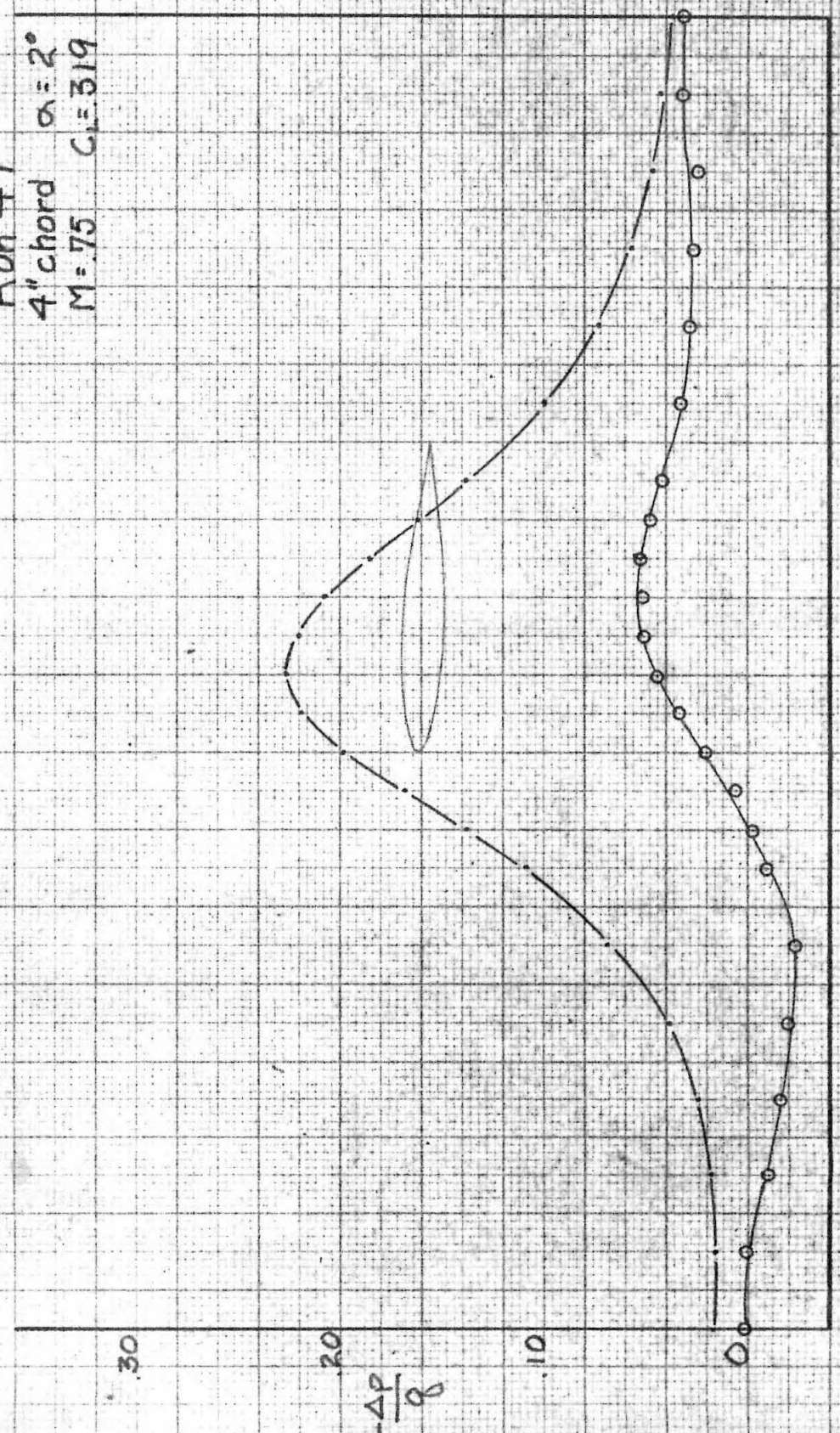


Fig. 39

Run 47

4" chord $\alpha = 2^\circ$

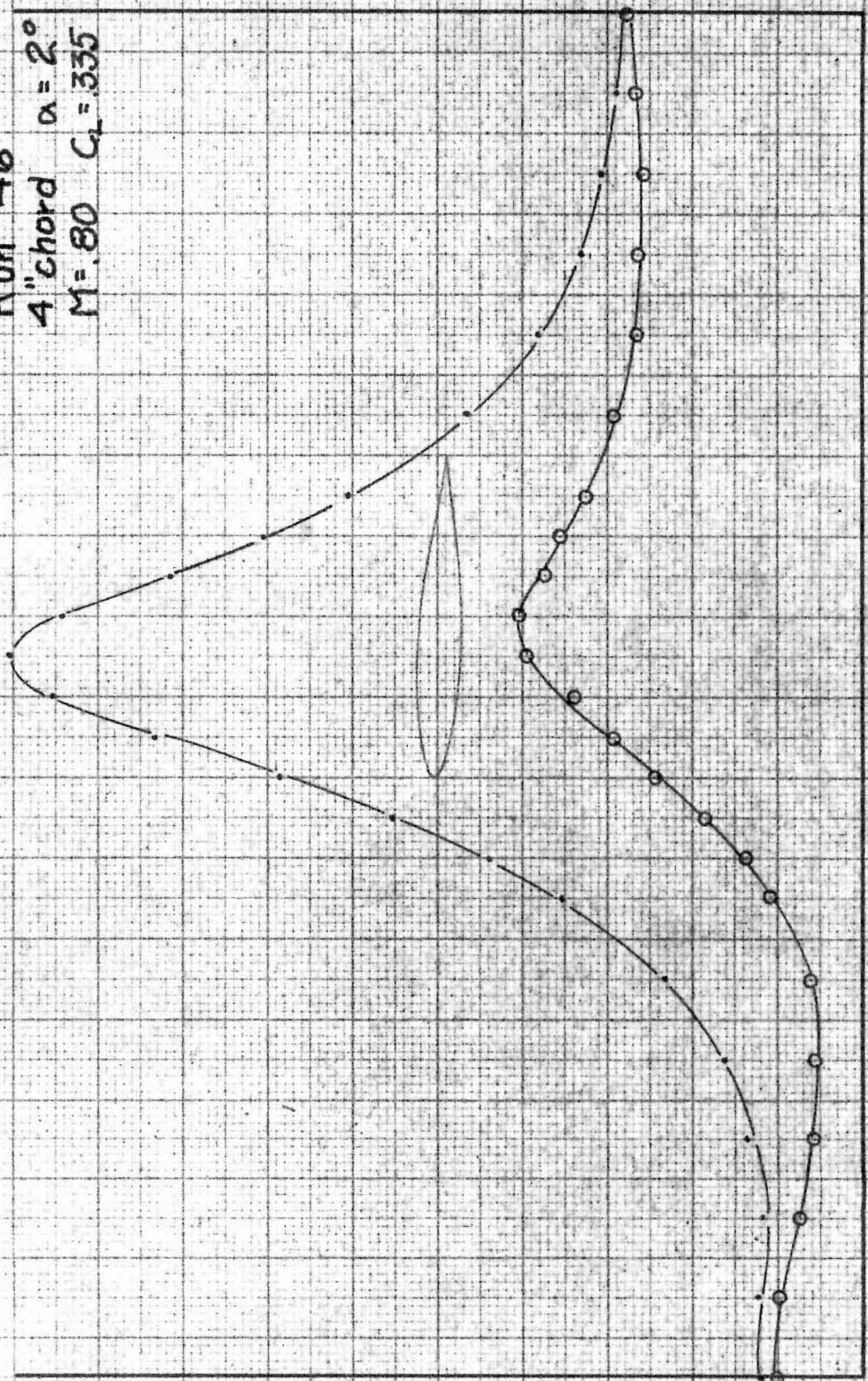
M = 75 C_r = 319



Chords from ac.

Fig. 40

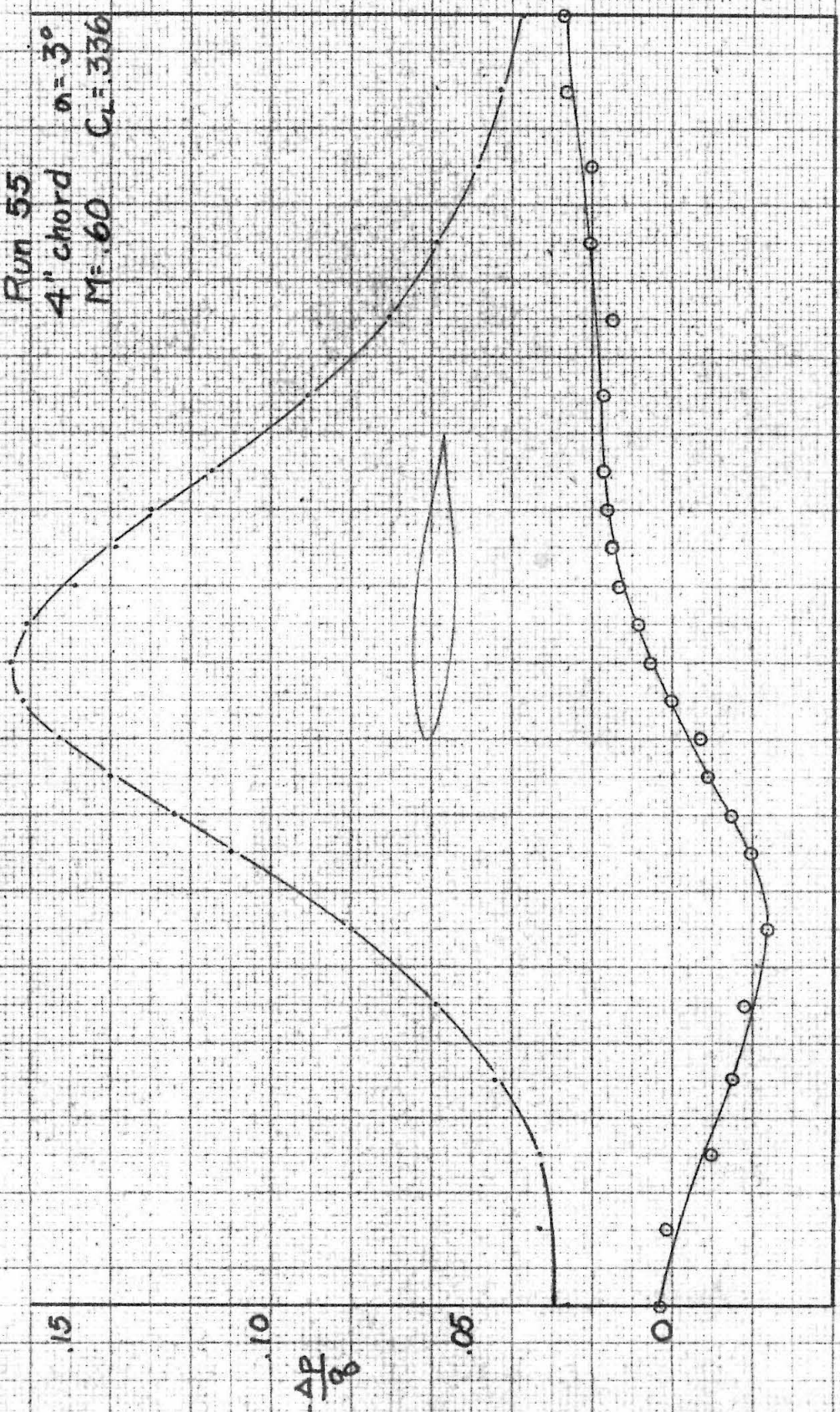
Run 46
4" chord $\alpha = 2^\circ$
M = .80 $C_L = .335$



Chords from a.c.

Fig. 41

Run 55
4" chord $\alpha = 3^\circ$
M: 60 $C_L = 336$



2

1

0

1

2

Chords from a.c.

Fig. 42

Run 54
4' chord $\alpha = 3^\circ$
M = 65 C.L. 379

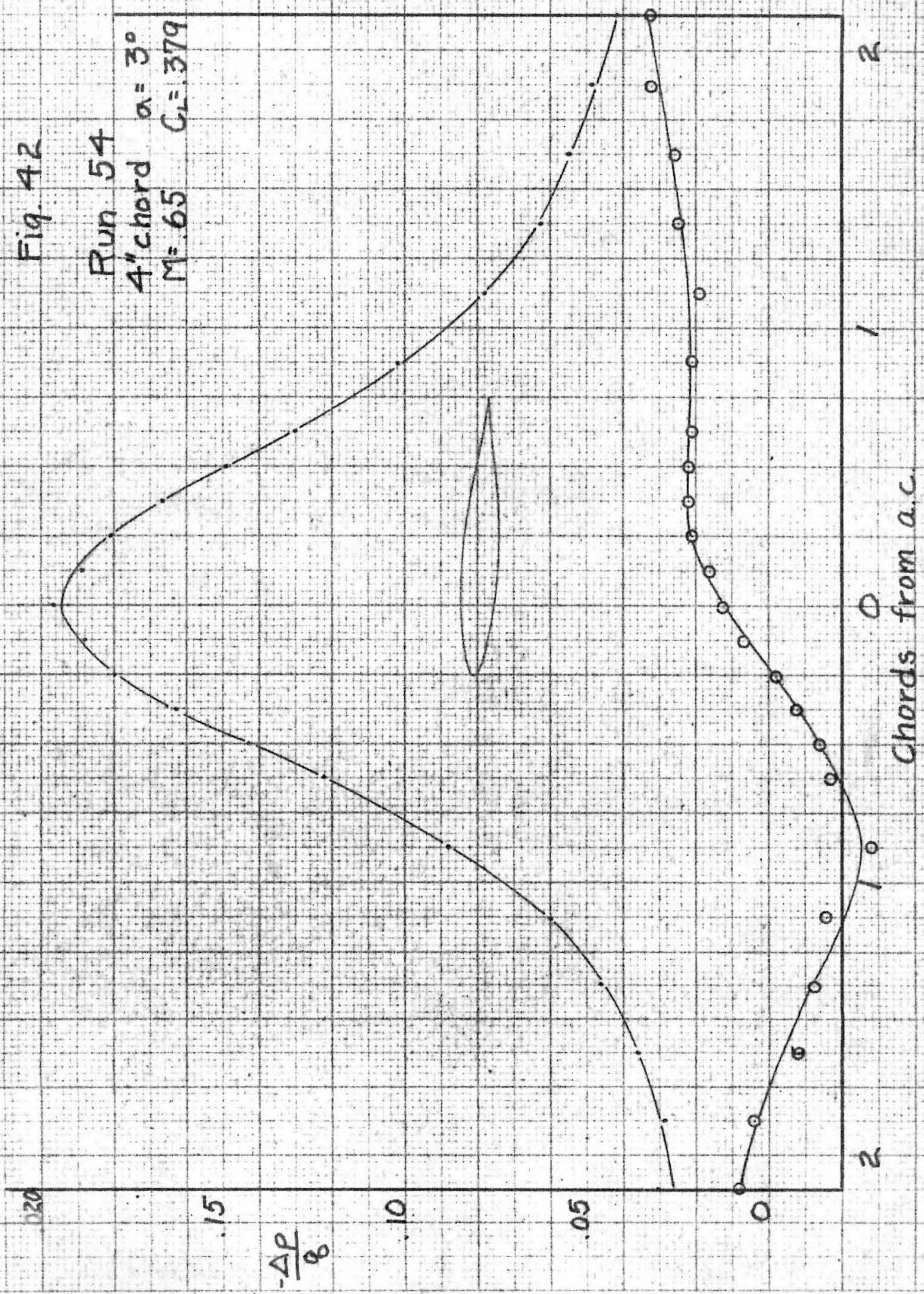


Fig 43

Run 53
4" chord $\alpha = 3^\circ$
M = 70 $C_L = 402$

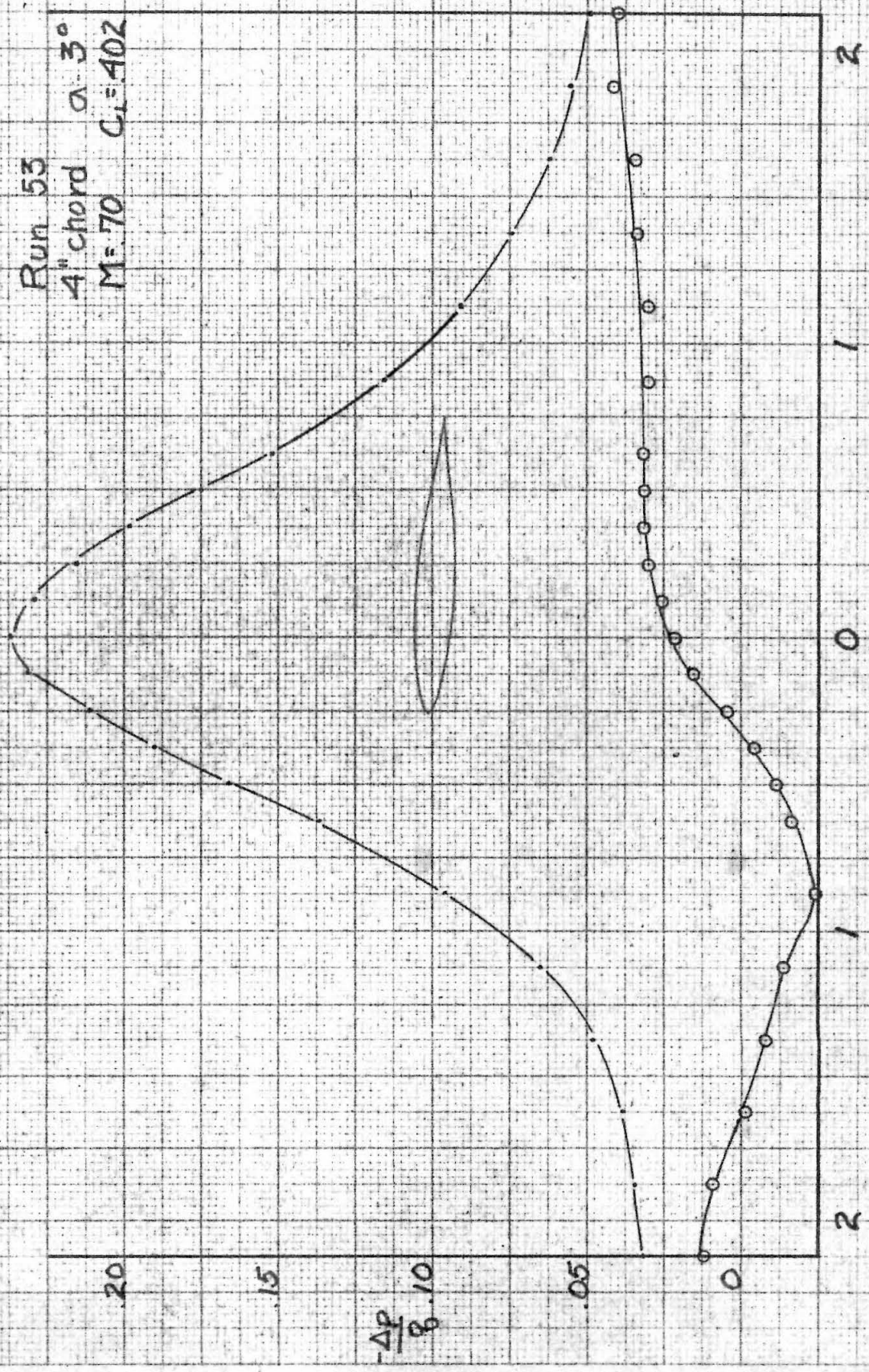


Fig. 44

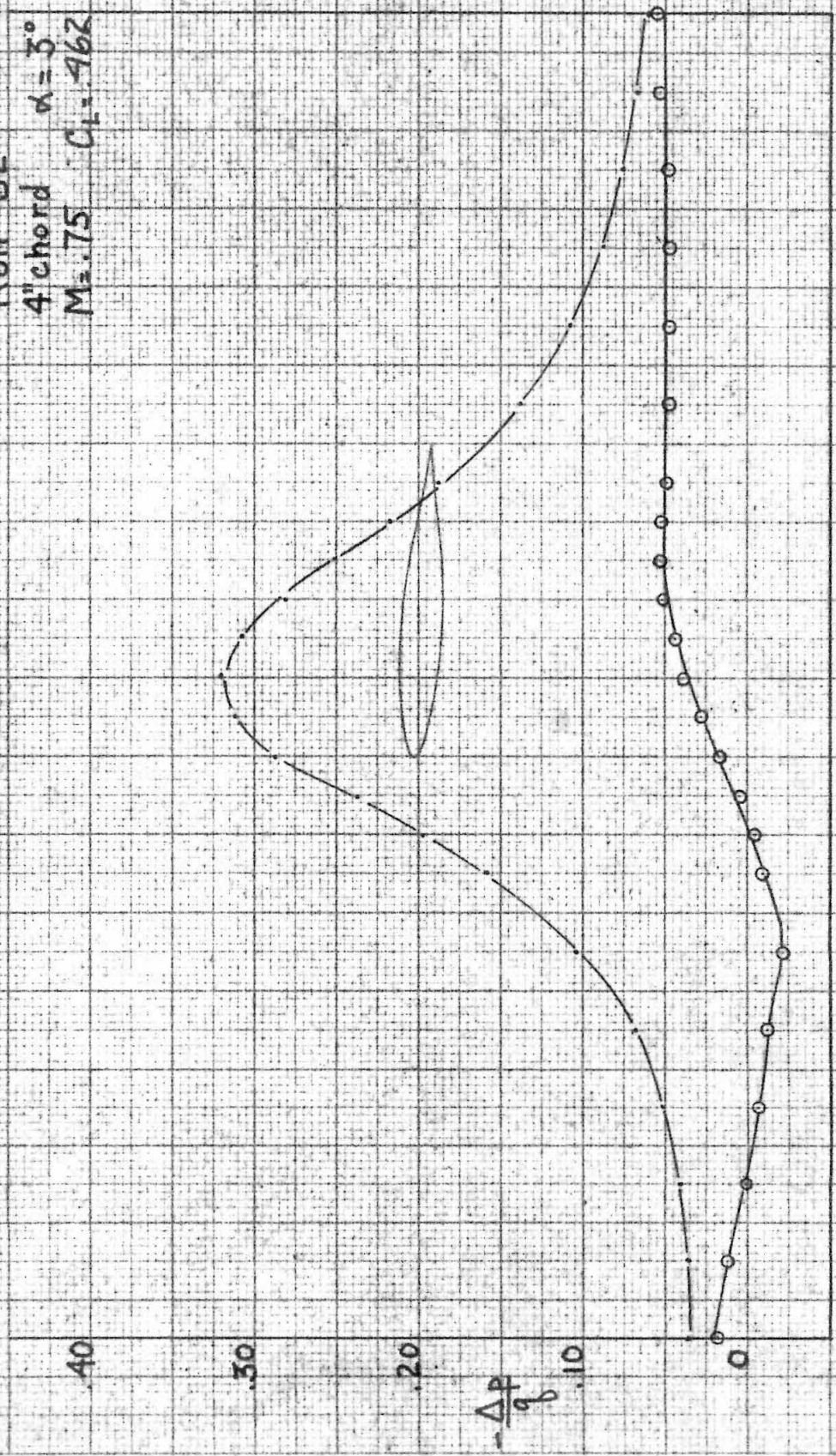
Run 52

4' chord

$\alpha = 3^\circ$

$M = .75$

$C_L = .962$



Chords from a.c.

Fig 45

Run 51
4" chord $\alpha = 3^\circ$
M=80 $C_L = 441$

$\frac{\Delta P}{8}$

2

1

0

2

Chords from a.c.

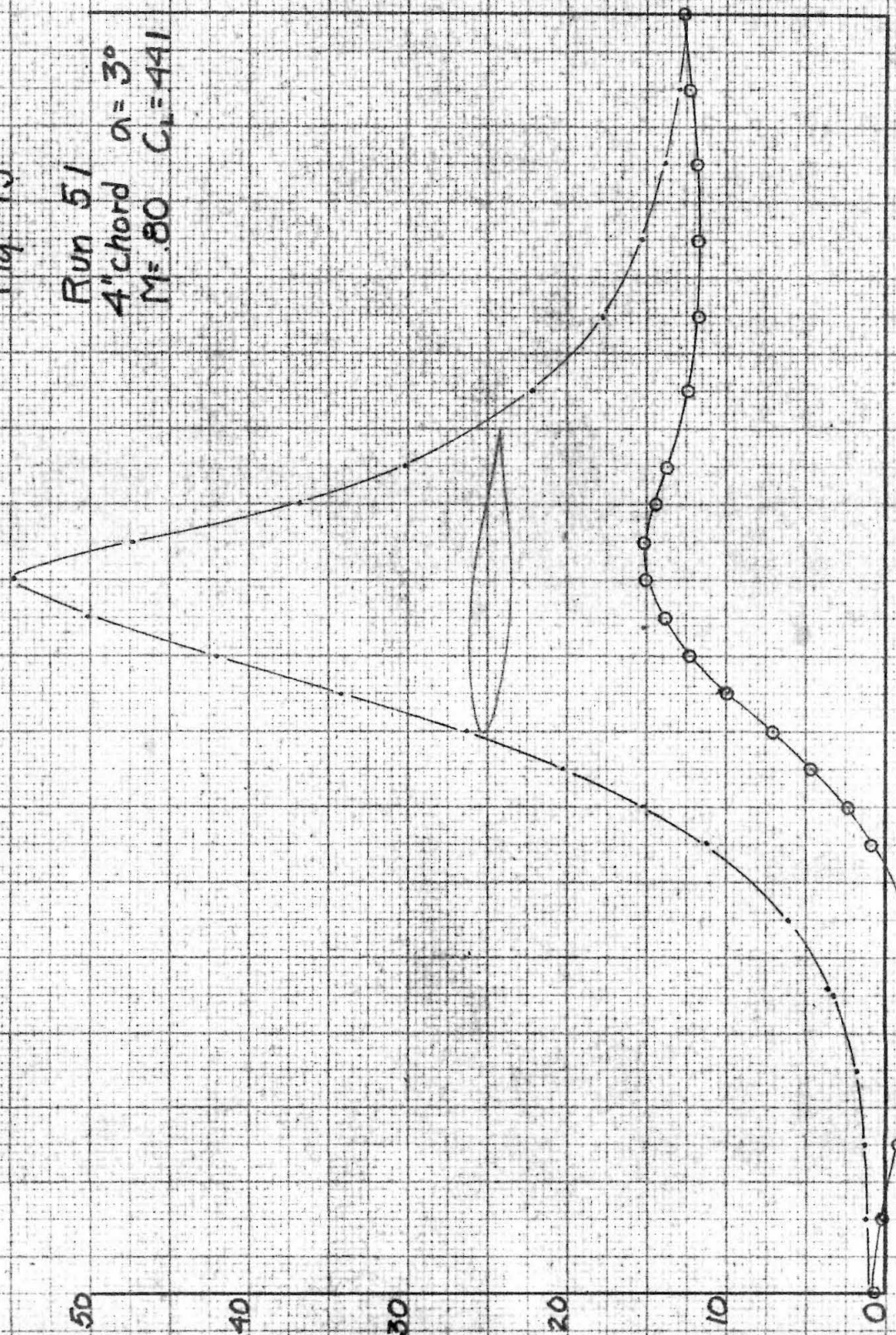


Fig. 46

Run 4
6" chord $\alpha = 1^\circ$
M = .60 $C_L = .088$

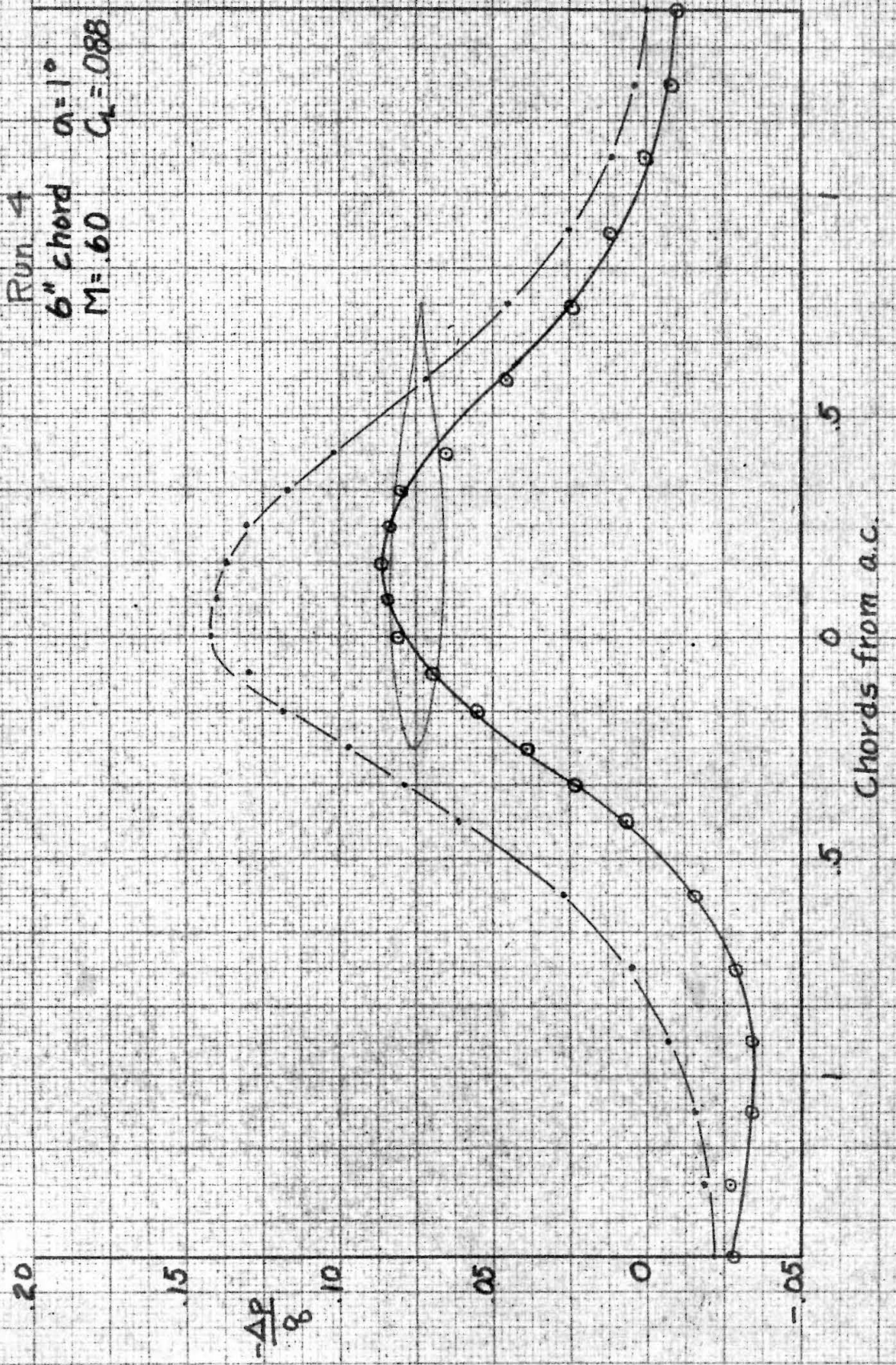


Fig. 47

Run 3
6" chord $\alpha = 1^\circ$
M = .65 $C_L = .094$

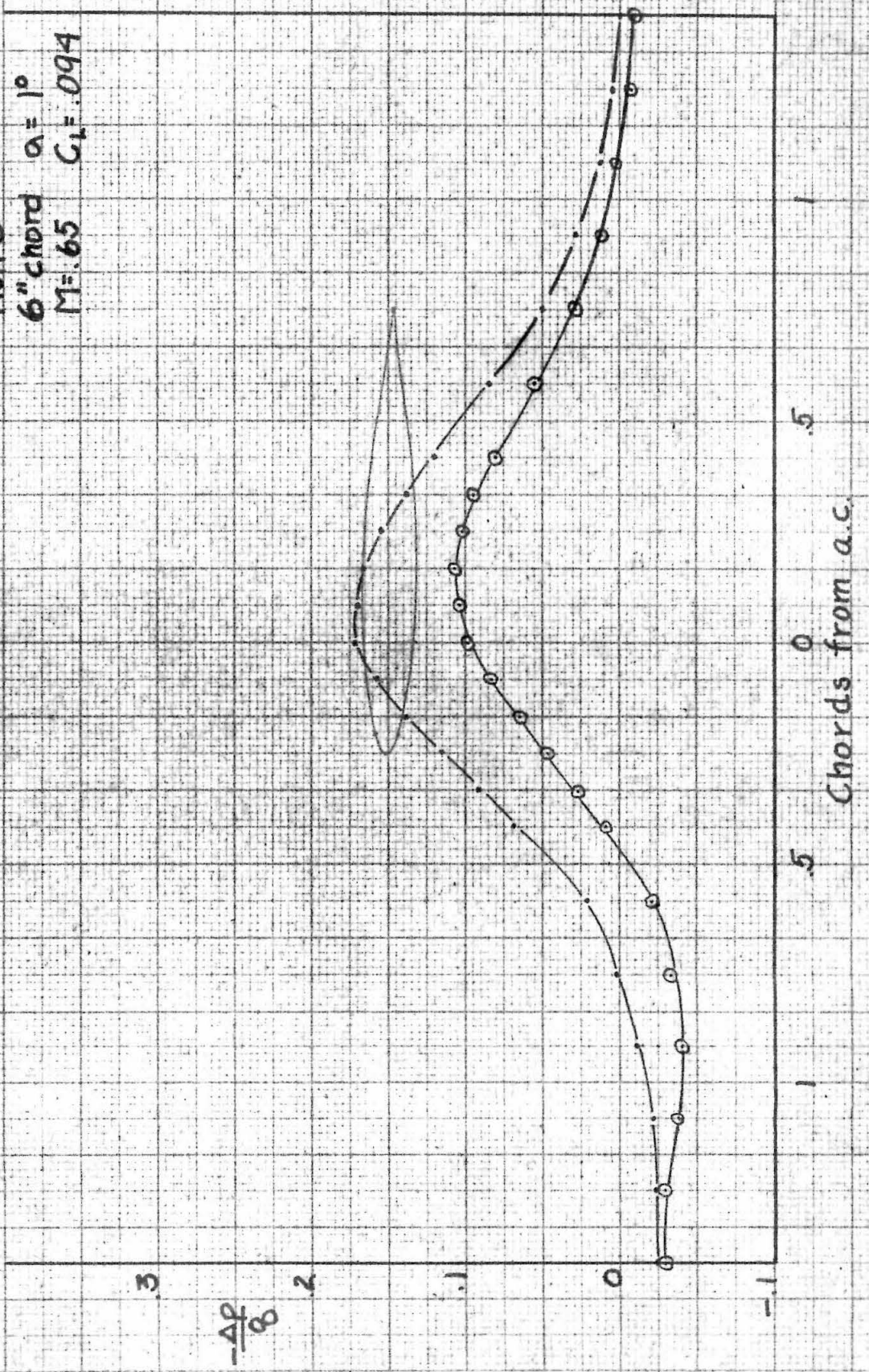


Fig. 48

Run 2
6" chord $\alpha = 1^\circ$
M = 70 $C_L = .115$

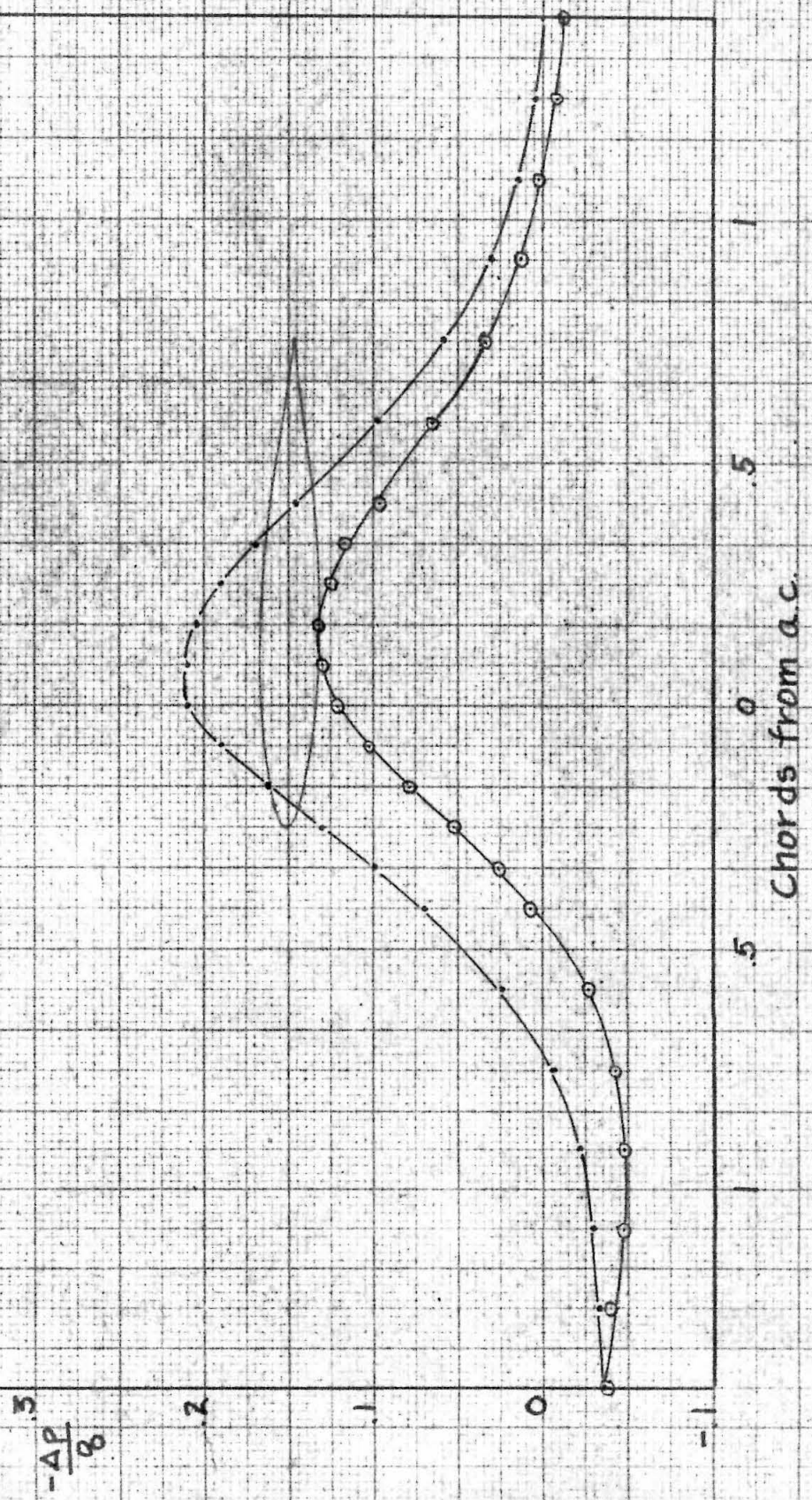


Fig. 49

Run 57
6" Chord $\alpha = 1^\circ$
M = .75 $C_c = 1.53$

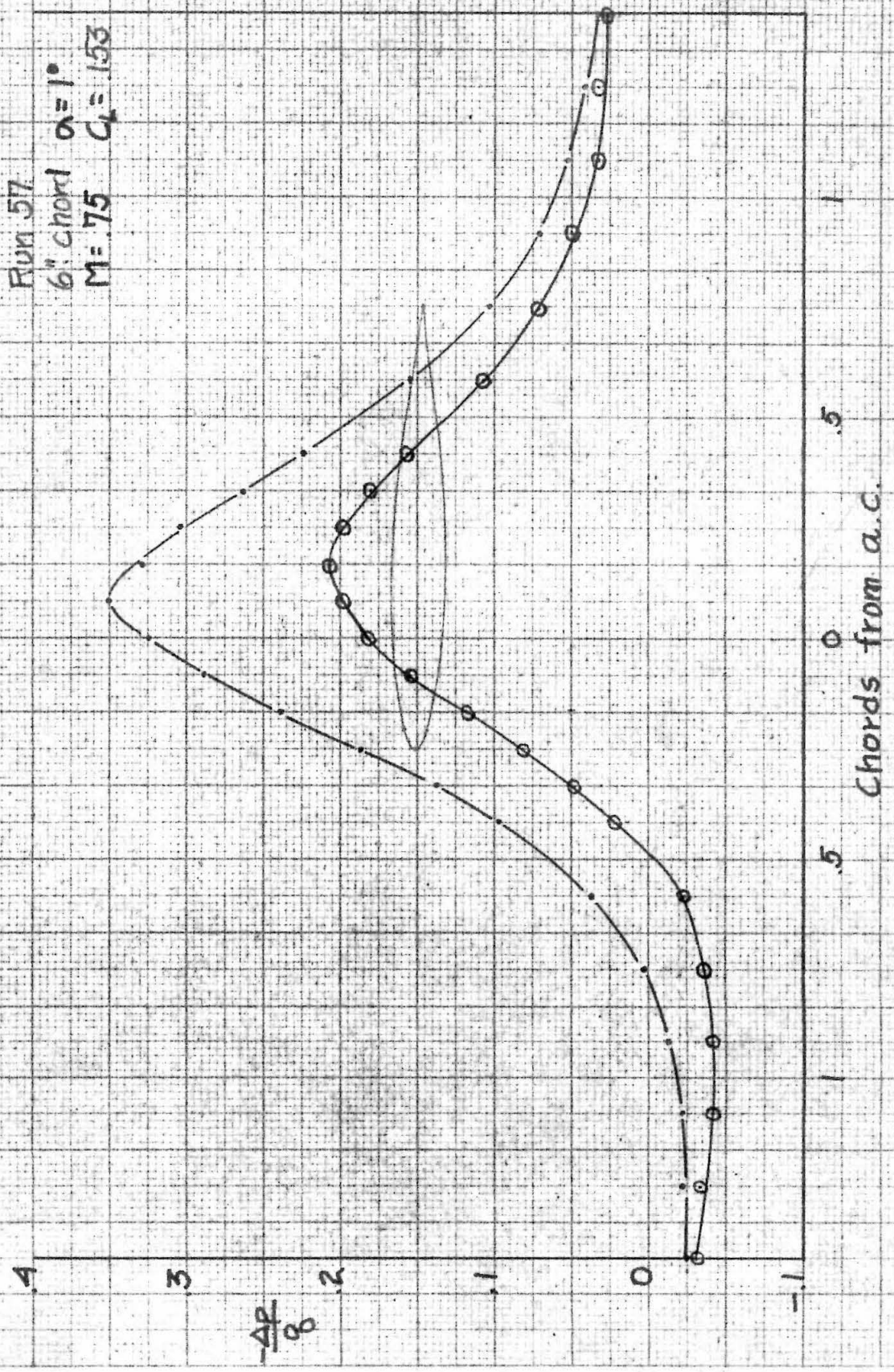


Fig. 50

Run 7
6" chord $\alpha = 2^\circ$
M = 60 $C_L = 2.40$

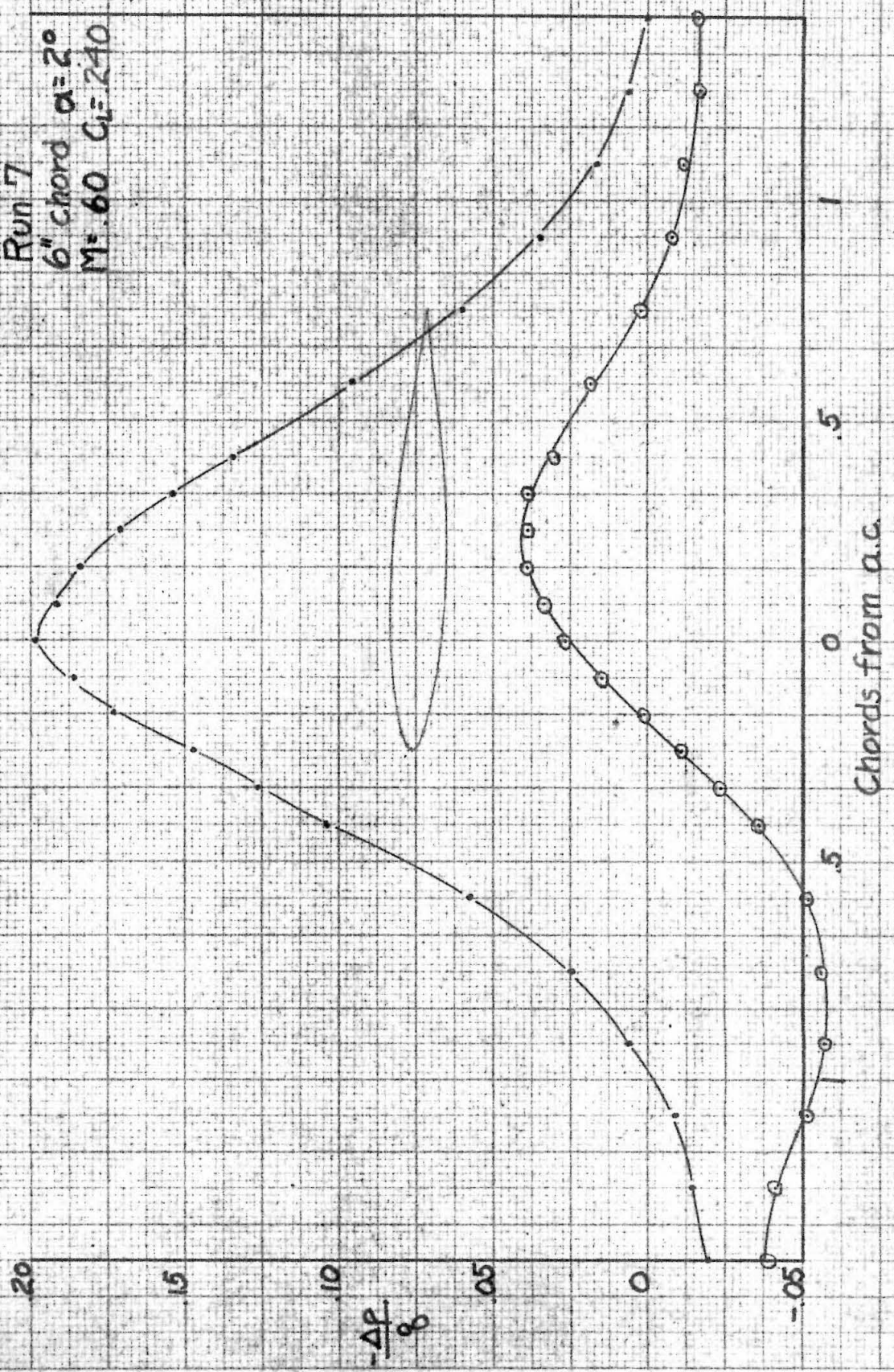


Fig. 51

Run 6
6" chord $\alpha = 2^\circ$
M: 65 $C_L = 255$

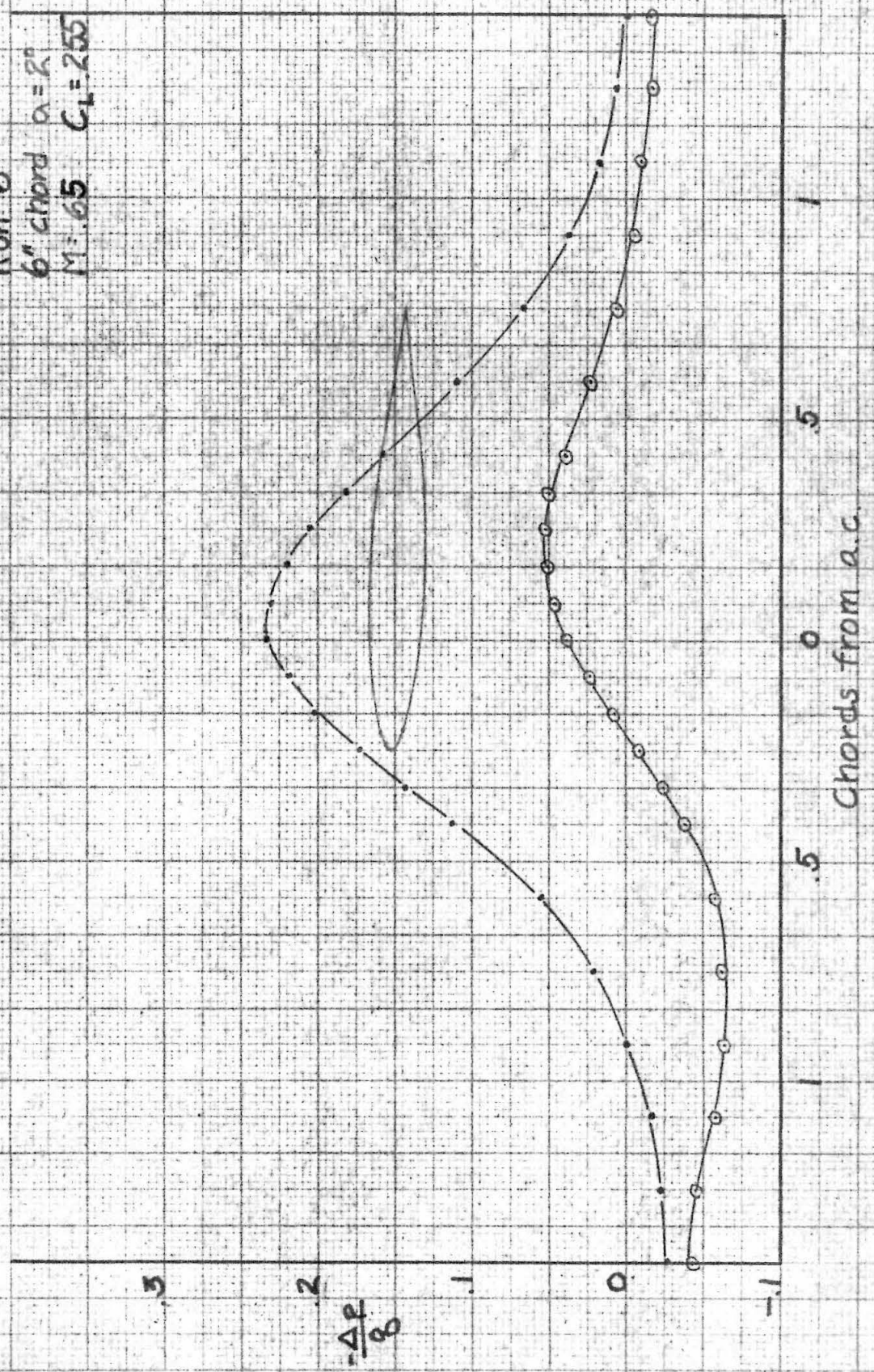


Fig 52

Run 5
6" chord $\alpha = 2^\circ$
M = .70 $C_L = 2.94$

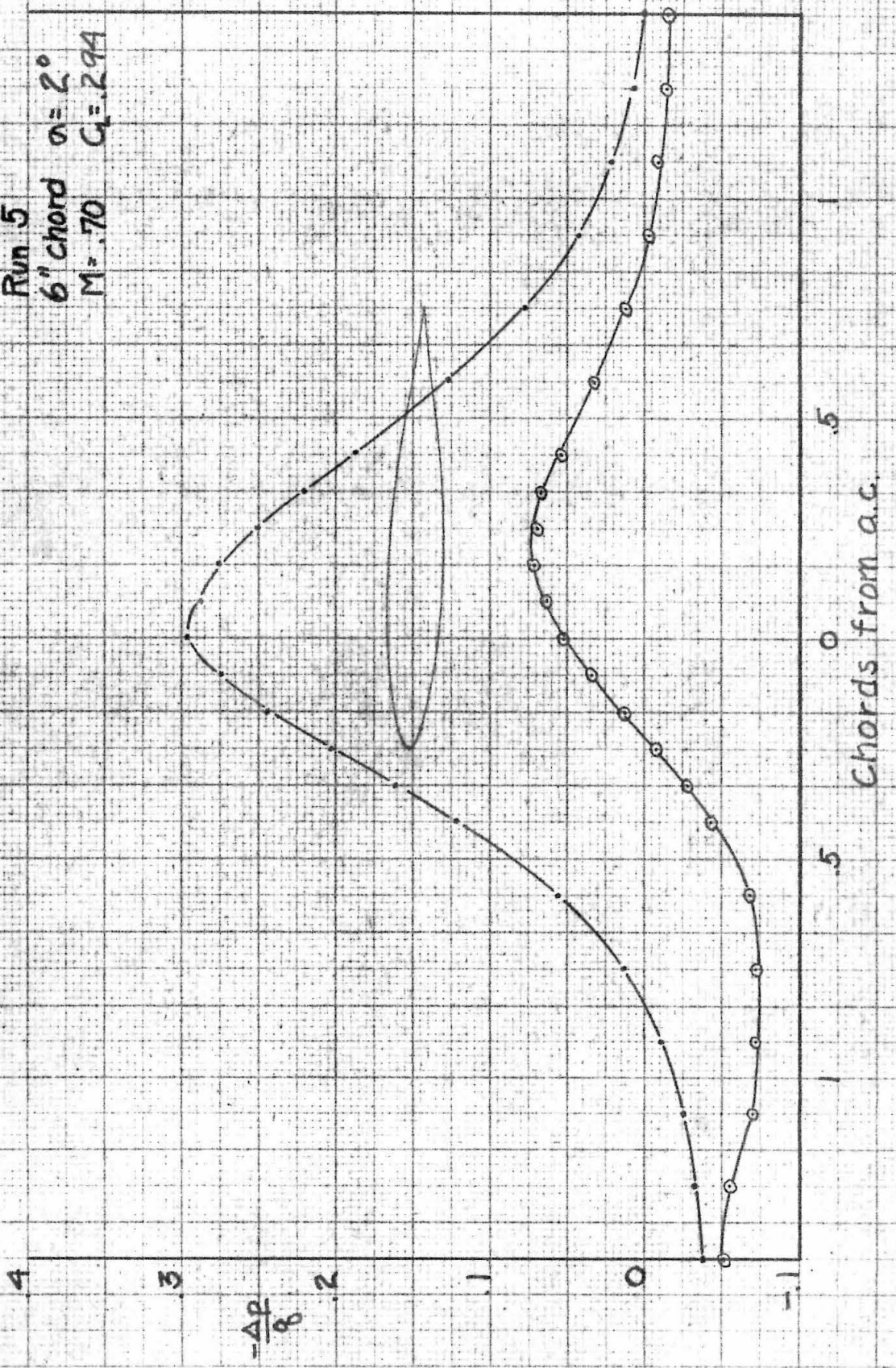


Fig. 53

Run 58
6" chord $\alpha = 2^\circ$
 $M = 75$ $C_r = 300$

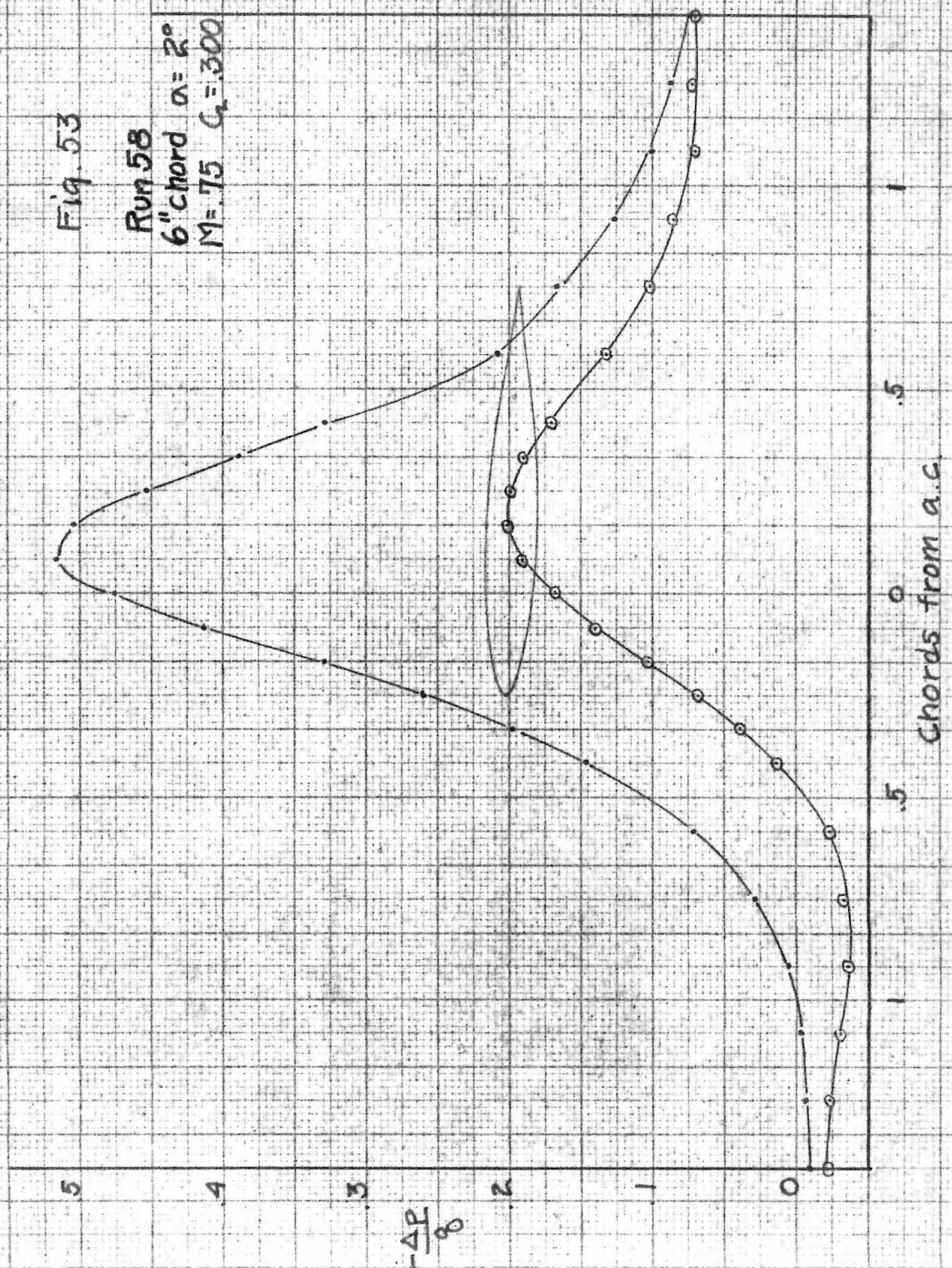


Fig 54

Run 9
6" chord $\alpha = 3^\circ$
M = 60 $C_L = 332$

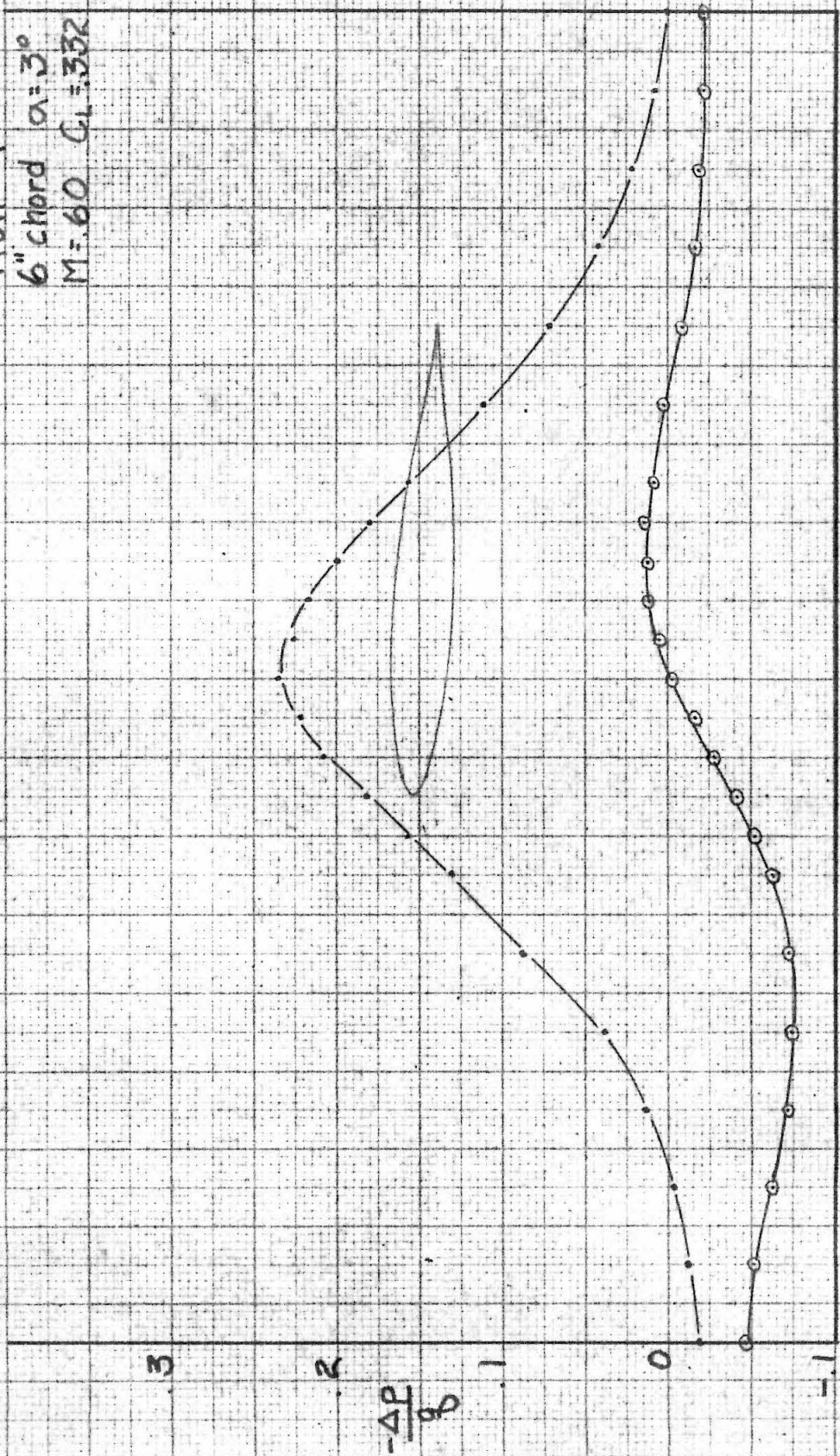


Fig. 55

Run 8

6" chord $\alpha = 3^\circ$

M = .65 $C_L = 364$

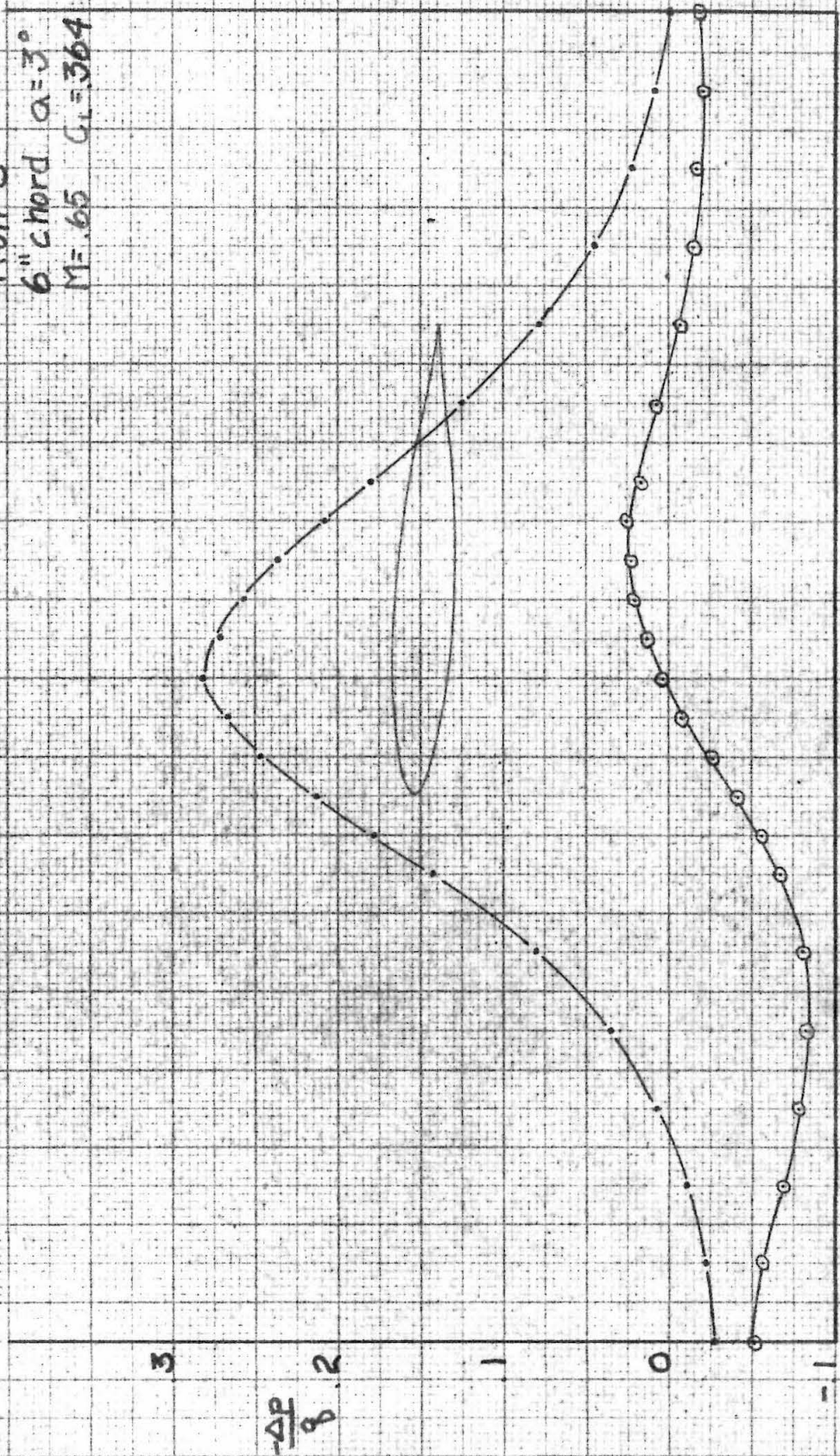


Fig. 56

Run 60
6" chord $\alpha = 3^\circ$
M = 70 $C_L = 426$

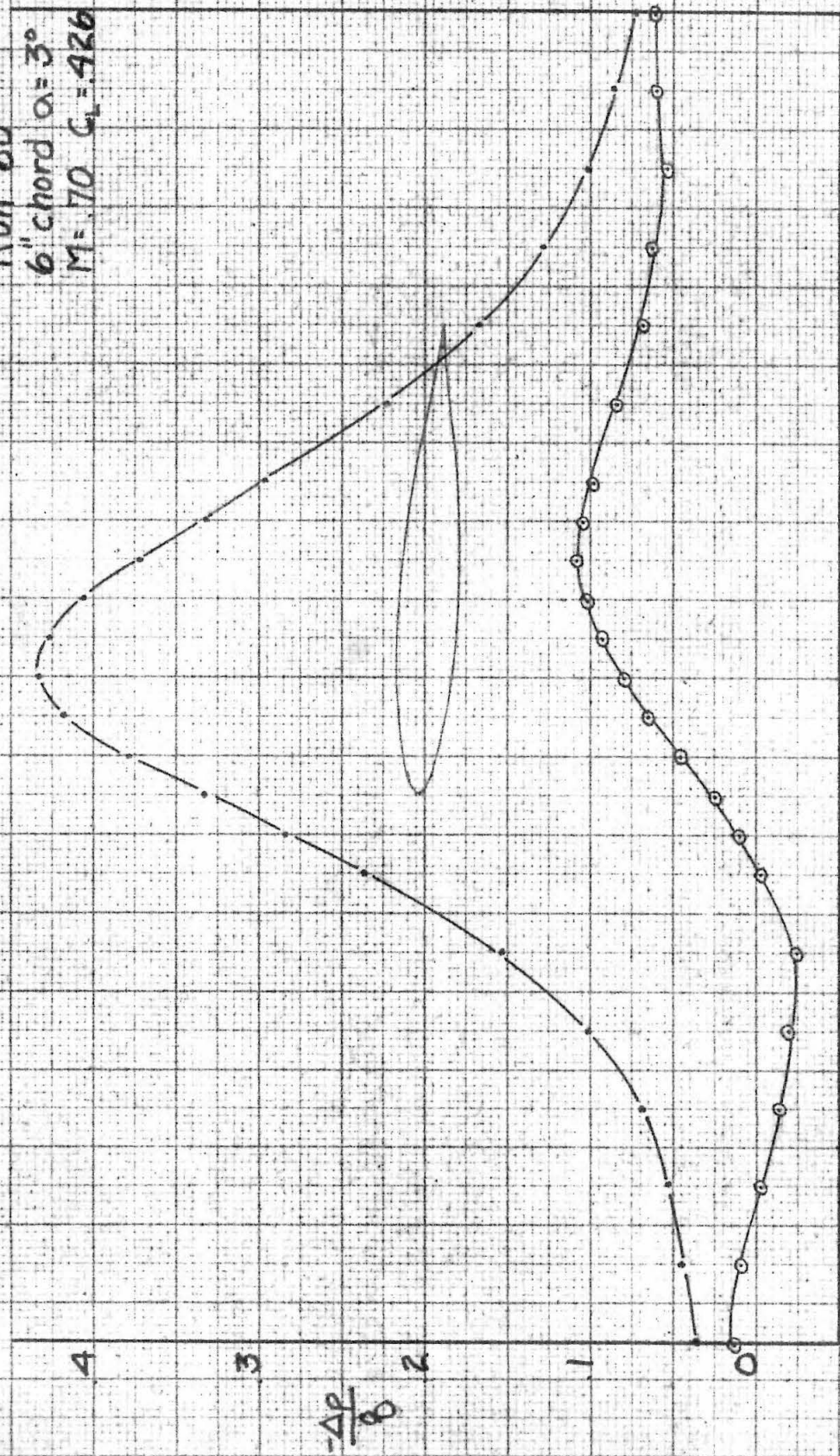
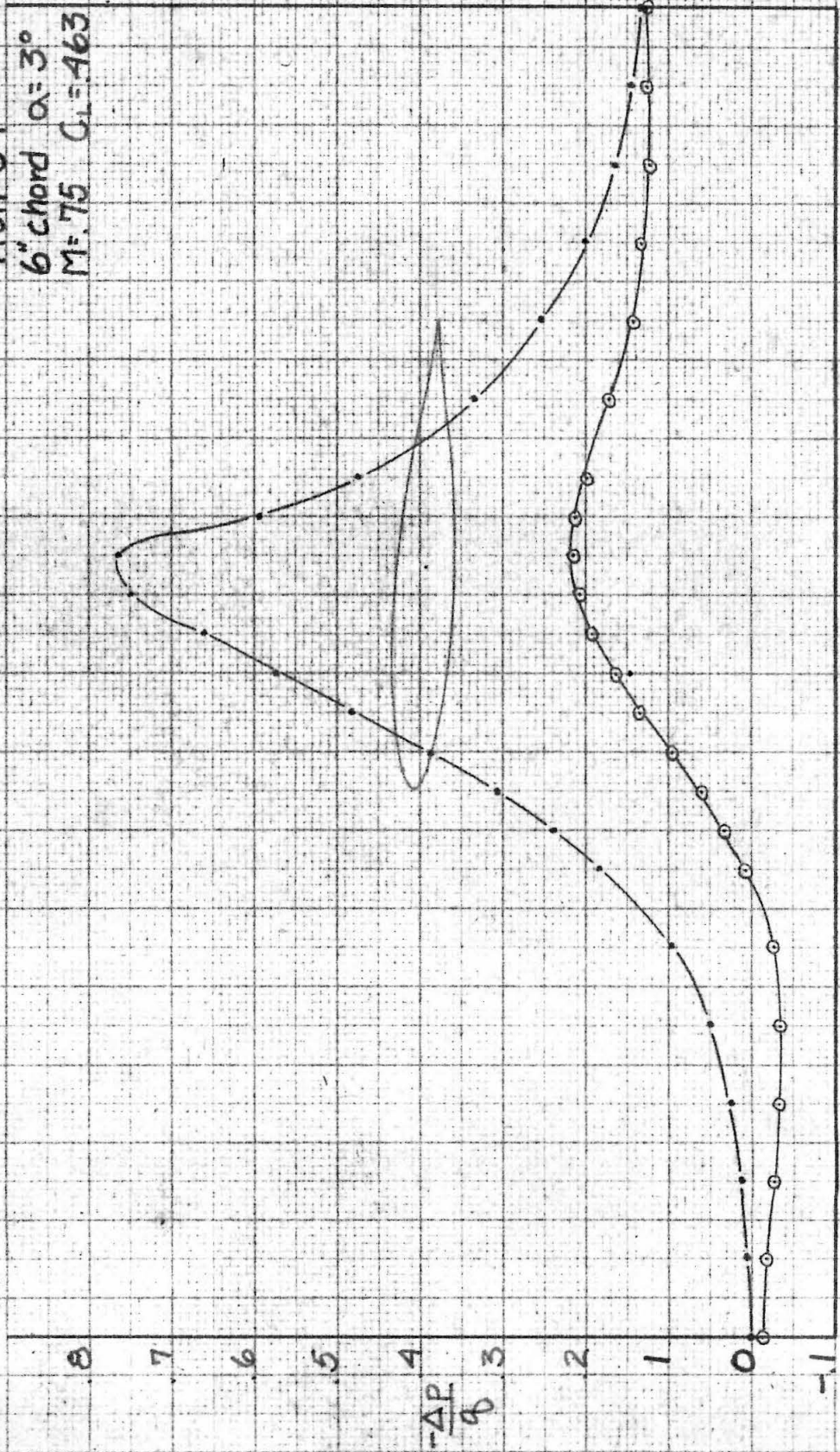


Fig 57

Run 59

6" chord $\alpha = 3^\circ$

M = .75 C.L. = 463

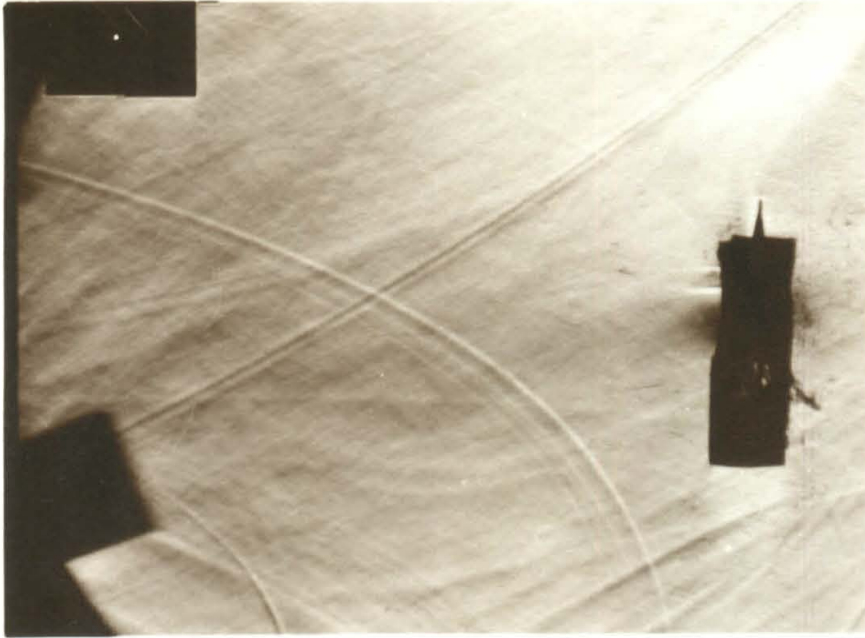


Chords from a.c.

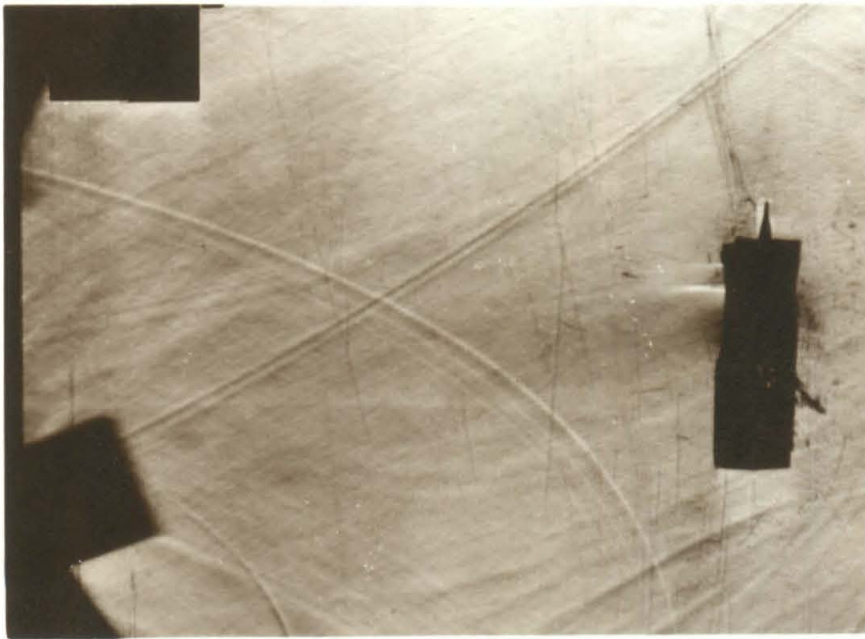
$-\Delta P/q$

CONFIDENTIAL

2.58



Run 16; 1" chord, $\alpha=2^\circ$ $M=.80$



Run 21; 1" chord, $\alpha=3^\circ$, $M=.80$

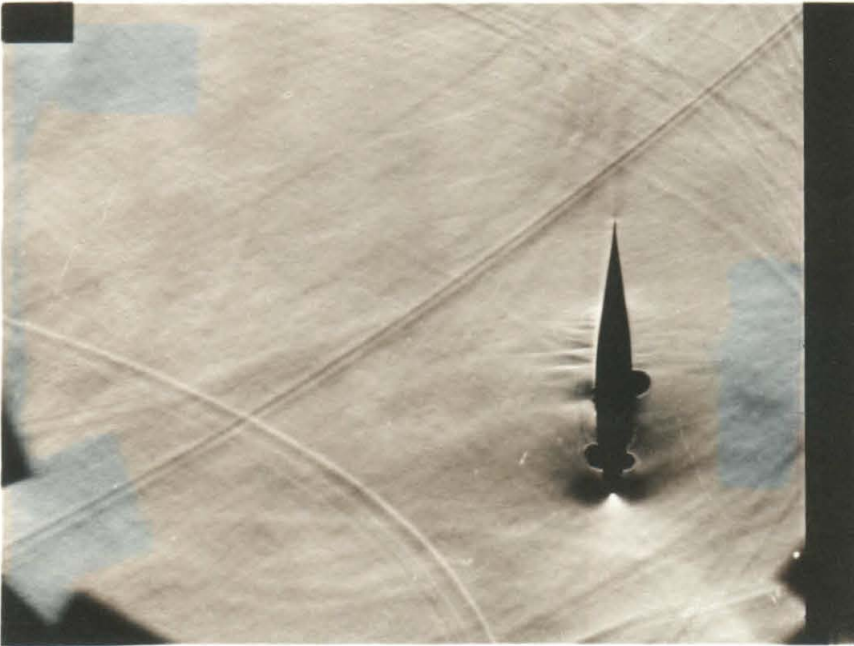
Only trailing edge of airfoil appears behind sealing tape. Tape is required for proper sealing of this small airfoil.

Fig 58

CONFIDENTIAL



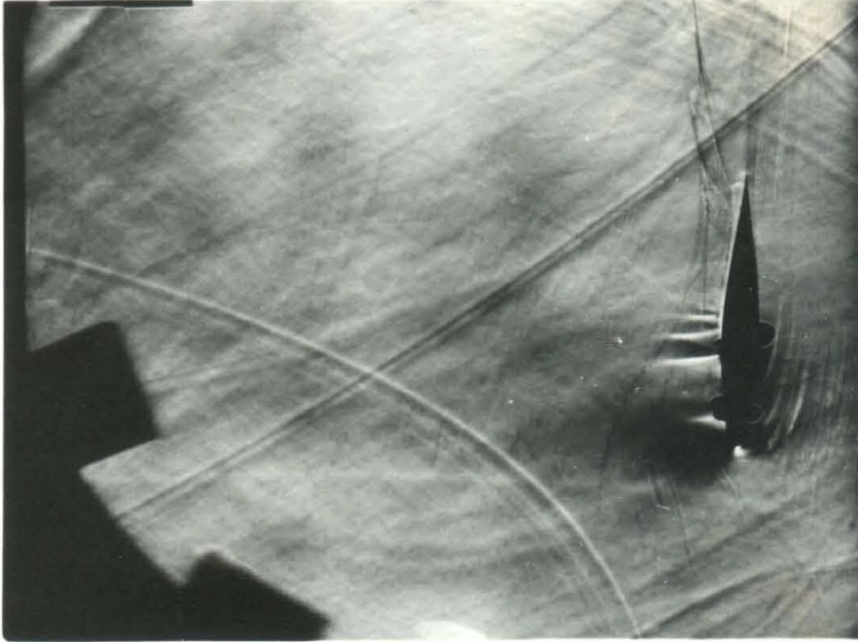
Run 31; 2" chord, $\alpha=1^\circ$, $M=.80$



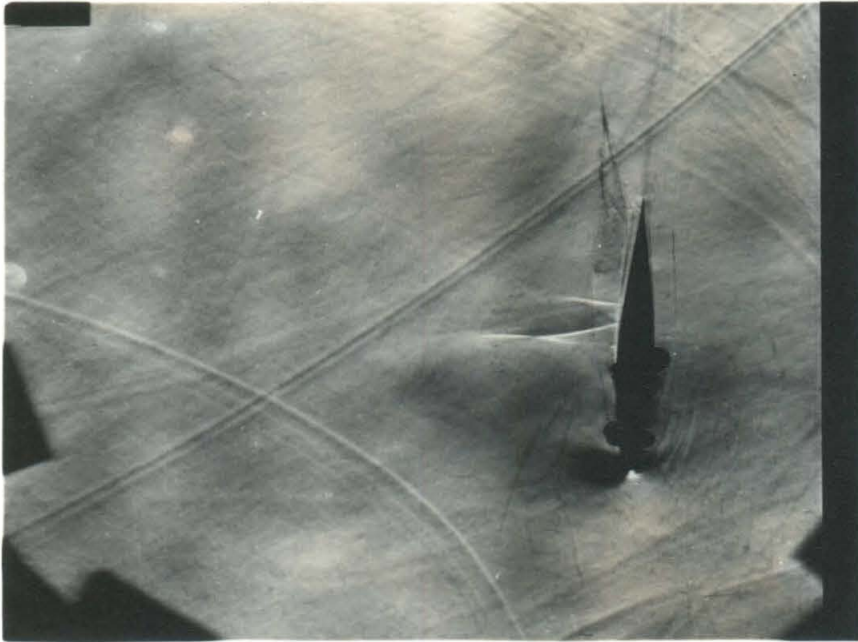
Run 36; 2" chord, $\alpha=2^\circ$, $M=.80$

Fig. 59A

CONFIDENTIAL



Run 42; 2" chord, $\alpha=3^\circ$, $M=.75$

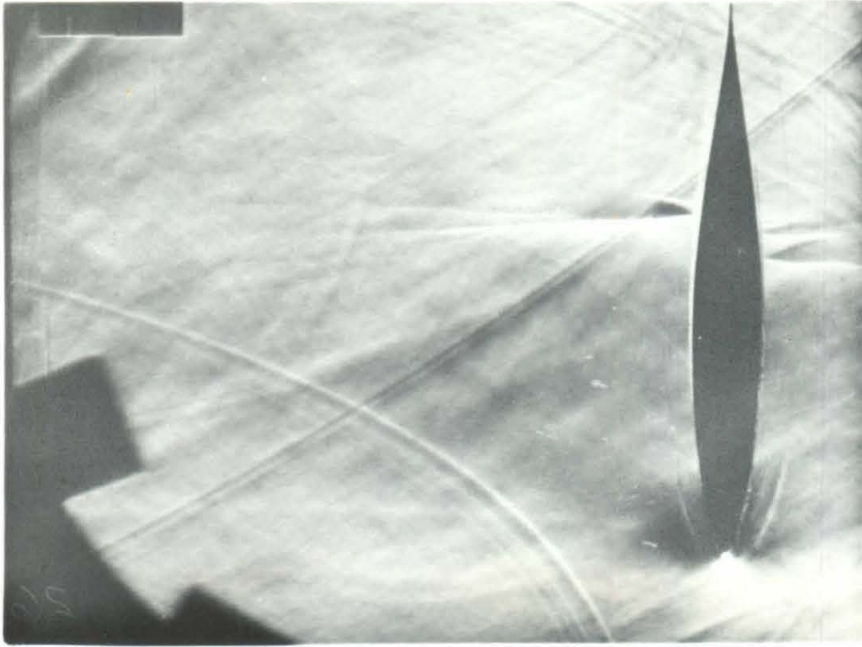


Run 41; 2" chord, $\alpha=3^\circ$, $M=.80$

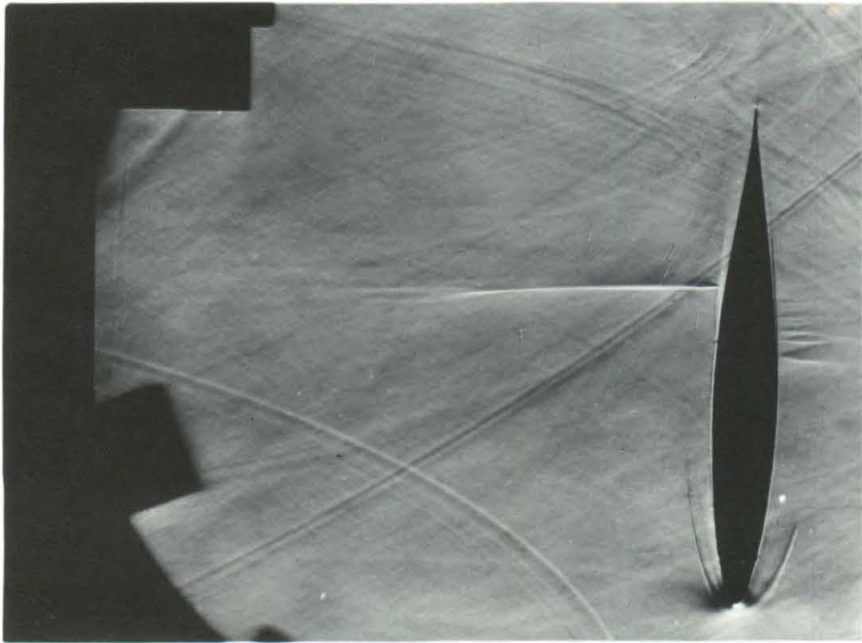
Fig. 59B

CONFIDENTIAL

CONFIDENTIAL



Run 26: 4" chord, $\alpha=1^\circ$, $M=.80$

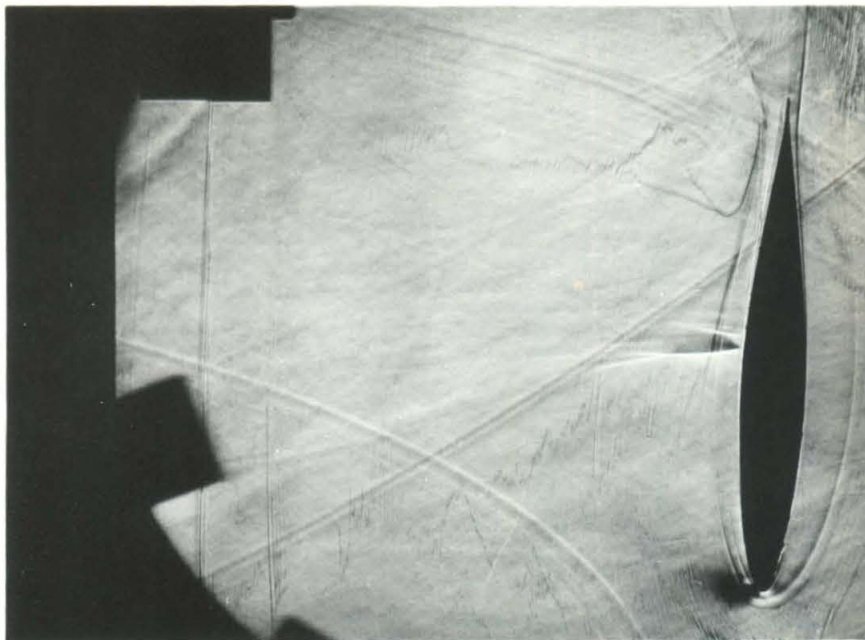


Run 46: 4" chord, $\alpha=2^\circ$, $M=.80$

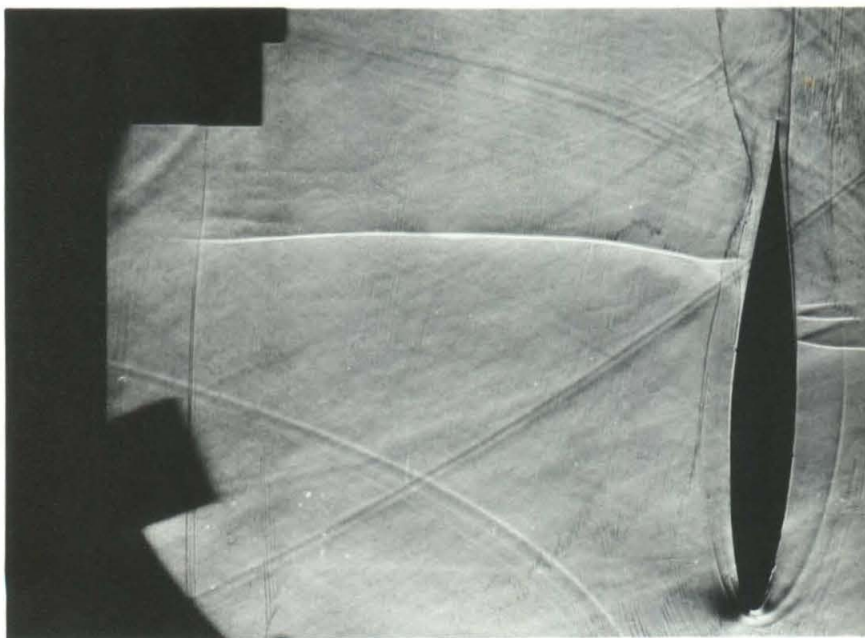
Fig. 60 A

CONFIDENTIAL

CONFIDENTIAL



Run 52; 4" chord, $\alpha = 3^\circ$, $M = .75$



Run 51; 4" chord, $\alpha = 3^\circ$, $M = .80$

Fig. 60B

CONFIDENTIAL

CONFIDENTIAL



Run 58; 6" chord, $\alpha=2^\circ$, $M=.75$



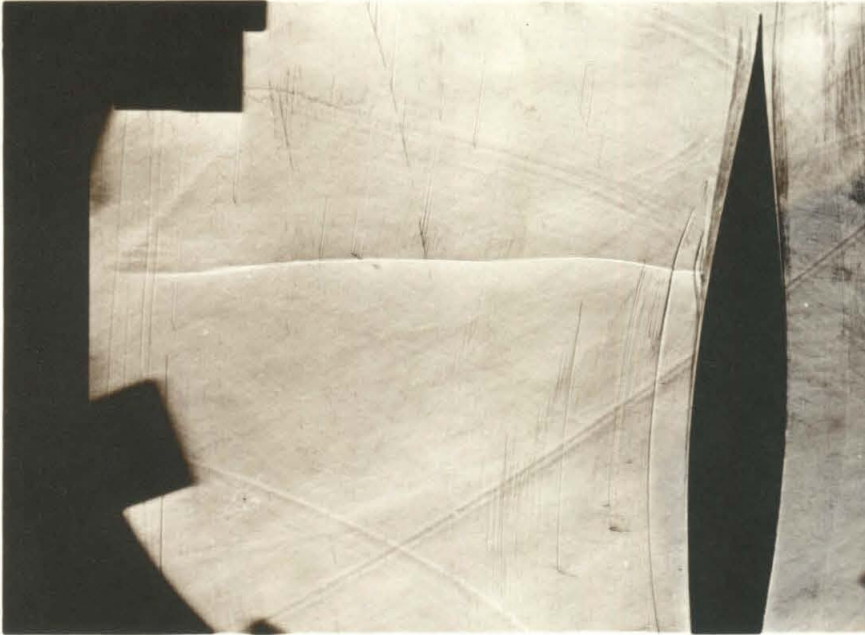
Run 57; 6" chord, $\alpha=1^\circ$, $M=.75$

Fig. 61

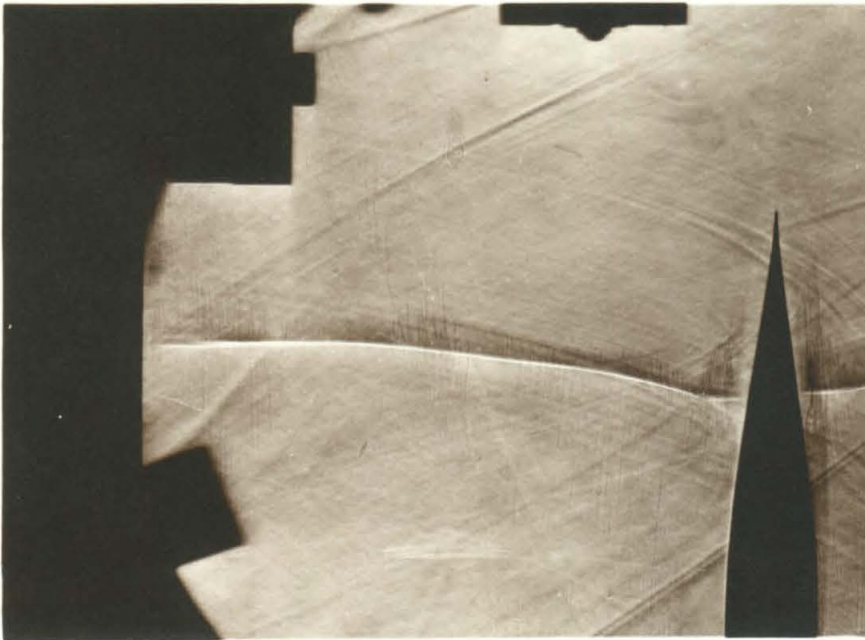
CONFIDENTIAL

CONFIDENTIAL

2.62



Run 59 6" chord, $\alpha=3^\circ$, $M=.75$



Run 56; 6" chord, $\alpha=1^\circ$, $M=.77$

Shock wave extends to top tunnel wall,
illustrating choked condition.

Fig. 62

CONFIDENTIAL

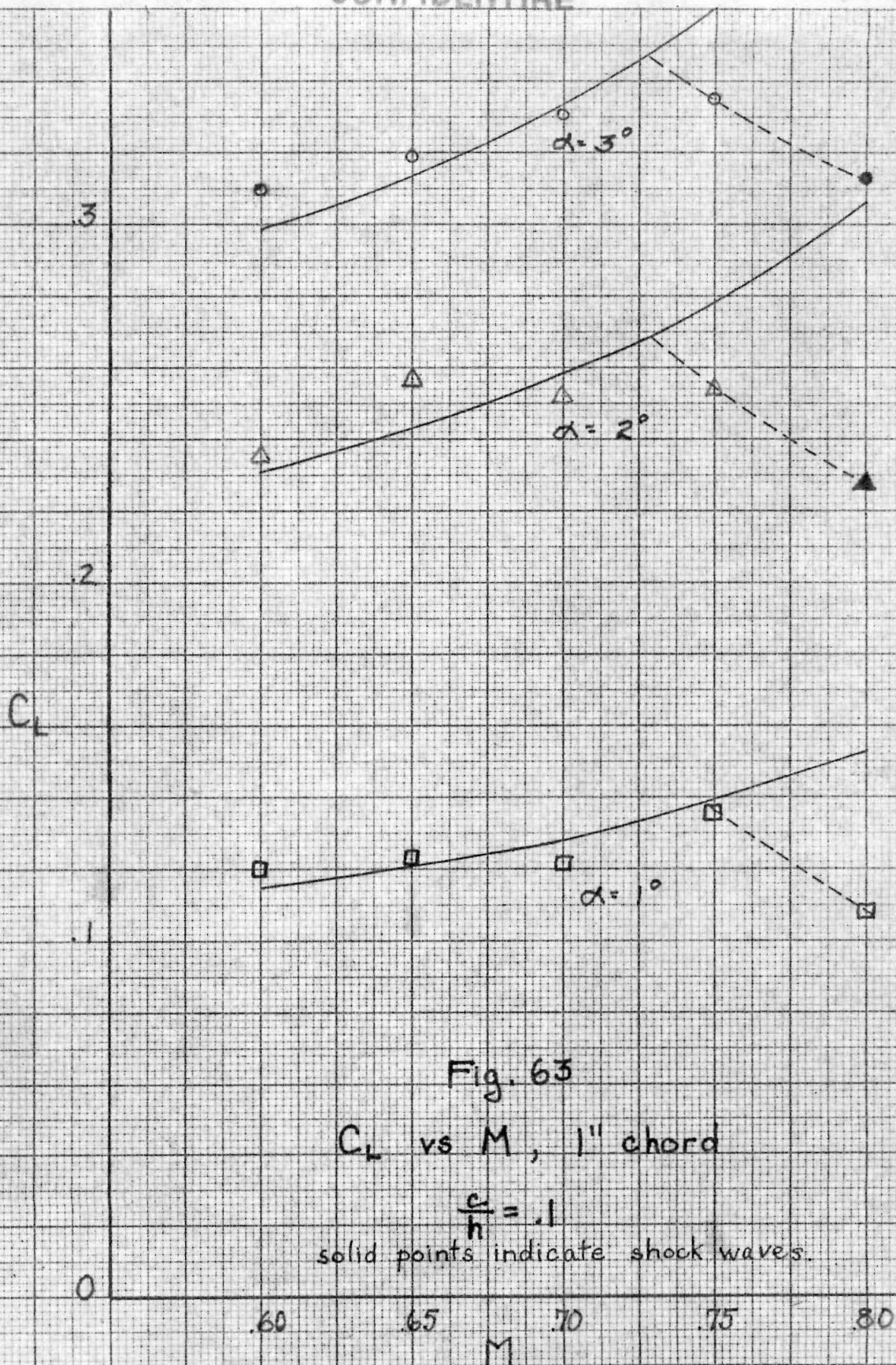


Fig. 63

C_L vs M , 1" chord

$$\frac{c}{h} = .1$$

solid points indicate shock waves.

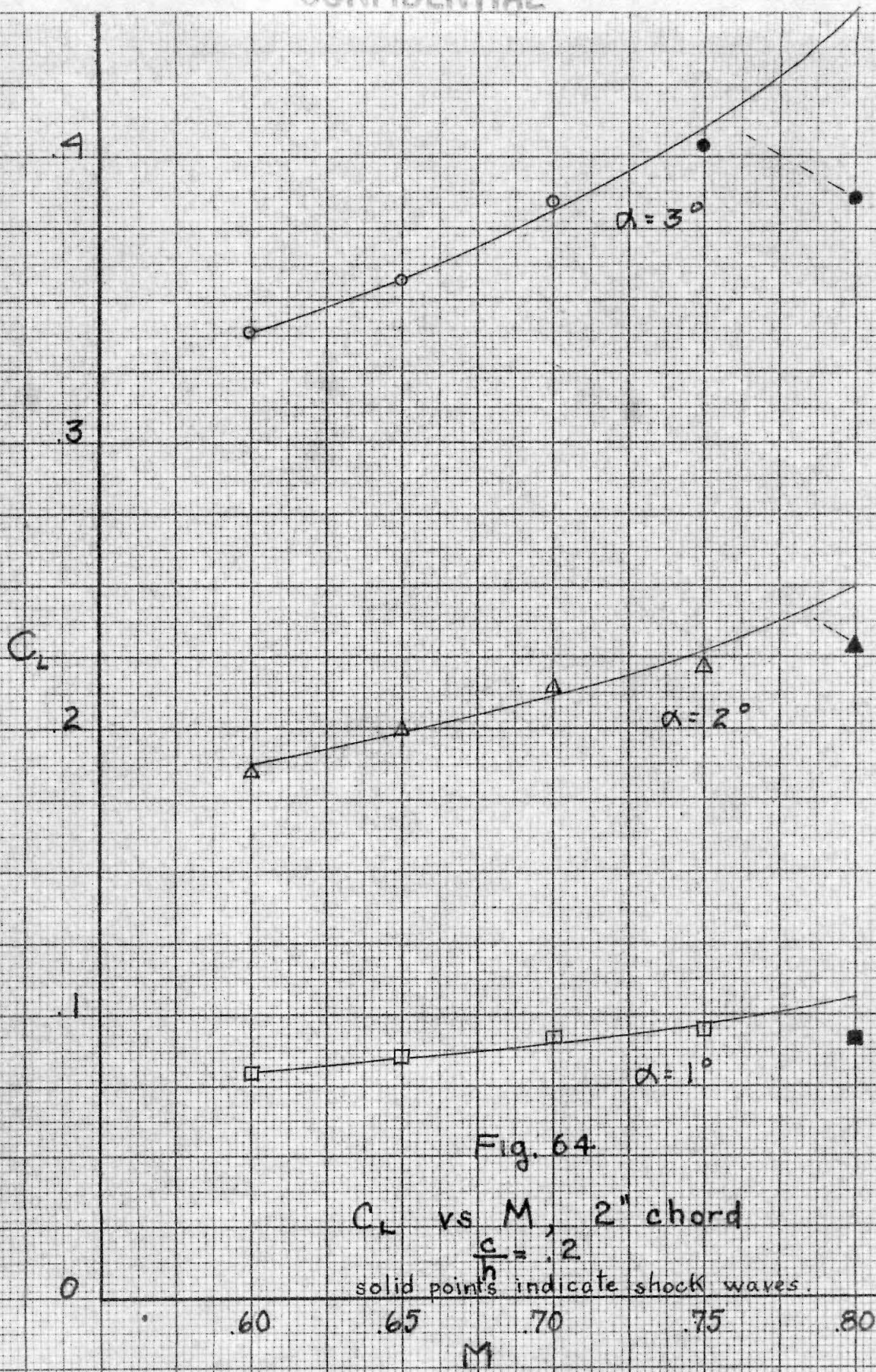
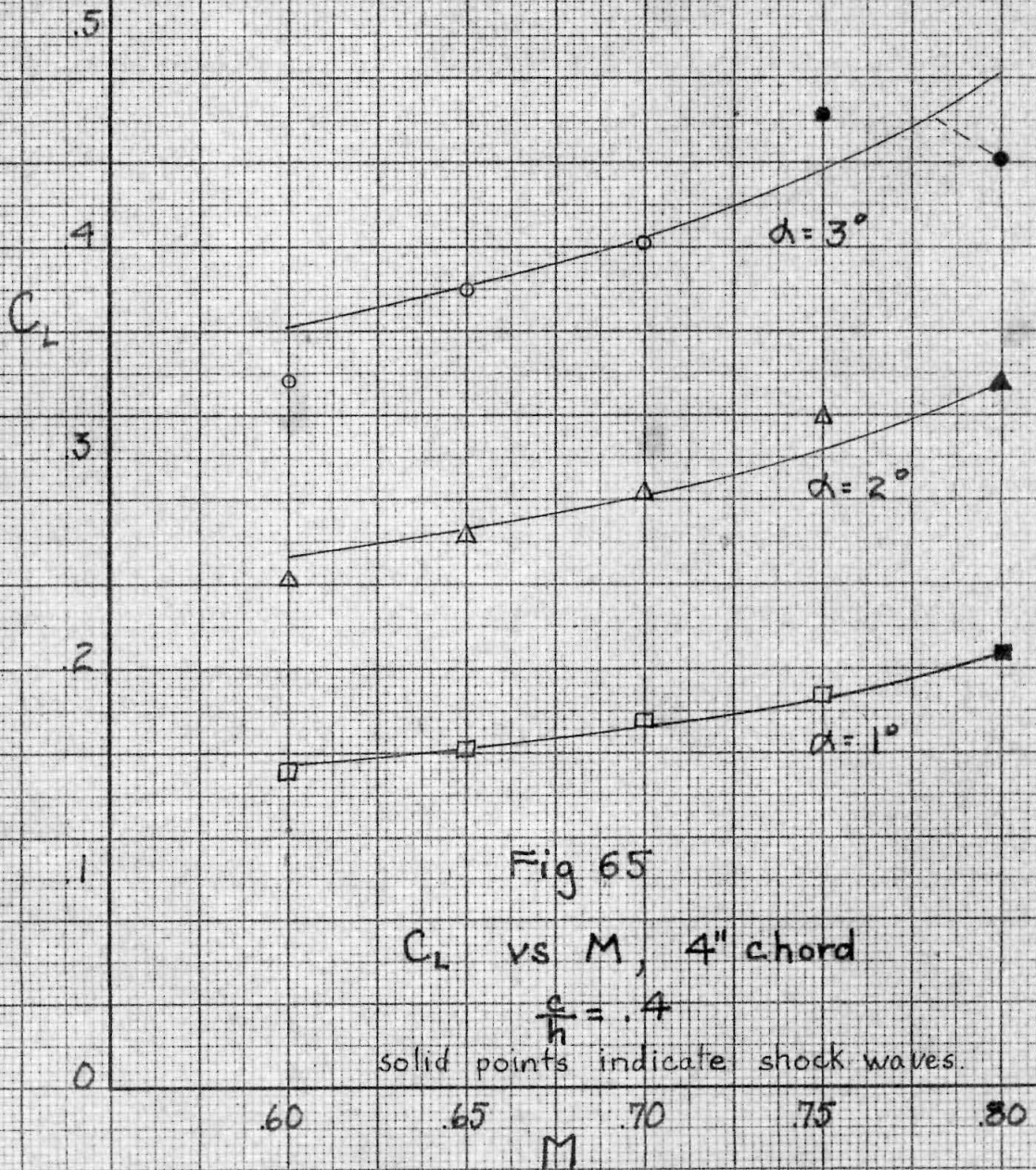


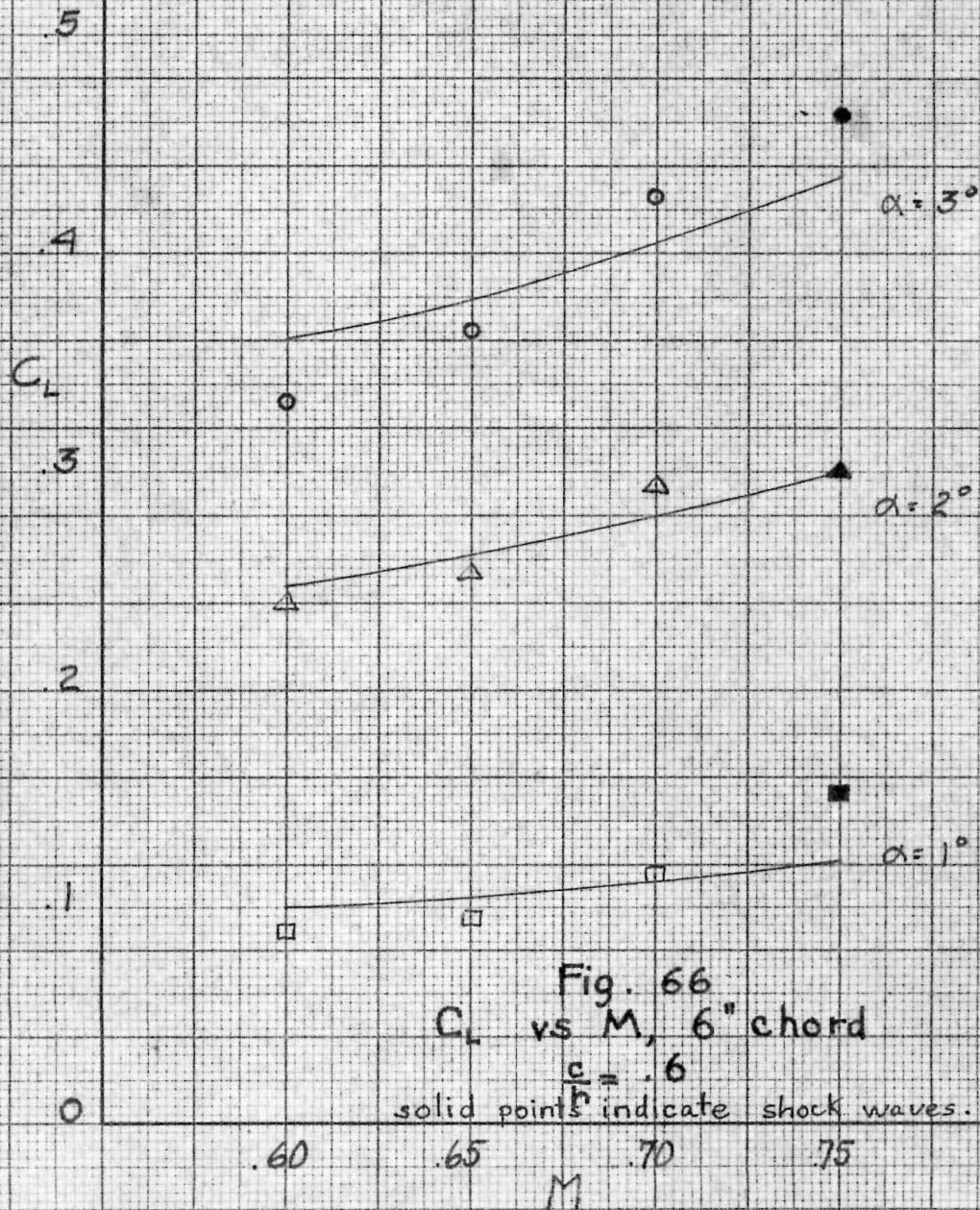
Fig. 64

C_L vs M , 2" chord

$\frac{c}{h} = .2$

solid points indicate shock waves.





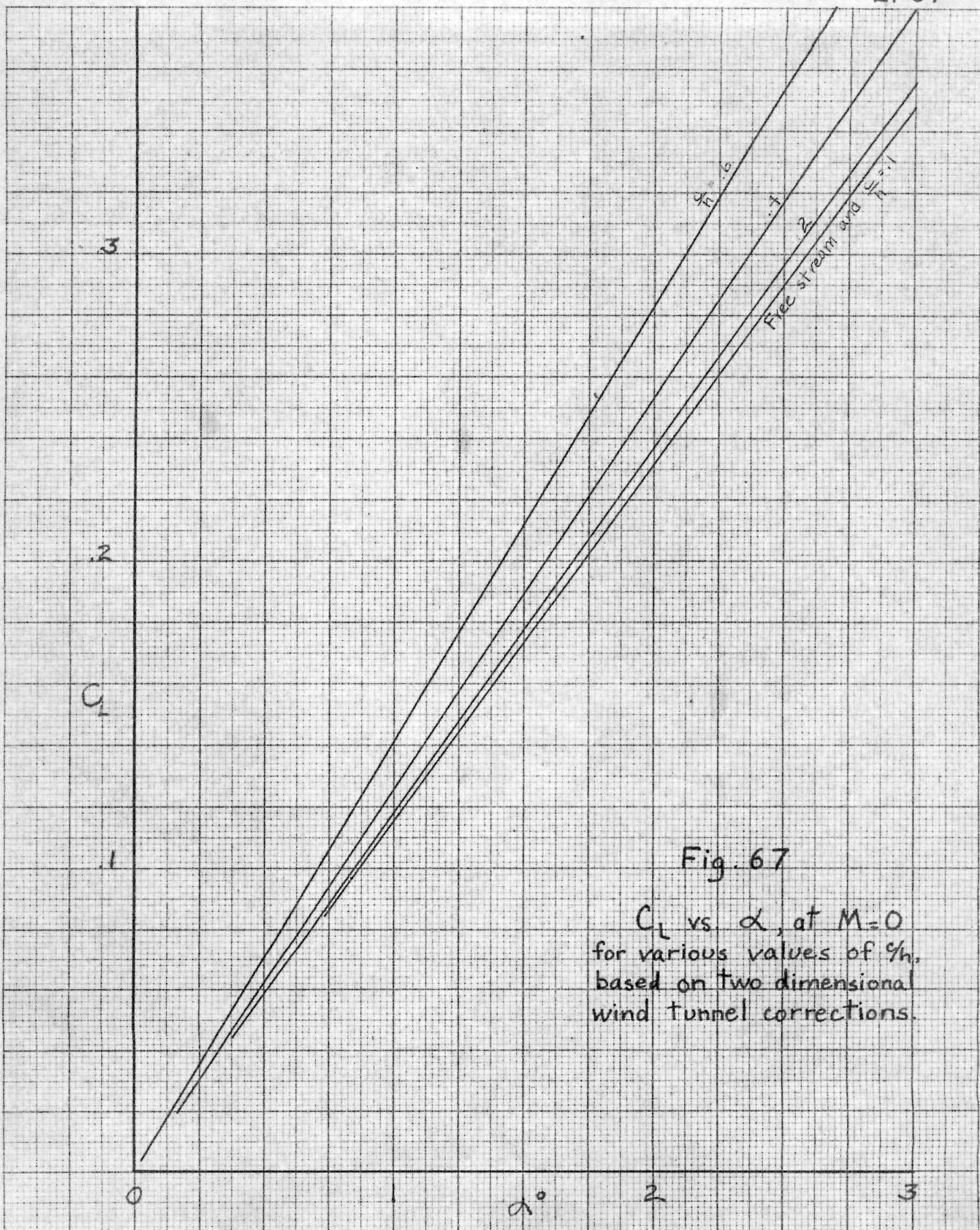
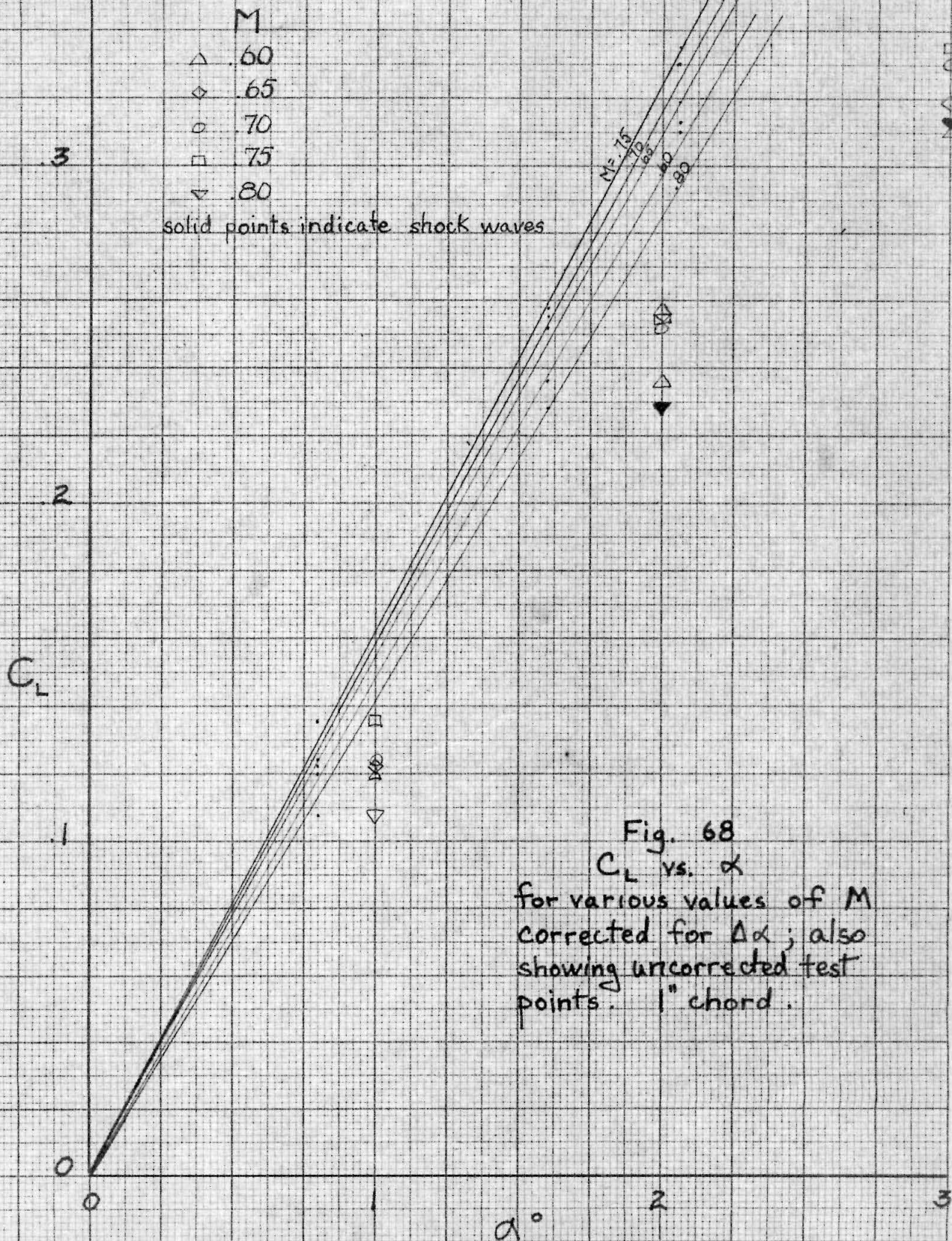


Fig. 67

C_L vs. α , at $M=0$
for various values of h/b ,
based on two dimensional
wind tunnel corrections.



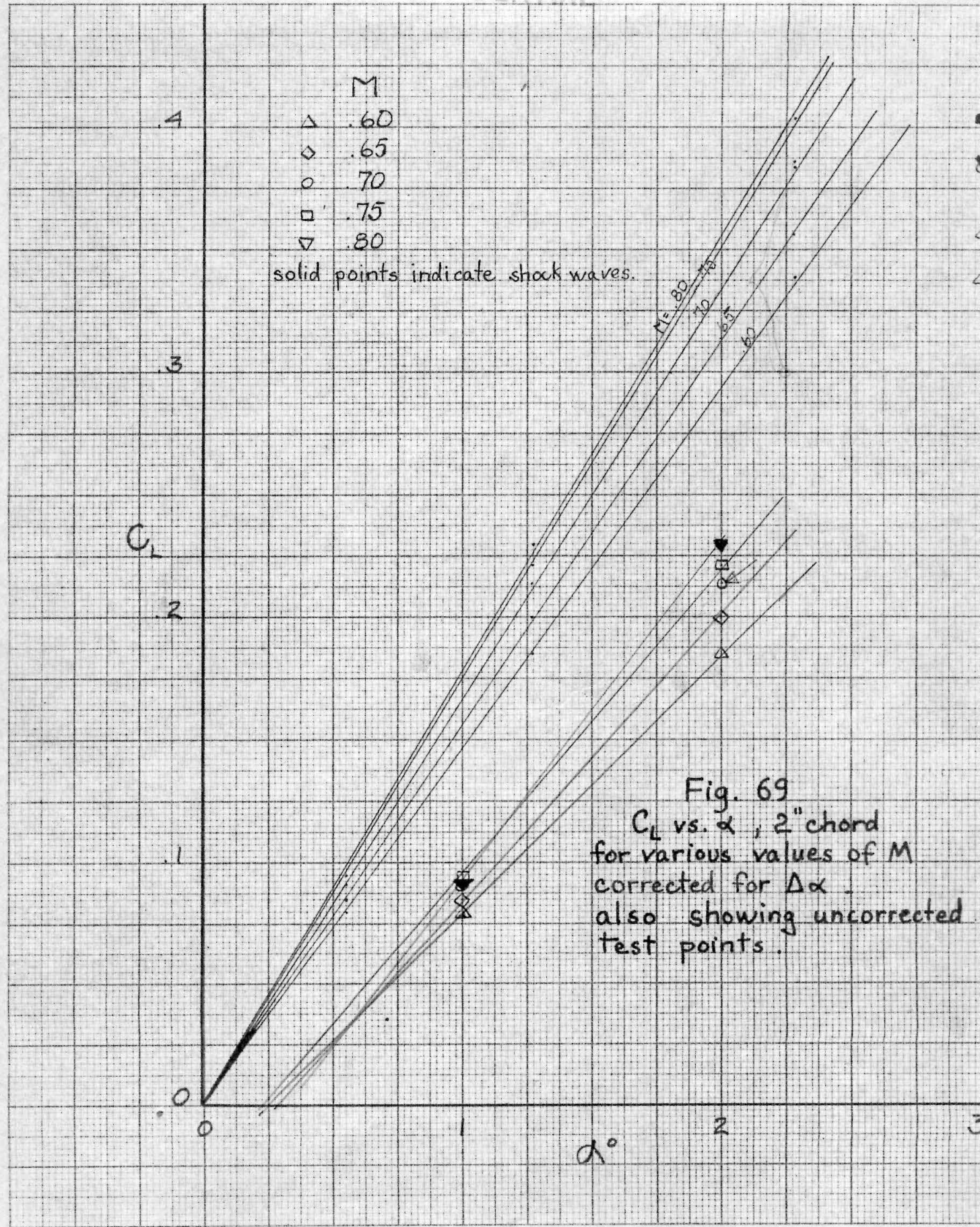


Fig. 69
 C_L vs. α , 2" chord
 for various values of M
 corrected for $\Delta\alpha$.
 also showing uncorrected
 test points.

- M
- △ 60
- ◇ 65
- 70
- 75
- ▽ 80

.5 solid points indicate shock waves

C_L

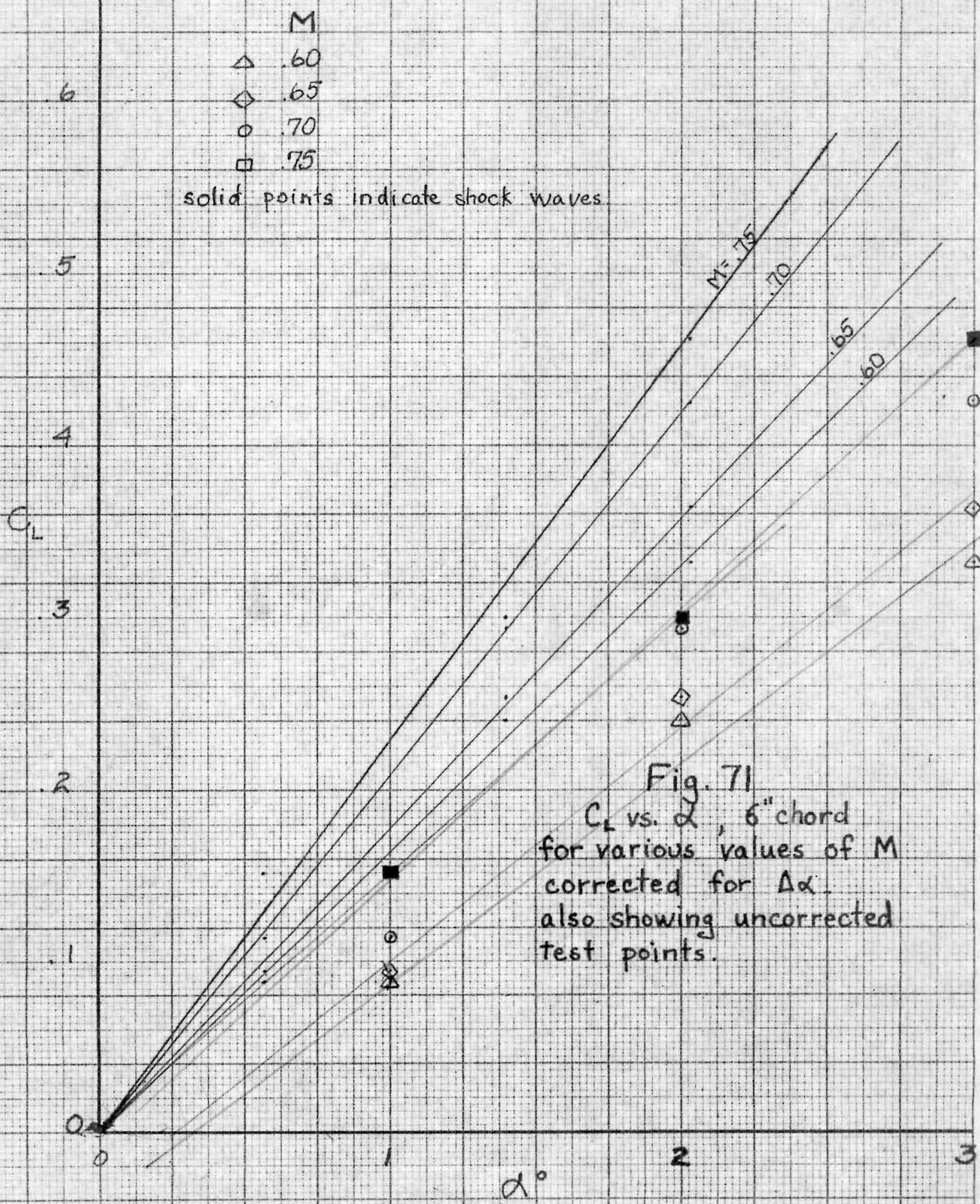
.2

.1

Fig. 70
 C_L vs. α , 4" chord
 for various values of M
 corrected for $\Delta\alpha$.
 also showing uncorrected
 test points.

M = 80
 .75
 70
 .65
 60

α°



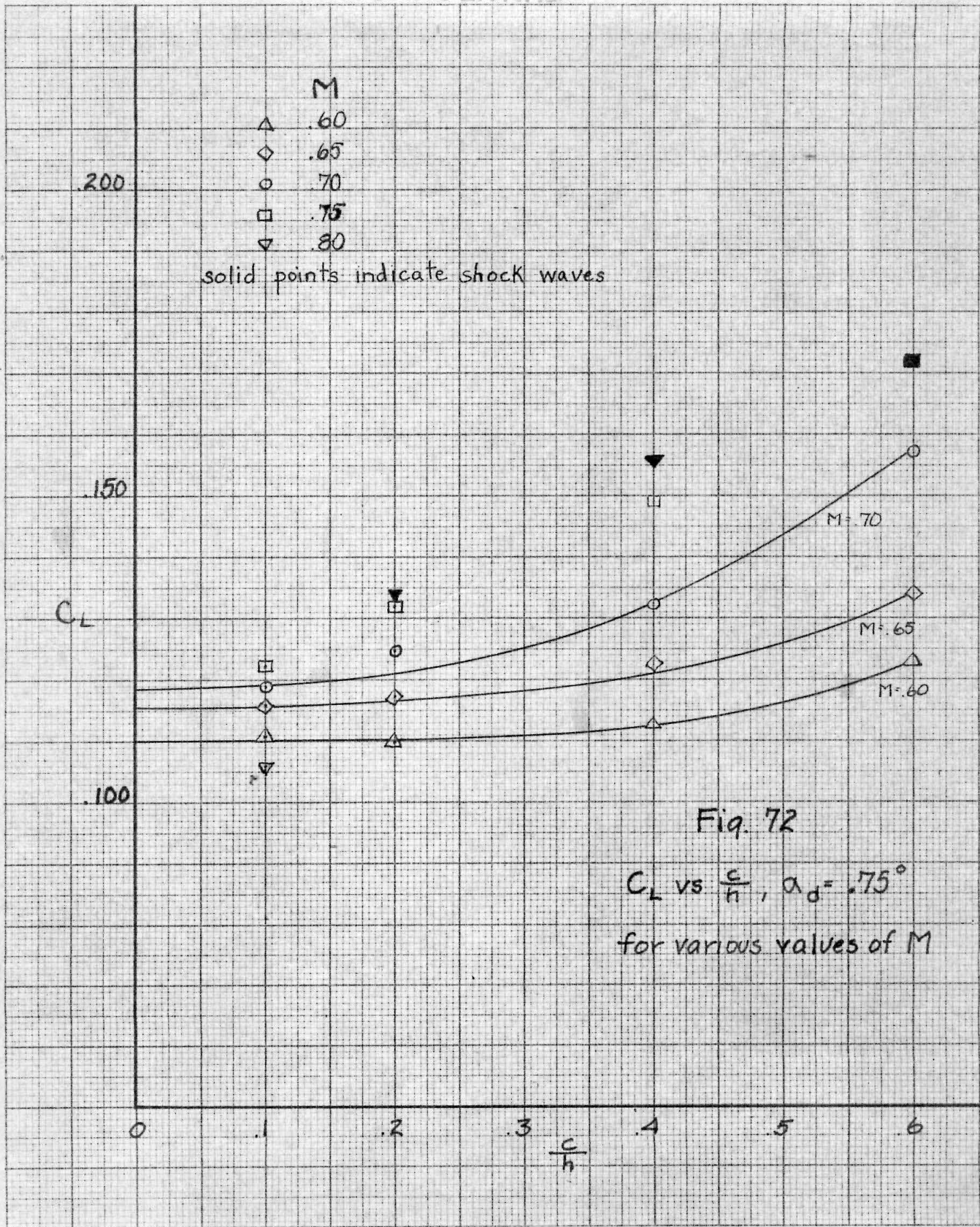


Fig. 72

C_L vs $\frac{c}{h}$, $\alpha_d = .75^\circ$
 for various values of M

- M
- △ .60
- ◇ .65
- .70
- .75
- ▽ .80

solid points indicate shock waves.

C_L

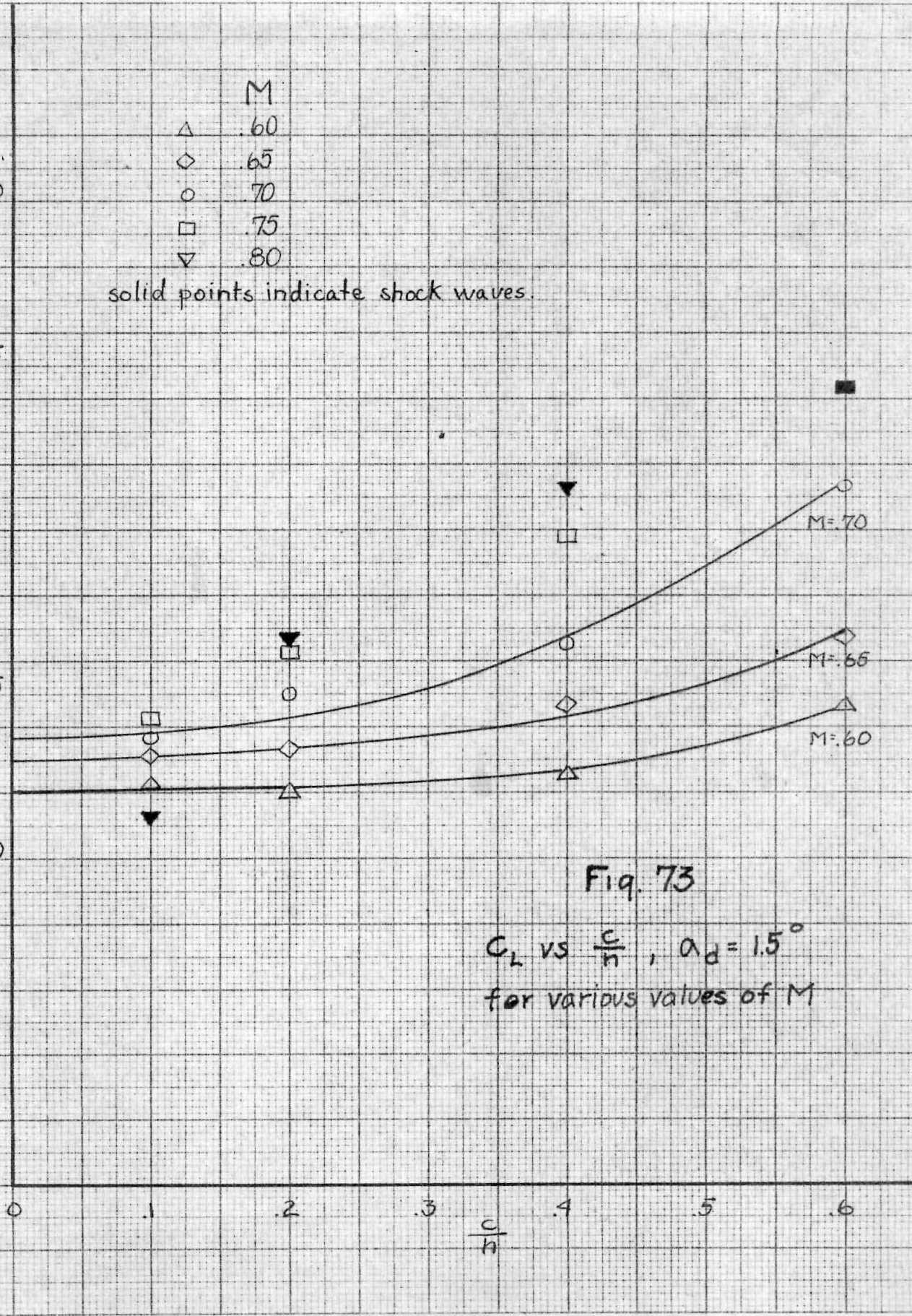


Fig. 73

C_L vs $\frac{c}{h}$, $\alpha_d = 1.5^\circ$
for various values of M

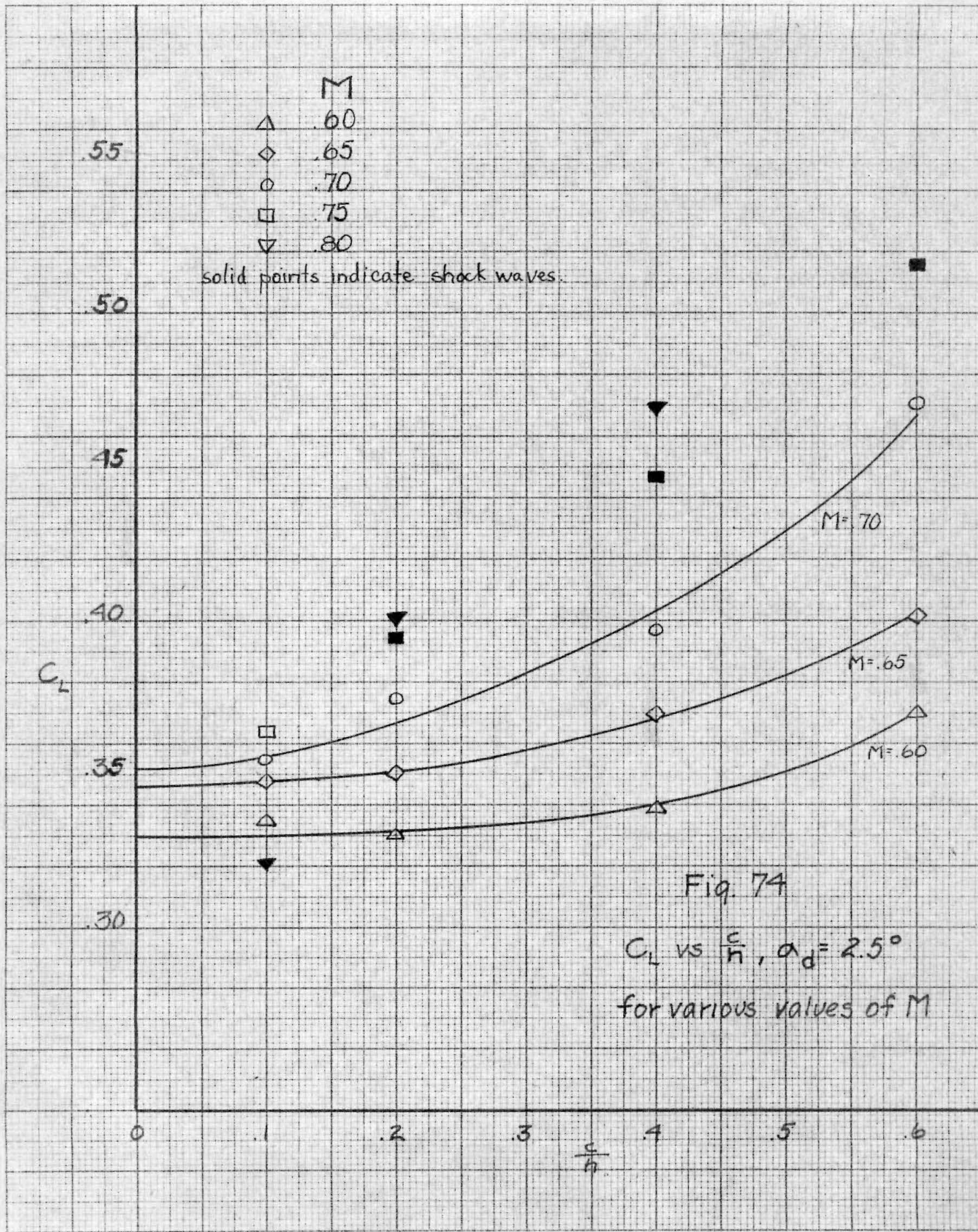


Fig. 74

C_L vs $\frac{c}{h}$, $\alpha_d = 2.5^\circ$
for various values of M

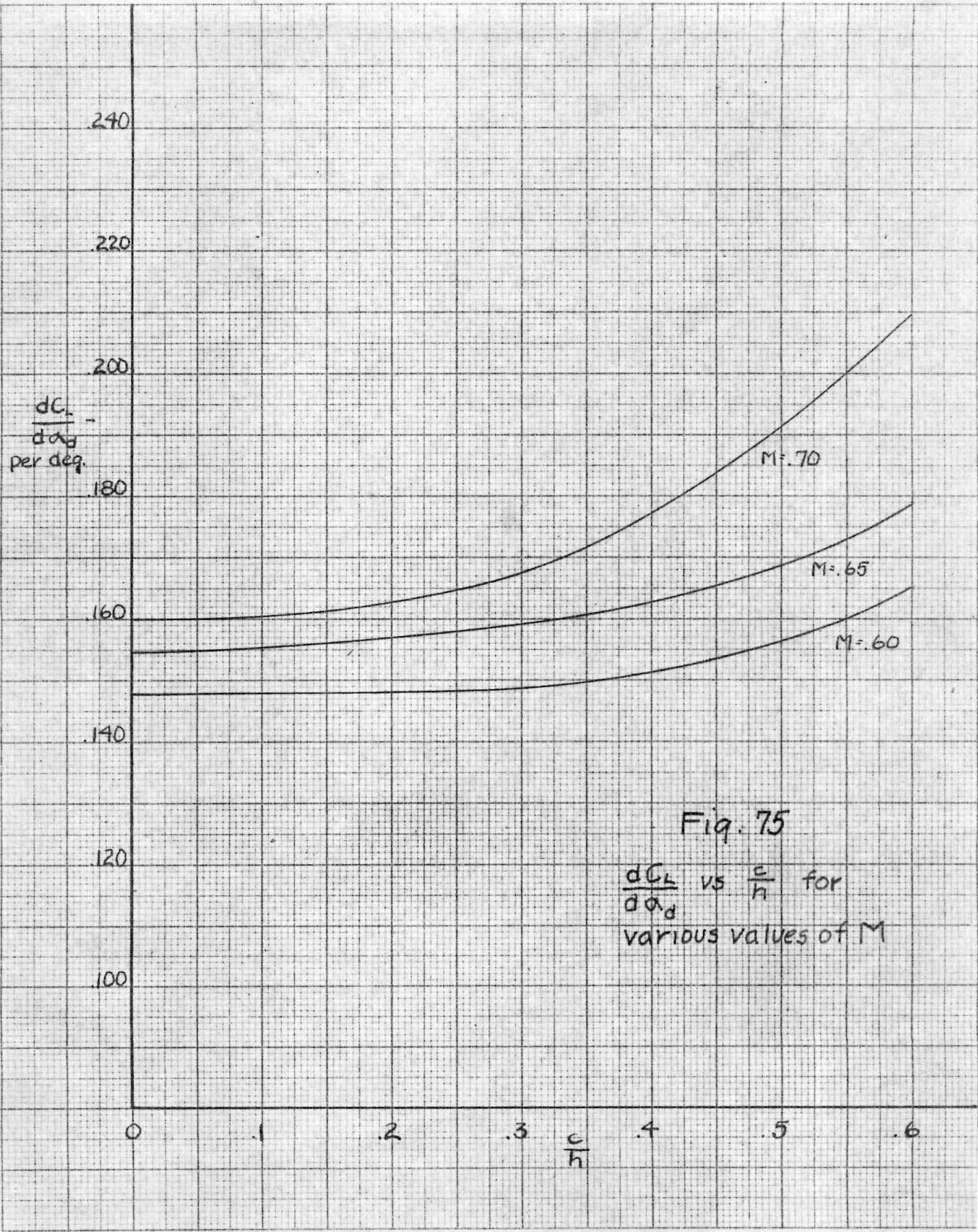


Fig. 75
 $\frac{dC_L}{d\alpha_d}$ vs $\frac{c}{h}$ for
various values of M